Bendix

Contract No.
NAS8-5407

Report No. BPAD-864-15651R

FINAL REPORT

FLUID STATE AMPLIFIER AND COMPENSATION

FOR THE MODEL NV-B1 GIMBAL ACTUATOR

Report Period

29 June 1964 to 29 March 1965

12 April 1965

Submitted to

National Aeronautics and Space Administration
George C. Marshall Space Flight Center
Huntsville, Alabama

By

Bendix Products Aerospace Division
The Bendix Corporation
South Bend, Indiana

Prepared Under
Direction Of: G. R. Howland

G. R. Howland
Project Supervisor

Approved By: D. J. Schaffer

D. J. Schaffer
Manager, Dynamic
Controls Engineering

ABSTRACT

23193

This report covers the analysis, design, and test effort performed from 29 June 1964 to 29 March 1965 on a pure fluid amplifier, servo-valve and compensation network for use with the Model NV-B1 Pneumatic Actuator for thrust vector control of the J-2 Rocket Engine.

The amplifier was designed as a breadboard device to demonstrate the feasibility of replacing the electronic components and the spool valve of the actuator by pure fluid components of the vortex design.

The results of the program indicated that such a concept is feasible and gave reasonably good dynamic performance. A follow-on development program is described to optimize the amplifier system design and performance.

TABLE OF CONTENTS

		Page
SECTION 1 -	INTRODUCTION	1-1
	1.1 Program Objective	1-1
SECTION 2 -	DESIGN APPROACH	2-1
	2.1 System Concept	2-1
	2.1.1 Analog Computer Simulation	2-1
	2.1.2 Fluid Amplifier Concepts	2-1
	2.2 System Design	2-3
	2.2.1 Configuration	2-3
	2.2.2 Vortex Amplifiers	2-5
	2.2.3 Servovalve Design	2-11
	2.2.4 Amplifier Design	2-14
	2.2.5 Rate Sensor Design	2-17
SECTION 3 -	COMPONENT ANALYSIS AND TEST RESULTS	
	3.1 Servovalve	3-1
	3.2 Amplifier	3-15
	3.3 Input Torque Motor Stage	3-31
	3.4 Rate Sensor	3-34

TABLE OF CONTENTS

	Page
SECTION 4 - SYSTEM ASSEMBLY AND TEST	4-1
4.1 Assembly Procedure	4-1
4.2 Test Procedure and Test Results	4-3
4.2.1 Amplifier and Servovalve	4-3
4.2.2 Rate Sensor	4-10
SECTION 5 - CONCLUSIONS AND RECOMMENDATIONS	5-1
5.1 Summary and Conclusions	5-1
5.2 Recommendations for Future Work	5-5
APPENDIX A - ANALOG COMPUTER STUDY OF VARIOUS COMPENSATION CONFIGURATIONS FOR THE J-2 ACTUATOR	A-1
APPENDIX B - DYNAMIC ANALYSIS OF VORTEX VALVES	B-1

LIST OF ILLUSTRATIONS

Figure	Title	Page
2-1	Computer Block Diagram	2-2
2-2	Fluid Amplifier System Schematic	2-4
2-3	Vortex Valve - Minimum and Maximum Impedance	2-6
2-4	Vortex Valve and Electron Tube	2-7
2-5	Vortex P_o Tap Characteristic	2-8
2-6	Vortex Flow Gain Characteristic	2-10
2-7(a)	Servovalve - Four-Way Bridge (Symbolic)	2-12
2-7(b)	Servovalve - Orifice Vent Control	2-12
2-7(c)	Servovalve - P_o Tap Vent Control	2-13
2-7(d)	Servovalve - Separate Valve Vent Control	2-13
2-8	Fluid Amplifier Block Diagram	2-15
2-9	Amplifier Schematic	2-16
2-10	Rate Sensor Schematic	2-18
3-1	Valve F - Flow Versus Control Pressure	3-3
3-2	Valve F - Load Characteristic	3-4
3-3	One Side of Servovalve Schematic	3-5
3-4	Valve F - Modified Load Characteristic	3-6
3-5	Valve B - Control Pressure Requirement	3-7
3-6	Valve B - Flow Versus Control Pressure	3-8
3-7	Servovalve Impedance Matching	3-10
3-8	Servovalve Pressure Characteristic	3-11
3-9	Differential Motor Pressure Versus Servovalve Input Signal	3-13
3-10	Servovalve - Partial Assembly	3-14
3-11	One Side of Amplifier Schematic	3-16
3-12	Push-Pull Amplifier Schematic	3-17
3-13	Gain Adjustment of Amplifier Stages	3-18
3-14	Valve L - Load Characteristic	3-19
3-15	Output Motor Pressure Versus Input to Last Stage Of Amplifier	3-22
3-16	Test Circuitry	3-23
3-17	Matching of Push-Pull Servovalve	3-25
3-18	Amplifier and Servovalve Pressure Levels	3-27

LIST OF ILLUSTRATIONS

Figure	Title	Page
3-19	Servovalve Output Pressure Versus Amplifier Input Pressure at 800 PSI	3-28
3-20	Servovalve Output Pressure Versus Amplifier Input Pressure at 400 PSI	3-29
3-21	Load Flow Characteristic	3-30
3-22(a)	Schematic of Pilot Stage (Forward Flow)	3-32
3-22(b)	Schematic of Pilot Stage (Reverse Flow)	3-33
3-23	Speed Transducer Calibration	3-35
4-1	Amplifier Assembly	4-2
4-2(a)	System Block Layout	4-4
4-2(b)	Rate Sensor Block Layout	4-5
4-3	System Calibration	4-7
4-4(a)	System Frequency Response - Gain Versus Frequency	4-8
4-4(b)	System Frequency Response - Phase Angle Versus Frequency	4-9
4-5(a)	Pressure Waveform Recordings	4-11
4-5(b)	Transient Response Recordings	4-12
4-6	Rate Sensor and Amplifier Calibration	4-14

LIST OF TABLES

Table	Title	Page
I	Performance Data	5-2

SECTION 1

INTRODUCTION

1.1 PROGRAM OBJECTIVE

The objective of this program was to demonstrate the feasibility of replacing the electronic amplifier and compensation required for an electropneumatic gimbal actuator, with a fluid amplifier design employing the actuator gas as the working fluid. The amplifier output will supply the power directly to the actuator motor, thereby eliminating the need for a spool-type servovalve.

Since an electropneumatic gimbal actuator for the J-2 engine had been developed under the first phase of this contract (NAS8-5407, reference Bendix Report No. BPAD-864-15479), the compensation requirements for this actuator to meet MSFC Specification 50M35003 were used as the basis for the design and evaluation of the fluid amplifier system.

The design approach taken in this program is outlined in Section 2. The component analysis and test results are described in Section 3, and the complete amplifier system test results are given in Section 4. The conclusions and recommendations for future work are discussed in Section 5. The two topical reports issued during the program period are included as appendices.

SECTION 2

DESIGN APPROACH

2.1 SYSTEM CONCEPT

2.1.1 Analog Computer Simulation

An analog computer program was initiated to evaluate various methods of compensating the J-2 electropneumatic actuator to provide the overall performance as specified in MSFC Specification 50M35003.

A detailed report of this phase of the program was submitted in Bendix Report No. BPAD-864-15472R and is included in this report as Appendix A. Six compensation techniques were considered and optimized. Consideration was made of each of the compensation techniques in terms of optimum overall performance and ease of adapting to fluid techniques. From these considerations, it was decided to employ system number four. This system consists of a straight gain amplifier with positive load feedback and negative rate feedback, as well as position feedback.

The static resolution is obtained from the gain of the amplifier and the positive load feedback. Stability is obtained by attenuating the forward gain as a function of frequency (by providing a lag in the load feedback), and motor speed (by means of the negative rate feedback).

A block diagram of the computer configuration is shown in Figure 2-1. For ease of computer simulation, the position feedback was summed upstream of the torque motor and the load and rate feedbacks were summed at the torque motor flapper.

2.1.2 Fluid Amplifier Concepts

Initial design studies were made to compare the estimated performance of an amplifier and servovalve using both jet-on-jet devices and vortex devices. The use of jet-on-jet devices for the servovalve presents three basic problems; a method of handling return flow, poor

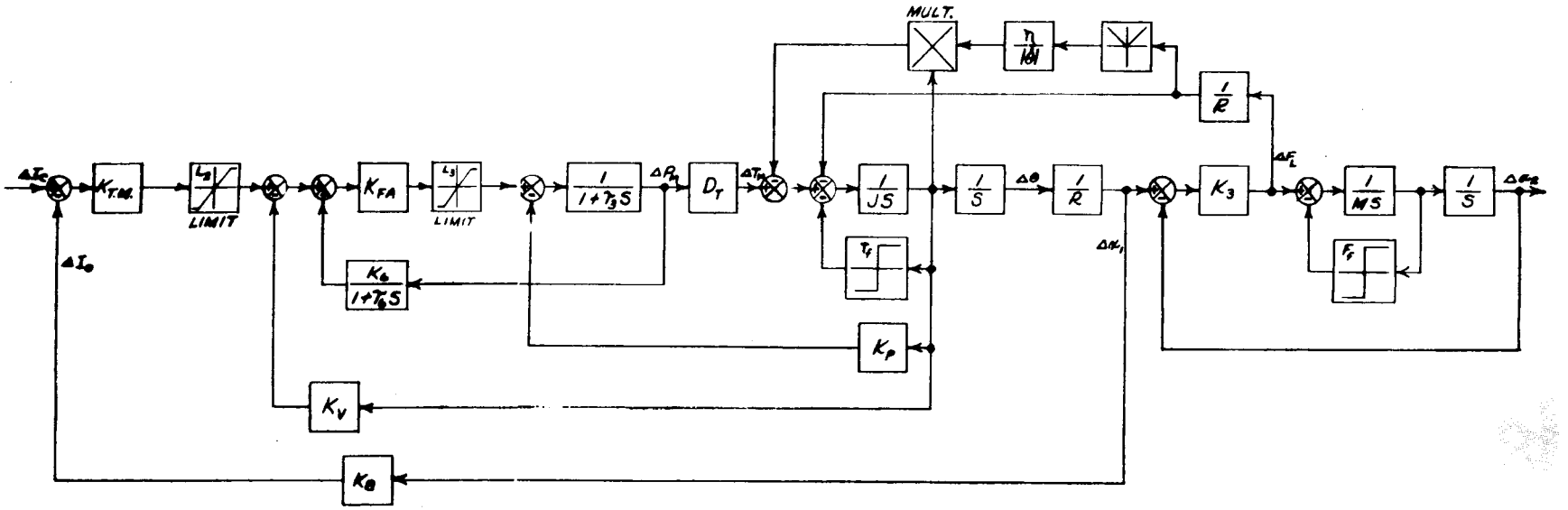

K_{FA} = FLUID AMPLIFIER GAIN = 2×10^6 P.S.I./IN.

K_6 = POS. PRESSURE FDBK GAIN = 0.25×10^{-6} IN./P.S.I.

K_V = MOTOR VELOCITY FDBK GAIN = 0.38×10^{-6} IN./RAD./SEC.

τ_6 = COMPENSATION LAG = 0.04 SEC.

FIGURE 1e SYSTEM NO. 4

COEFFICIENTS COMMON TO SYSTEMS 1 THROUGH 5

$K_{T.M.}$ = TORQUE MOTOR GAIN = 0.35×10^{-3} IN./MA.

K_θ = ACTUATOR FDBK GAIN = 27.4 MA/IN.

L_2 = TORQUE MOTOR LIMIT = 0.014 IN.

L_3 = STALL PRESSURE LIMIT = 400 P.S.I.

MOTOR, TRANSMISSION, AND LOAD COEFFICIENTS

D_T = MOTOR TORQUE DISPLACEMENT = 0.3 IN^3/RAD.

R = TRANSMISSION RATIO = 221 RAD./IN.

J = MOTOR PLUS TRANSMISSION INERTIA = 3.07×10^{-3} IN. LB. SEC.^{2}

M = LOAD INERTIA = 116.7 LB. SEC.^{2}/IN.

K_3 = LOAD STRUCTURAL SPRING RATE = 73,000 OR 391,000 LB./IN.

η = TRANSMISSION EFFICIENCY = 0.7

K_P = MOTOR PRESSURE SPEED CHARACTERISTIC = 0.9 P.S.I./RAD./SEC. FOR N_2 OR 0.45 FOR H_2

F_f = LOAD FRICTION FORCE = 7,300 OR 1,460 LBS.

T_f = MOTOR FRICTION TORQUE = 40 IN. LBS.

τ_3 = MOTOR COMPRESSIBILITY TIME CONSTANT = 0.005 SEC. FOR N_2 AND 0.003 FOR H_2

FIGURE 2-1 COMPUTER BLOCK DIAGRAM

maximum pressure recovery and high quiescent flow. In order to obtain a minimum acceptable pressure recovery would require the power nozzle to operate in the supersonic region. Experience both at Bendix and from a literature survey has indicated that the performance of a supersonic proportional amplifier is, at least at the present state of the art, both poor and unreliable.

It was therefore decided to employ four vortex valves in a bridge circuit. A detailed discussion of the servovalve is given in Section 2.2.

After initial evaluation of the servovalve was performed, consideration was given to employing jet-on-jet devices for the amplifier circuit. It was found that vortex amplifiers operating in push-pull provided the required pressure levels and gains with a minimum power loss. The sizing of the vortex devices indicated a smaller volume and, therefore, better frequency response potential than the equivalent jet-on-jet devices.

2.2 SYSTEM DESIGN

2.2.1 Configuration

The complete fluid amplifier system is shown schematically in Figure 2-2. The system consists of a four-way bridge vortex servovalve powered by a three-stage vortex push-pull amplifier. Amplifier gain adjustment is provided at the second and third stages. The input to the first stage is a pressure differential generated by the combined effects of the input torque motor flapper position, the position feedback bleed areas, the rate sensor output and the load feedback.

The rate sensor consists of a rotating input vortex valve which controls two vortex valves in push-pull, to generate a differential pressure output.

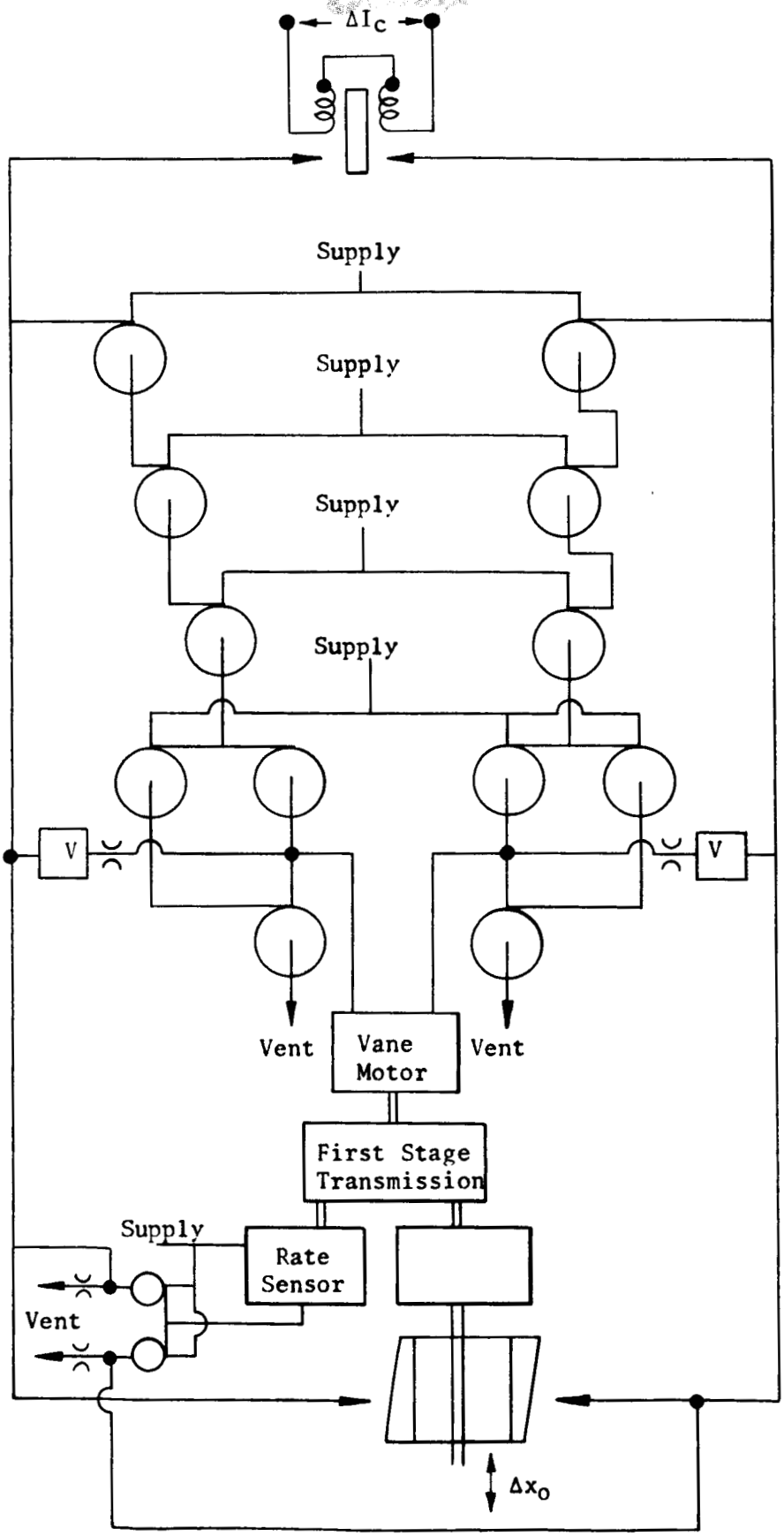

FIGURE 2-2 FLUID AMPLIFIER SYSTEM SCHEMATIC

Since the control pressure to each stage of amplification must be higher than the corresponding stage supply pressure, the supply pressures are obtained by orifices from the source pressure. Design optimization of each stage minimizes the stage pressure drop and provides the maximum pressure differential at the load.

2.2.2 Vortex Amplifiers

Before proceeding with a detailed description of the amplifier system, it is necessary to describe the basic characteristics of the vortex devices. The vortex amplifier, shown schematically in Figure 2-3, consists of a hollow cylindrical chamber. The supply flow is provided through a radial slot to the periphery of the chamber. The control flow is provided through a slot tangential to the periphery. The total flow exits by means of a hole in one (or both) chamber ends at the chamber axis of symmetry. The dimensioning of the chamber is such that the exit hole provides the majority of the valve impedance. In the absence of control flow, the chamber is at essentially supply pressure and the flow rate is determined by the exit hole area and the supply to exhaust pressure ratio. If a control flow is introduced at the tangential slot, the resultant momentum interchange will cause the total flow to rotate in a spiral to the exit. In order to conserve angular momentum, the tangential velocity of the flow must increase as the radius of rotation reduces. If sufficient control momentum is injected, the centrifugal pressure generated will equal the supply pressure, reducing the supply flow to zero. The output flow is then equal to the injected control flow. Since the control flow required to obtain this condition is less than the initial supply flow, a flow amplification results. The vortex amplifier, being a flow throttling device, has a performance comparable to the conventional electron triode tube. This similarity is shown symbolically in Figure 2-4. Addition and subtraction of control signals can be obtained by adding a number of control ports around the periphery of the chamber.

Flow can be removed from the chamber at either wall. If the concentric exit holes have equal diameters, the total flow through the valve is double that of a single exit. If one hole is smaller than the other, a flow transfer occurs which can be used to improve the valve gain. Figure 2-5 shows the deadended pressure (P_o) measured at one exit port (d_o)

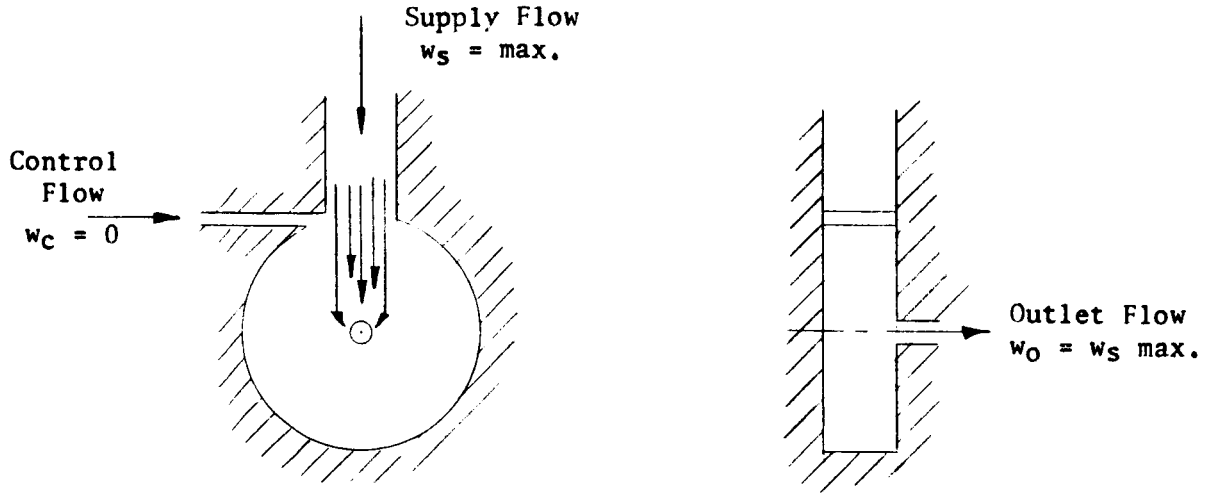

MINIMUM IMPEDANCE

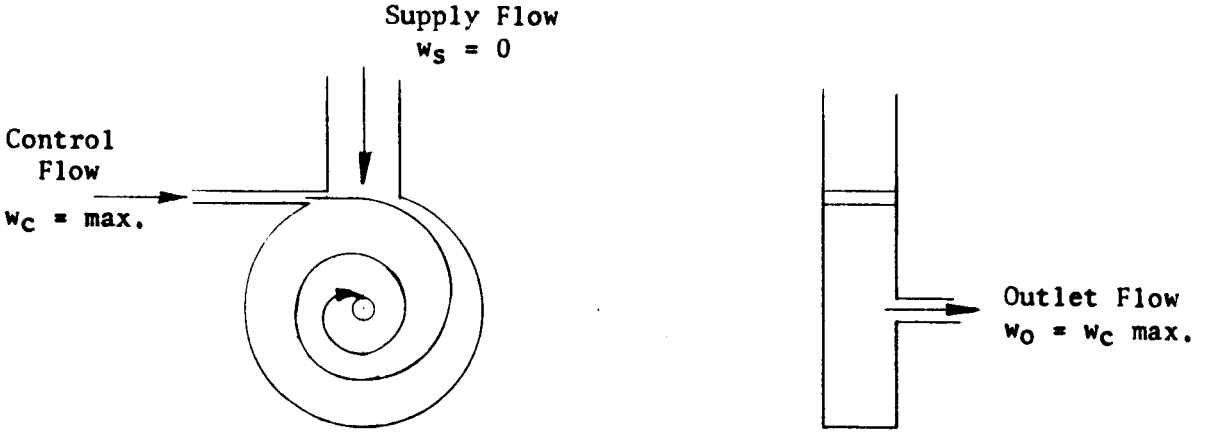

MAXIMUM IMPEDANCE

FIGURE 2-3 VORTEX VALVE - MINIMUM AND MAXIMUM IMPEDANCE

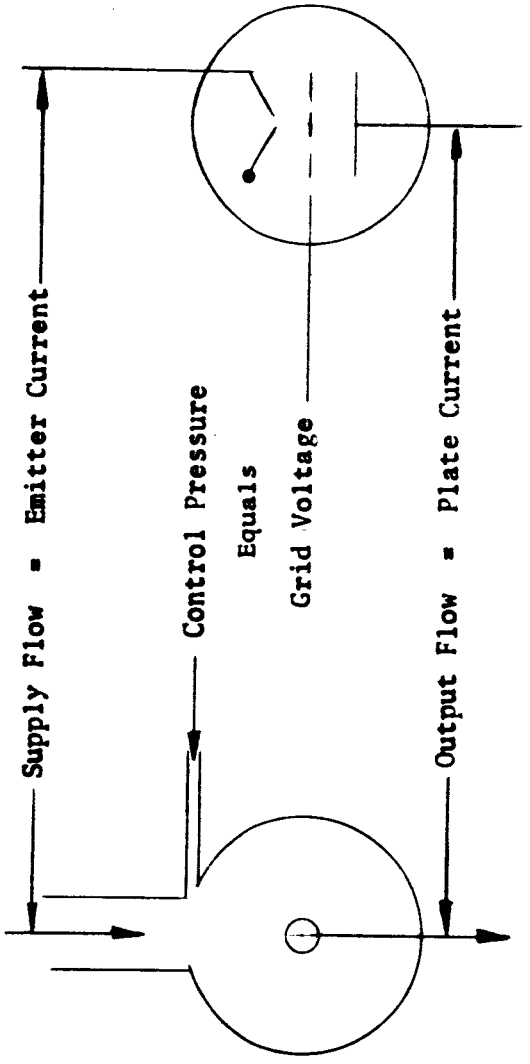

FIGURE 2-4 VORTEX VALVE AND ELECTRON TUBE

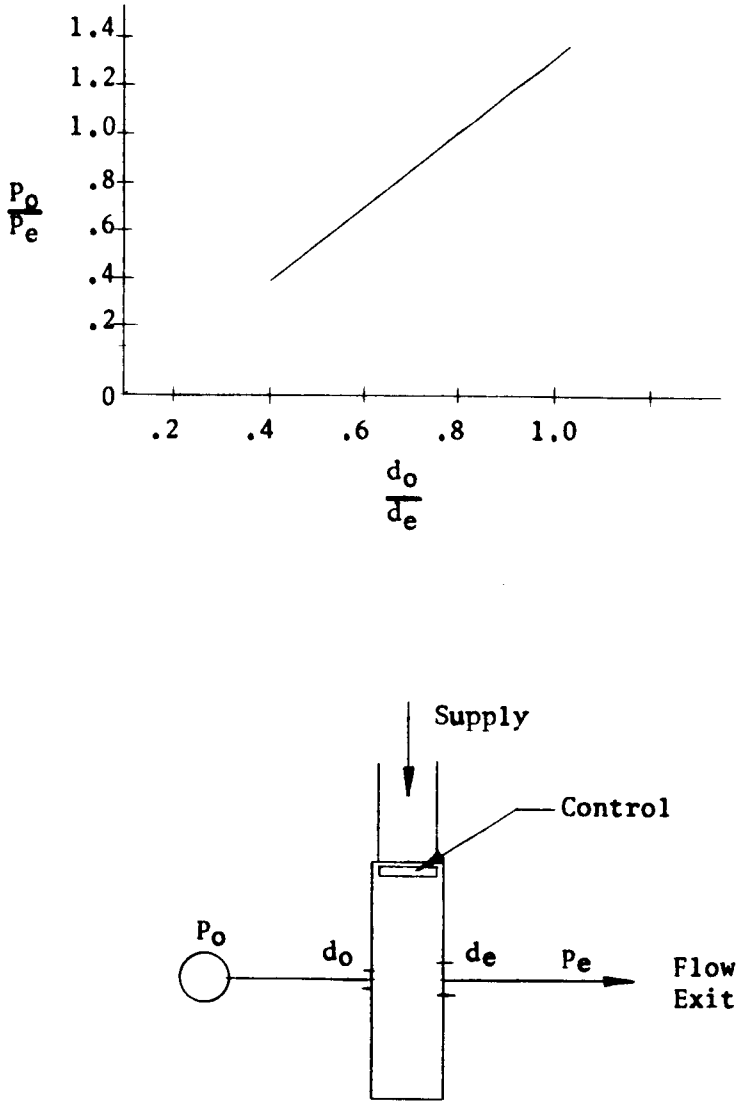

FIGURE 2-5 VORTEX P_o TAP CHARACTERISTIC

when the total flow is venting through the opposing exit hole (d_e) to a vent pressure P_e, at the full turndown condition. It can be seen that if d_o is less than 0.8 d_e, then P_o is less than the downstream pressure P_e. When no control flow is present, P_o is essentially equal to the supply pressure. This "P_o tap" can then be used to provide an output pressure which varies between supply pressure and a pressure less than the vent pressure. This wide a pressure range is not possible with a conventional jet-on-jet device. Figure 2-6 indicates how the "P_o tap" can be used in conjunction with the exit hole to obtain various valve characteristics.

Since the generation of the vortex swirl is dependent on the control to supply momentum interchange, high flow amplification can be obtained by using a smaller area control port. The high flow amplification is obtained at the expense of a high control pressure requirement. When staging vortex amplifiers, a high control pressure requirement results in larger stage losses and a lower available load pressure differential. A tradeoff must therefore be made between stage amplification and pressure loss. Various vortex chamber configurations were built and tested to evaluate the effects of the critical geometric dimensions on the performance of the valve. Using the criteria of maximum pressure recovery and maximum flow turndown for minimum control to supply pressure differential, the following parametric ratios were evolved:

a. Control port area to outlet area ratio - 0.5

b. Inlet port area to outlet area ratio - 3 (minimum

c. Chamber diameter to outlet diameter ratio - 8 to 12

d. Chamber thickness to outlet diameter ratio - 1 (minimum)

The outlet area is determined by the maximum flow and pressure drop requirements. Once this area is determined, the remaining valve dimensions can be obtained from the above listed ratios. In order to minimize the chamber volume, the chamber diameter to outlet diameter ratio used was 7.5. This provided the minimum chamber size without appreciable performance degradation.

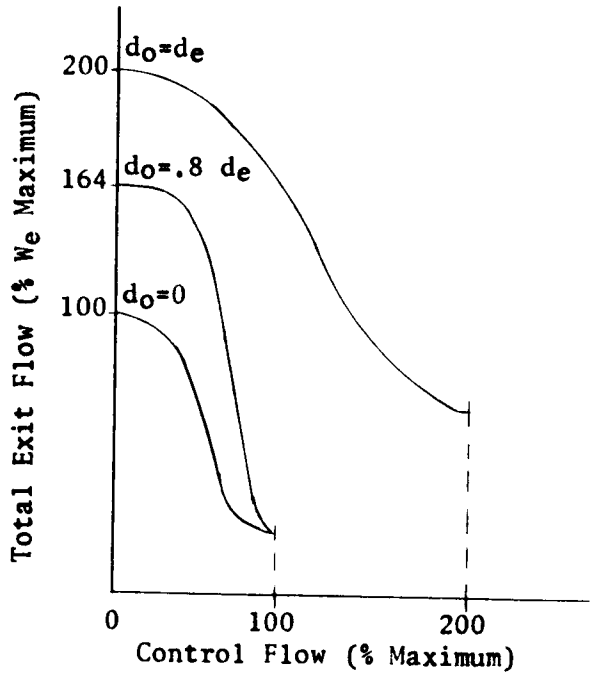

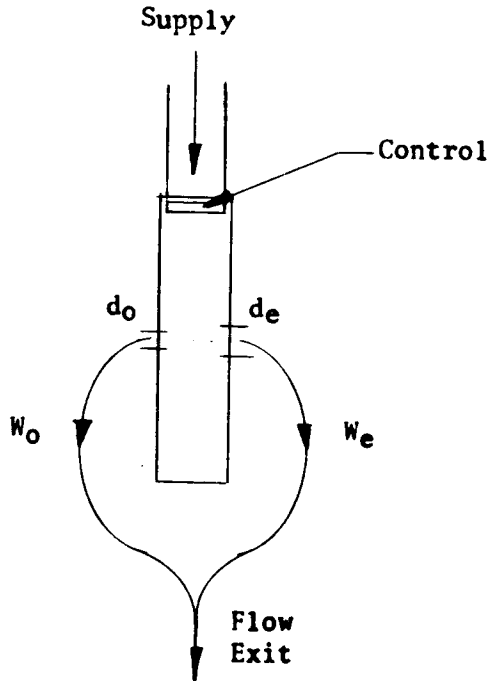

FIGURE 2-6 VORTEX FLOW GAIN CHARACTERISTIC

A digital computer program was evolved to provide both steady state and transient data on the performance characteristics of a vortex chamber of given dimensions. The details of this program and the extremely close correlation with experimental results is given in Bendix Report No. BPAD-15530R and is included in Appendix B of this report. This program provides a powerful tool in the design and optimization of vortex amplifiers.

2.2.3 Servovalve Design

As mentioned previously, consideration was given to the use of a jet-on-jet device for the servovalve. This device was discarded as being unfeasible for the application because of flow and pressure level requirements.

A bridge circuit consisting of four throttling vortex valves was then analyzed. The bridge circuit is shown schematically in Figure 2-7(a). Valves F_1 and B_2 operate together in push-pull with valves F_2 and B_1 to provide the reversible load differential. This type of circuit provides the throttling action required to minimize the quiescent flow. Figure 2-7(b) indicates the use of vortex amplifiers to provide the bridge elements. The main problem that arises from the use of the circuit as shown in Figure 2-7(b) becomes apparent when the control pressure level requirements are considered. The control pressure required at the supply valves (F_1 and F_2) will vary between the supply pressure (P_SF) and some percentage above P_SF. The control pressure to the vent valves must vary from above the maximum load pressure to the vent pressure (or equal to the minimum load pressure). Since the load pressure will approach P_SF under a blocked load condition, the range of control pressure required by valves B_1 and B_2 is much greater than that required for valves F_1 and F_2. Obviously, an orifice arrangement in the control lines as indicated in Figure 2-7(b) would not provide adequate range of control pressure. Figure 2-7(c) indicates one method of matching the control pressure requirements to the four valves. It will be recalled from the vortex valve discussion in Section 2.2.2 that the "P_o tap" pressure will vary between supply pressure and vent pressure over the range of control pressure if d_o is 80% of the exit hole diameter d_e. This pressure range is then adequate to control the vent valves.

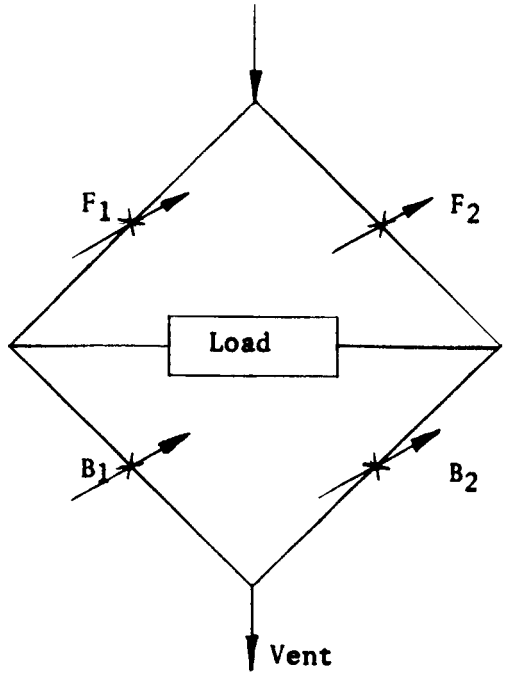

FIGURE 2-7(a) SERVOVALVE - FOUR-WAY BRIDGE (SYMBOLIC)

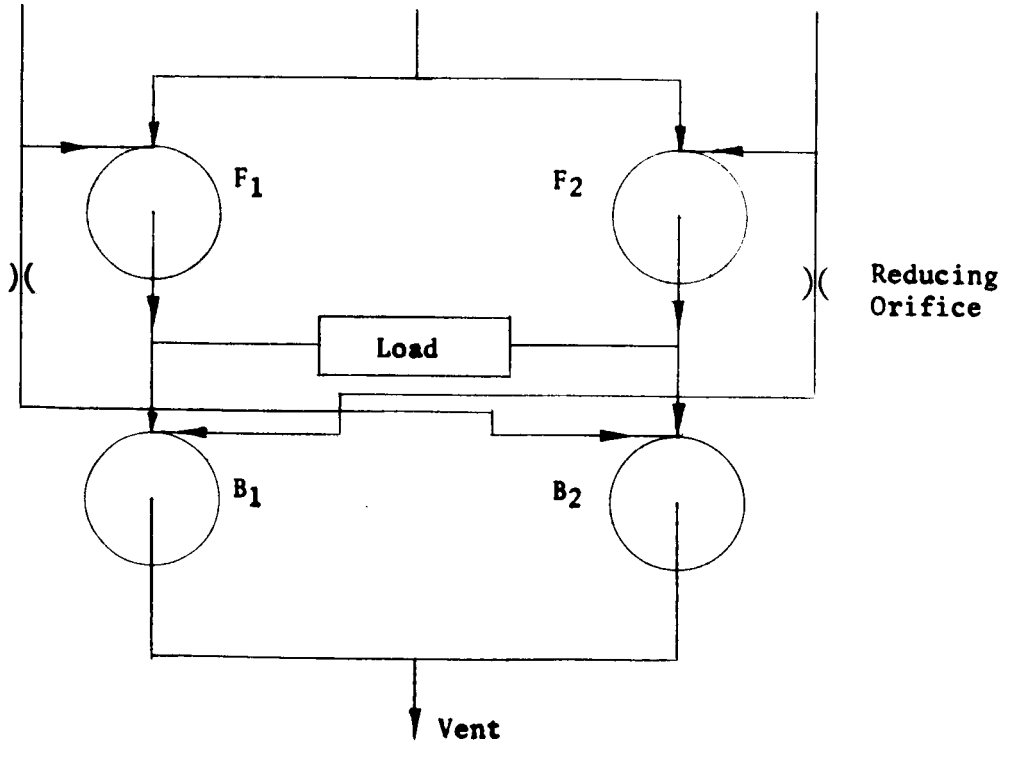

FIGURE 2-7(b) SERVOVALVE - ORIFICE VENT CONTROL

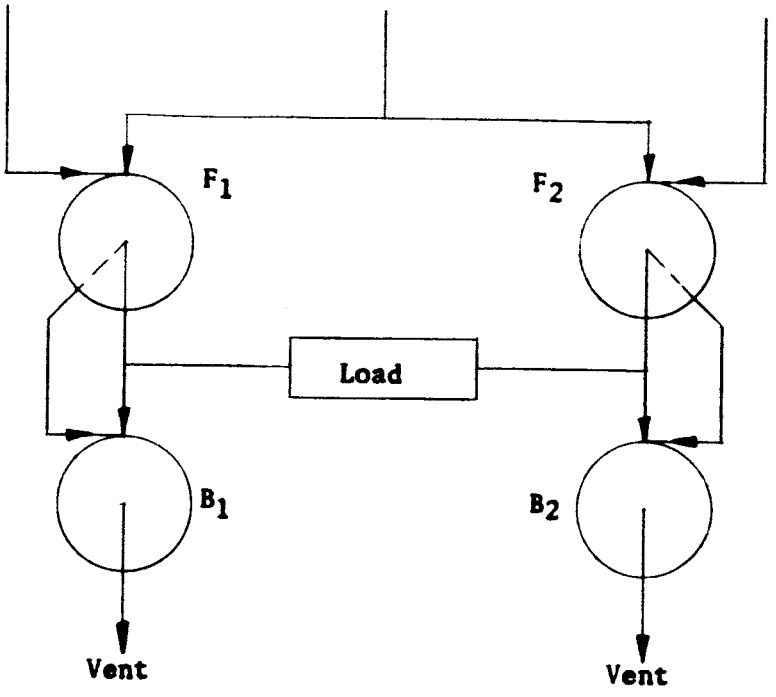

FIGURE 2-7(c) SERVOVALVE - P_o TAP VENT CONTROL

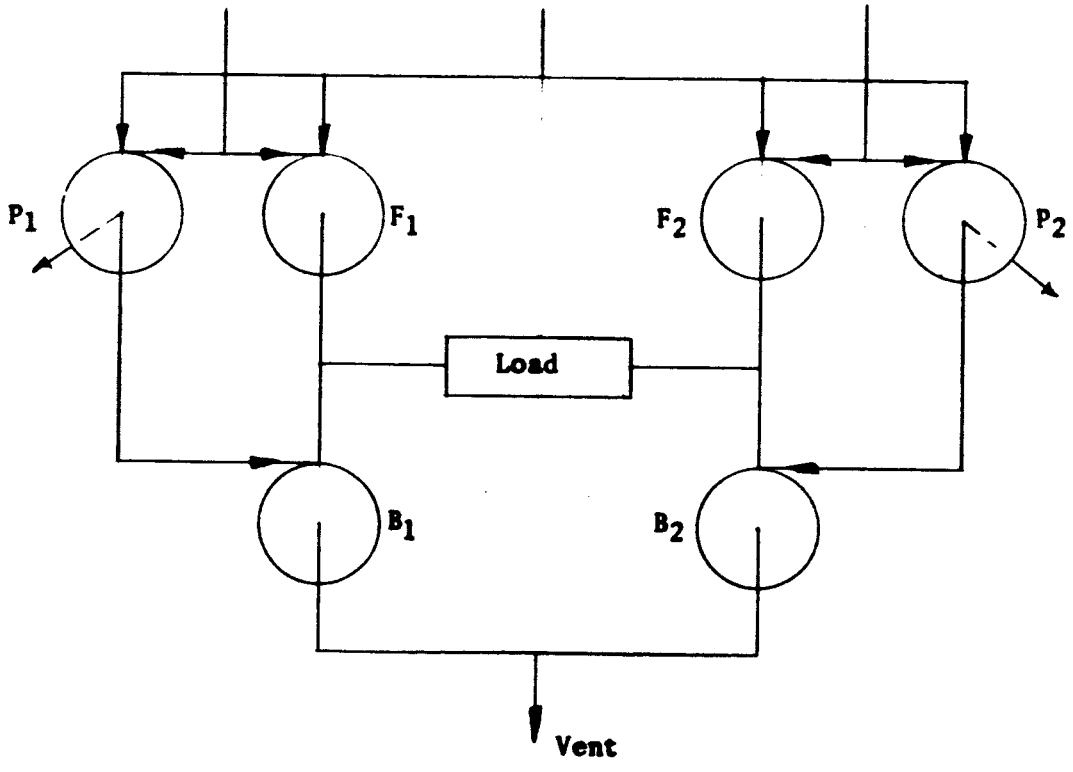

FIGURE 2-7(d) SERVOVALVE - SEPARATE VALVE VENT CONTROL

The complete bridge can then be controlled by connecting the P_o tap of valves F_1 and F_2 to the control ports of the corresponding B_1 and B_2 valves. A more flexible arrangement of this configuration is shown in Figure 2-7(d). In this arrangement, the power flow control function of valves F_1 and F_2 are separated from the B_1 and B_2 valve control by using an additional pair of vortex valves (P_1 and P_2) to provide the required control flows. This allows a minimum size vortex valve based on the load flow requirements. It was felt that the improvement in frequency response and the design flexibility of configuration (d) warranted its use despite the increase in vent flow which results. Test results obtained with this design have proven to be superior to the results anticipated for circuit (c).

2.2.4 Amplifier Design

The purpose of the amplifier is to provide sufficient flow and pressure to drive the servovalve, using as input the pressure differential generated by the torque motor flapper. From the analog computer studies, the overall system gain was determined as shown in Figure 2-1. An analysis of the torque motor and bleed orifice arrangement determined a torque motor gain of 0.38 psi/ma. The pure fluid amplifier and servovalve combination must then have a forward gain of 1860 psi/psi. Once the forward gain is known, the feedback gains can be determined. Figure 2-8 shows the block diagram of the complete actuator system with the transfer function characteristics required for the fluid amplifier components. This diagram is derived from the computer simulation diagram of Figure 2-1.

The amplifier schematic is shown in Figure 2-9. The amplifier consists of three stages of vortex valves in push-pull. The push-pull operation allows compatibility with the pressure differential output of the torque motor and the control requirements of the servovalve. Operating in a push-pull mode also reduces the sensitivity of the amplifier to noise and source pressure variations. The supply pressures to the various stages are determined by fixed orifices in parallel from the source pressure.

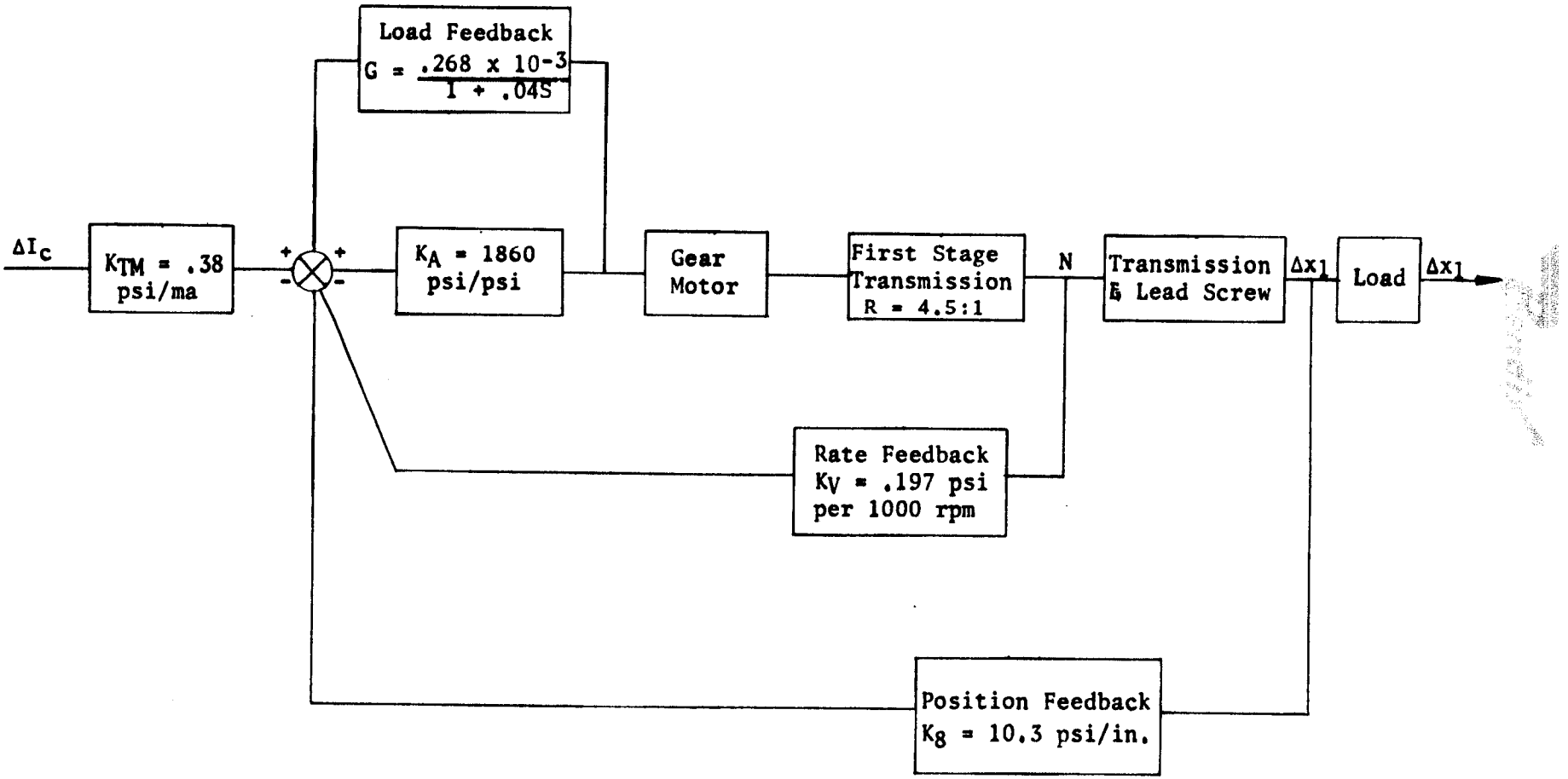

FIGURE 2-8 FLUID AMPLIFIER BLOCK DIAGRAM

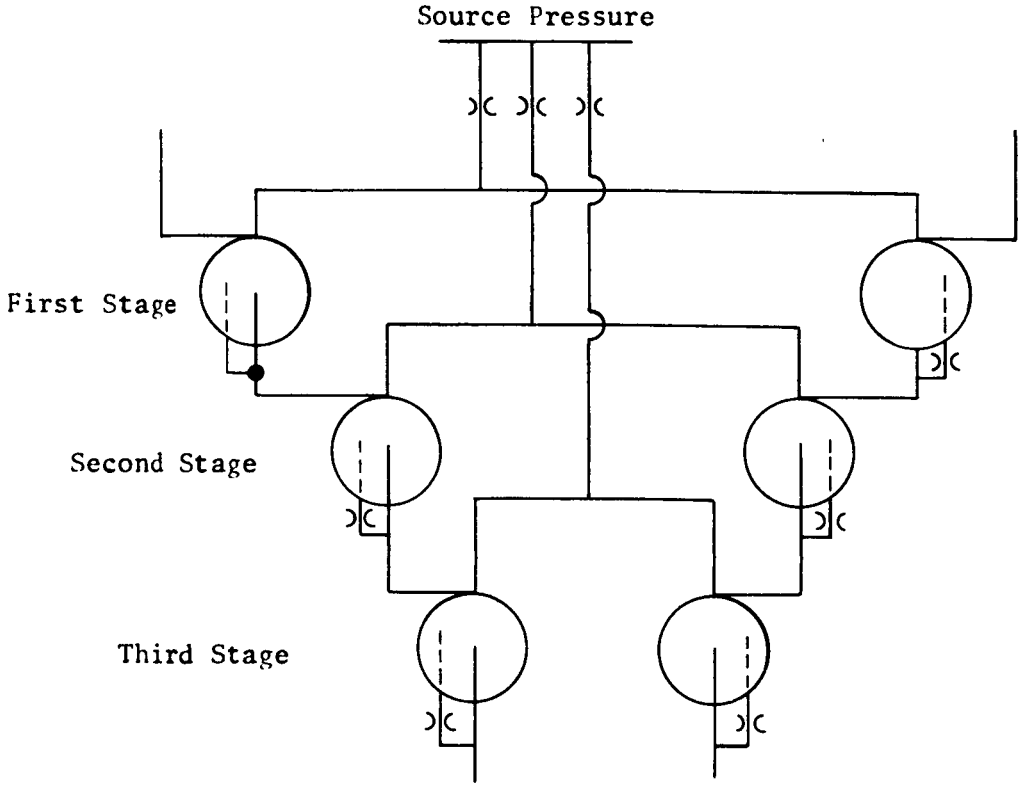

FIGURE 2-9 AMPLIFIER SCHEMATIC

The flows into the control ports of the first stage are provided by orifices from the source pressure. The total flow through these orifices provides both the control flows and the bleed flows from the command and feedback units. The flow available for control of the amplifier is therefore dependent upon the sum of the equivalent bleed areas. These bleed areas are determined by the torque motor flapper position (command signal), the output position bleed (position feedback), the rate sensor impedance (rate feedback), and the load pressure level (load feedback).

The output of each vortex stage consists of the exit hole and the "P_o tap". A variable restrictor is placed downstream of the P_o tap in the second and third stages to vary the maximum flow output and therefore the gain of the stage. This adjustment can also be used to obtain symmetrical performance of the amplifier.

2.2.5 Rate Sensor Design

The rate sensor is shown schematically in Figure 2-10. The sensor consists of a speed to pressure transducer with a single stage push-pull output amplifier. The transducer is a vortex chamber in which the supply flow is obtained from radial holes in a cylindrical button. The button forms one end of the vortex chamber. A bias flow is introduced into the chamber through a tangential control slot. When the button is rotated, the incoming supply flow is given a swirl component which is proportional to the speed of rotation. The rotating supply flow will either add to or tend to cancel the bias swirl, depending on the direction of rotation of the button relative to the control slot. Since the impedance of the vortex valve is dependent on the magnitude of the generated swirl, the flow through the valve will be proportional to the speed and direction of rotation.

In order to match the output of the speed transducer to the push-pull input of the amplifier, a single stage of amplification is incorporated in the rate sensor. This stage consists of two vortex valves with a common control input. One valve is biased to the full turndown

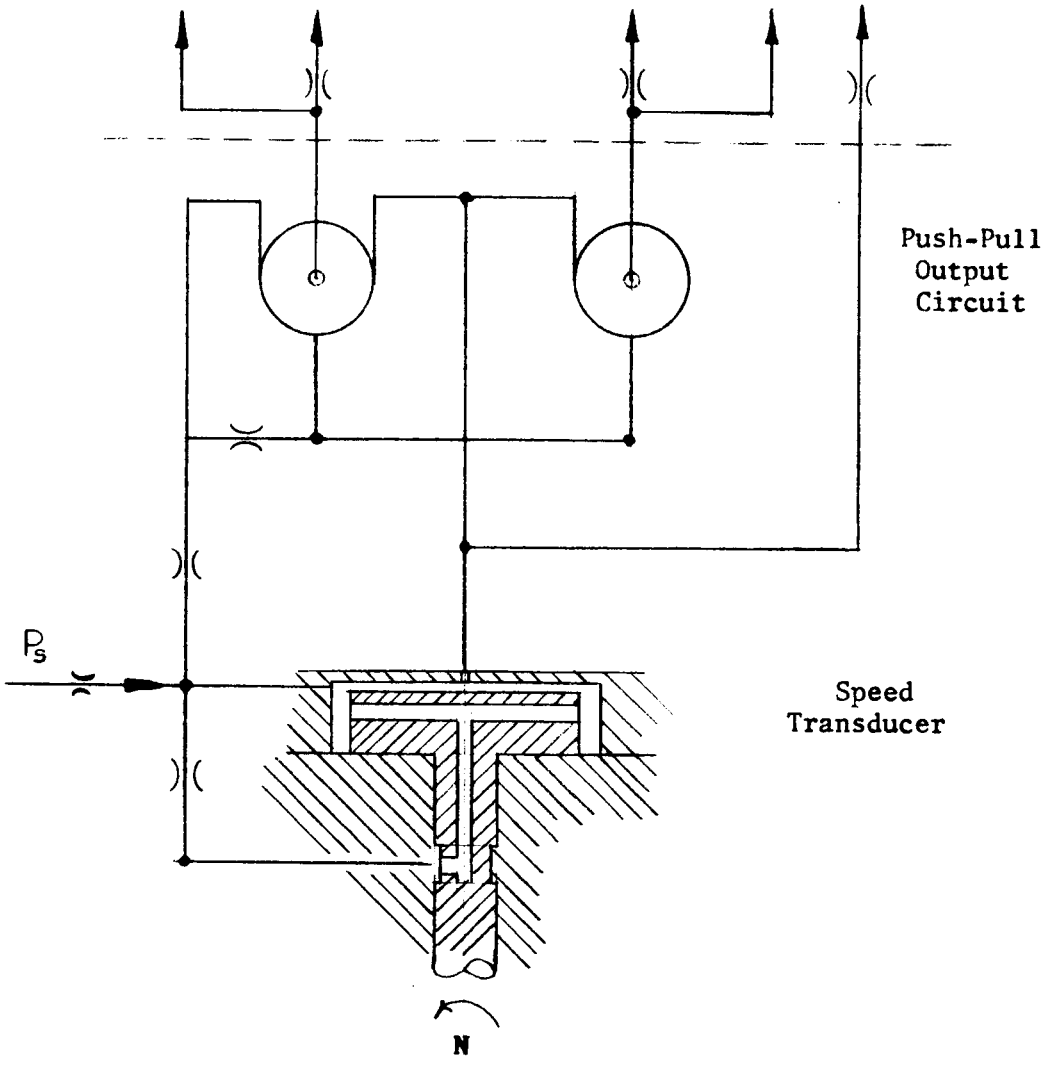

FIGURE 2-10 RATE SENSOR SCHEMATIC

condition. With no control flow, the output flow of the unbiased valve will be maximum while the biased valve will have a minimum output flow. Increasing the control flow will cause one output to decrease and the second output to increase. If load orifices are placed downstream of the vortex outlets, the load pressure differential will vary as a function of the speed and direction of rotation of the rate sensor. This pressure differential is applied to the input stage of the amplifier.

The flange and square end shaft of the sensor are designed for incorporation with the present actuator. Bendix drawing NPX-102-440 shows the sensor installation on the actuator. Since the sensor is driven by the idler gear of the transmission, a 4.5:1 speed reduction from the vane motor results.

SECTION 3

COMPONENT ANALYSIS AND TEST RESULTS

3.1 SERVOVALVE

The development program followed for the servovalve was divided into the following tasks.

A. Select circuitry based on prior experience and some exploratory tests.

B. Establish basic dimensions of valve inlet and exhaust areas and analyze theoretical performance.

C. Build breadboard hardware and compare actual test results with theoretical steady state analysis.

D. Define control signal input requirements which will determine amplifier output stage design.

The selection of the servovalve concept is discussed in Section 2.2.3 and is shown in Figure 2-7(d). The outlet areas of the valves F_1, F_2, B_1, and B_2 are based on the flow areas used in the servovalve of the J-2 actuator. The exhaust valve outlet areas (B_1 and B_2) were increased to accept the turndown flow of valves F_1 and F_2 without increasing the load back pressure.

The servovalve was sized as follows:

	Valve F	Valve B
Chamber Depth	0.200	0.200
Supply Port Width	0.350	0.350
Control Port Width	0.020	0.060
Chamber Diameter	1.0	1.0
Outlet Diameter	0.136	0.136
P_o Tap Diameter	0.125	0.136

Figure 3-1 shows the relationship between the supply flow (W_{SF}) and control flow (W_{CF}) of valve F versus the control pressure (P_{CF}). The load pressure (P_{M1}) was 230 psia and the supply pressure (P_{SF}) was held constant at 585 psia. For a given ratio of P_{CF}/P_{SF}, holding P_{SF} constant, the exit flow from valve F will follow the sharp edged orifice characteristic. The relationship of W_{EF} versus P_M/P_{SF} for various turn-down ratios R of valve F can then be plotted as shown in Figure 3-2. The outlet flow

$$W_{EF} = W_L + W_{SB}$$

where,

W_L = load flow - lbs./sec.

W_{SB} = supply flow into valve B - lbs./sec.

The load flow W_L can be divided into leakage flow from the pneumatic motor of the actuator and the flow through the motor to the other side of the servovalve.

Therefore;

$$W_L = W_{LE} + W_{LT}$$

where,

W_{LE} = leakage flow - lbs./sec.

W_{LT} = load flow through motor - lbs./sec.

From tests on the actuator vane motor, the leakage flow is .0275 lb./sec. of nitrogen at 60 psi supply for the S/N 2 motor and .05 lb./sec. at 100 psi supply pressure for the S/N 1 motor. For development tests conducted on the vortex servovalve, this load leakage has been simulated by two orifices vented to ambient pressure as shown schematically in Figure 3-3. A diameter of 0.120 inch on each side of the load is required to simulate the motor leakage. The leakage flow can then be subtracted from the total output flow of valve F to determine the flow available to the load and valve B. This flow (W_{LT} and W_{SB}) versus load pressure ratio is shown in Figure 3-4.

Test results on vortex valve B are shown in Figures 3-5 and 3-6.

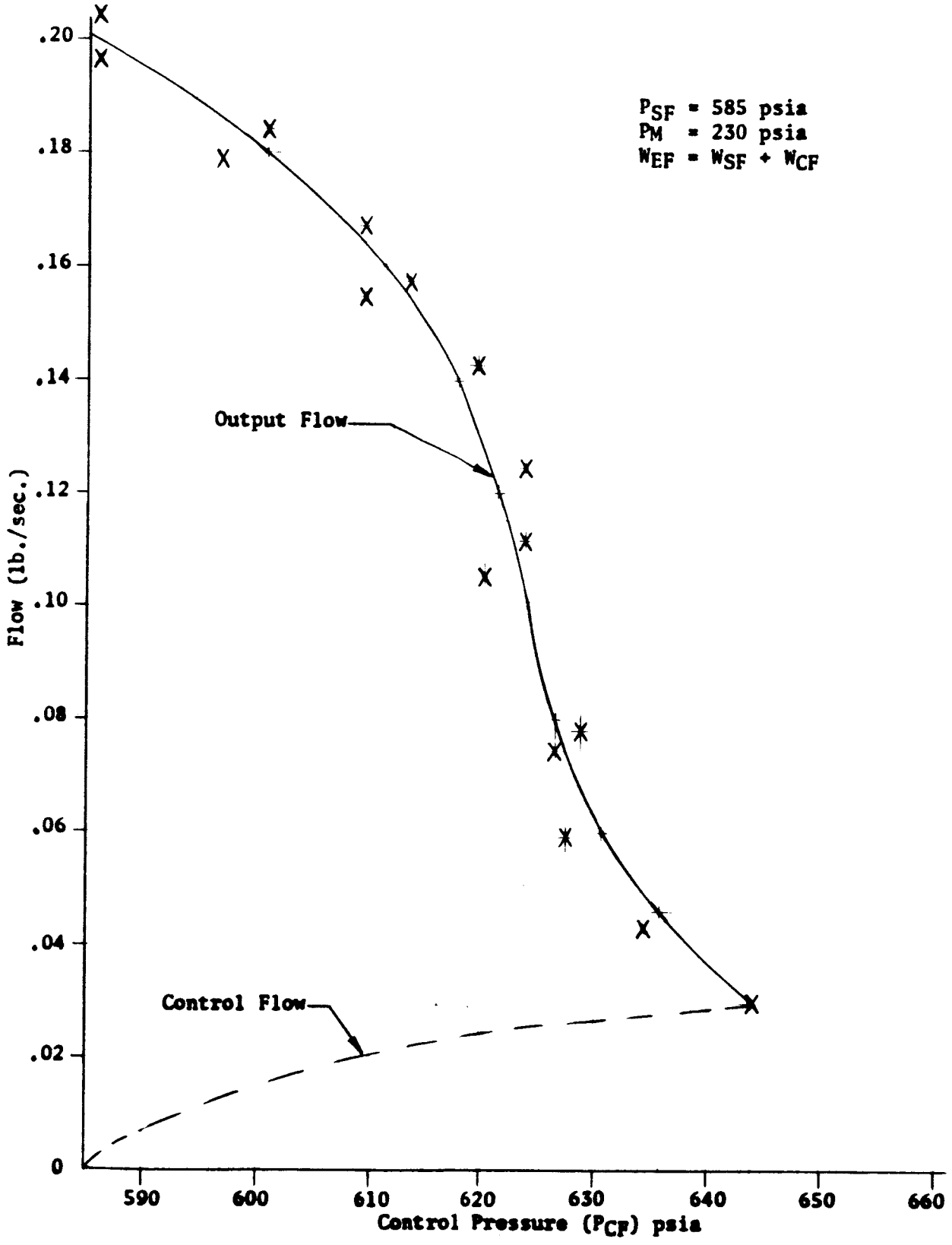

FIGURE 3-1 VALVE F - FLOW VERSUS CONTROL PRESSURE

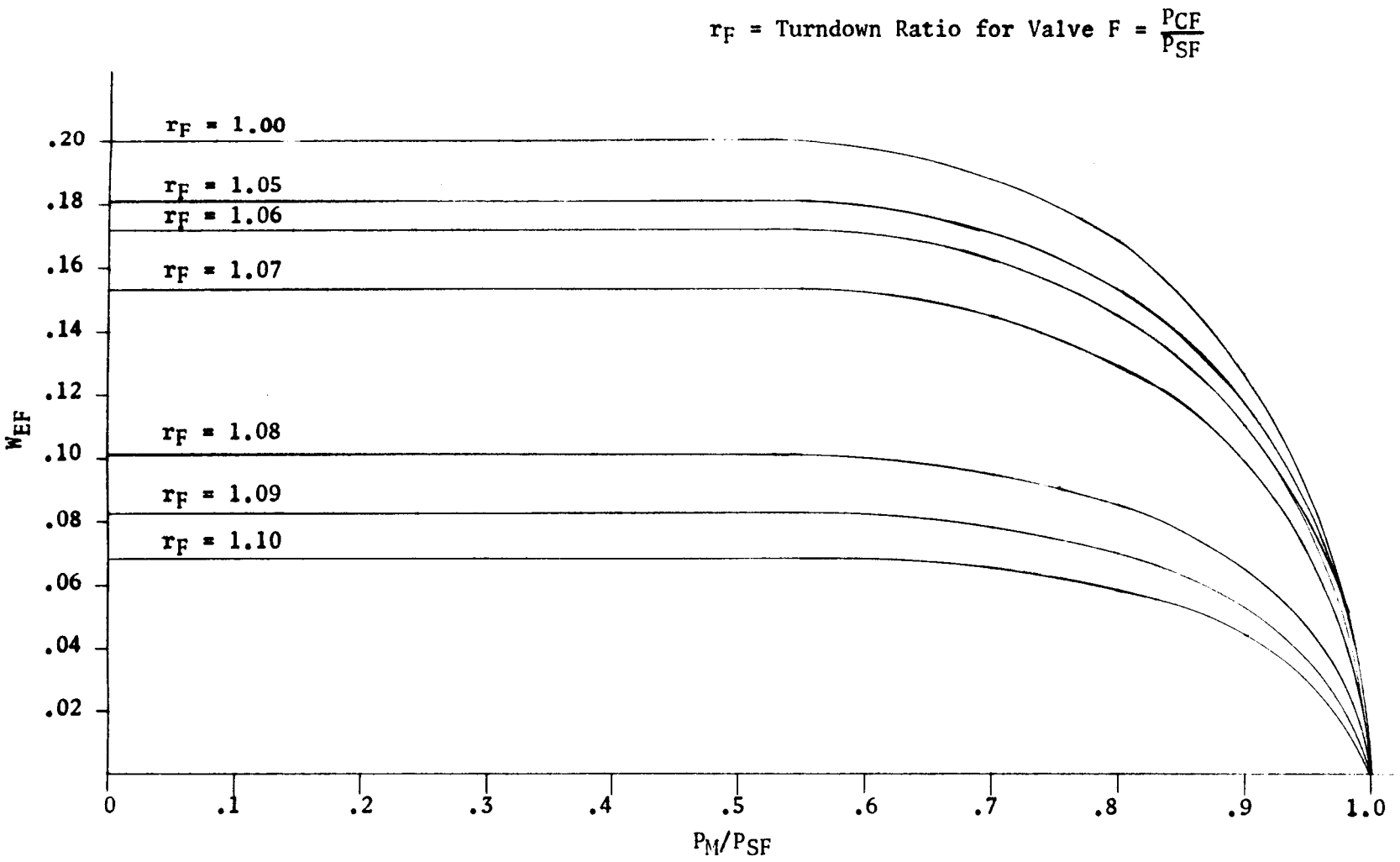

FIGURE 3-2 VALVE F LOAD CHARACTERISTIC

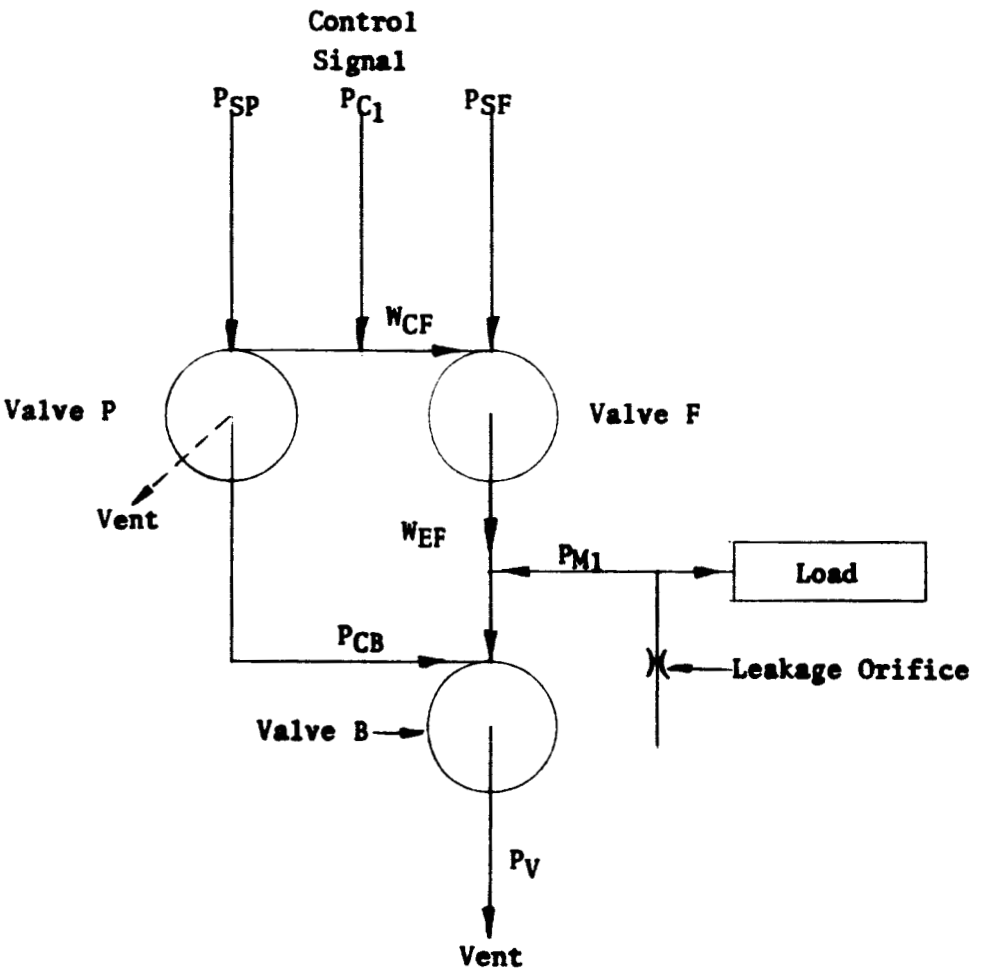

FIGURE 3-3 ONE SIDE OF SERVOVALVE SCHEMATIC

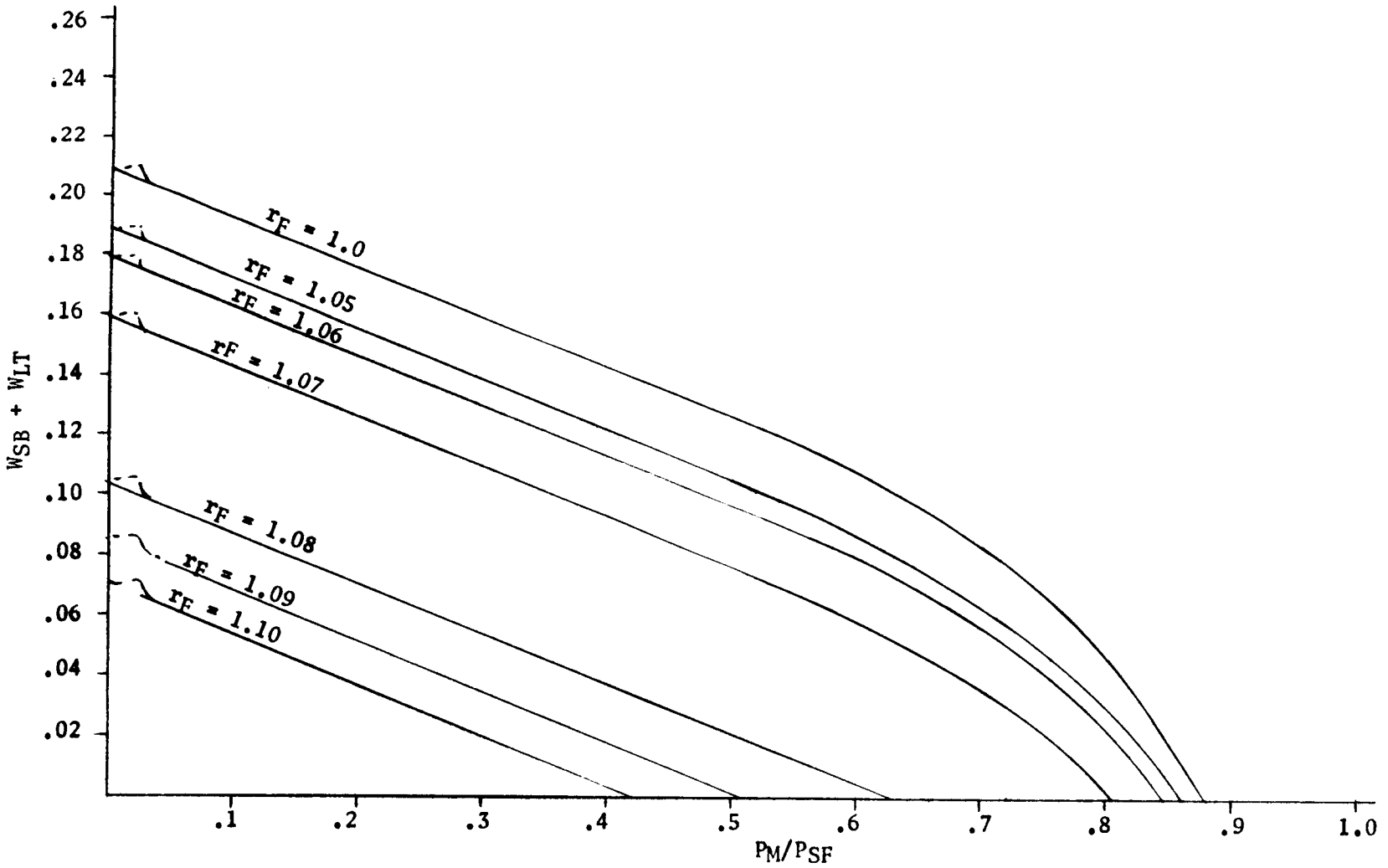

FIGURE 3-4 VALVE F MODIFIED LOAD CHARACTERISTIC

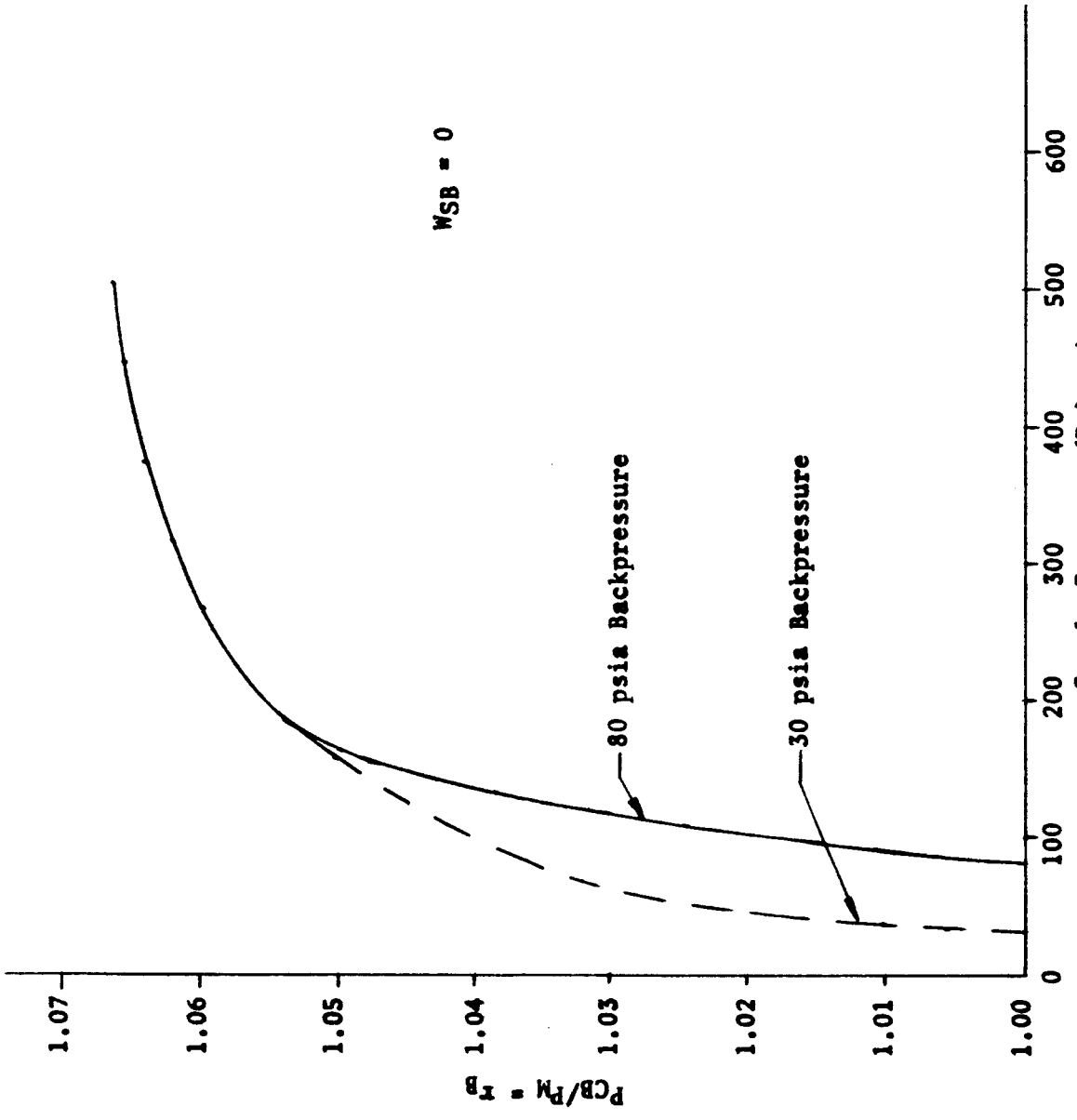

FIGURE 3-5 VALVE B CONTROL PRESSURE REQUIREMENT

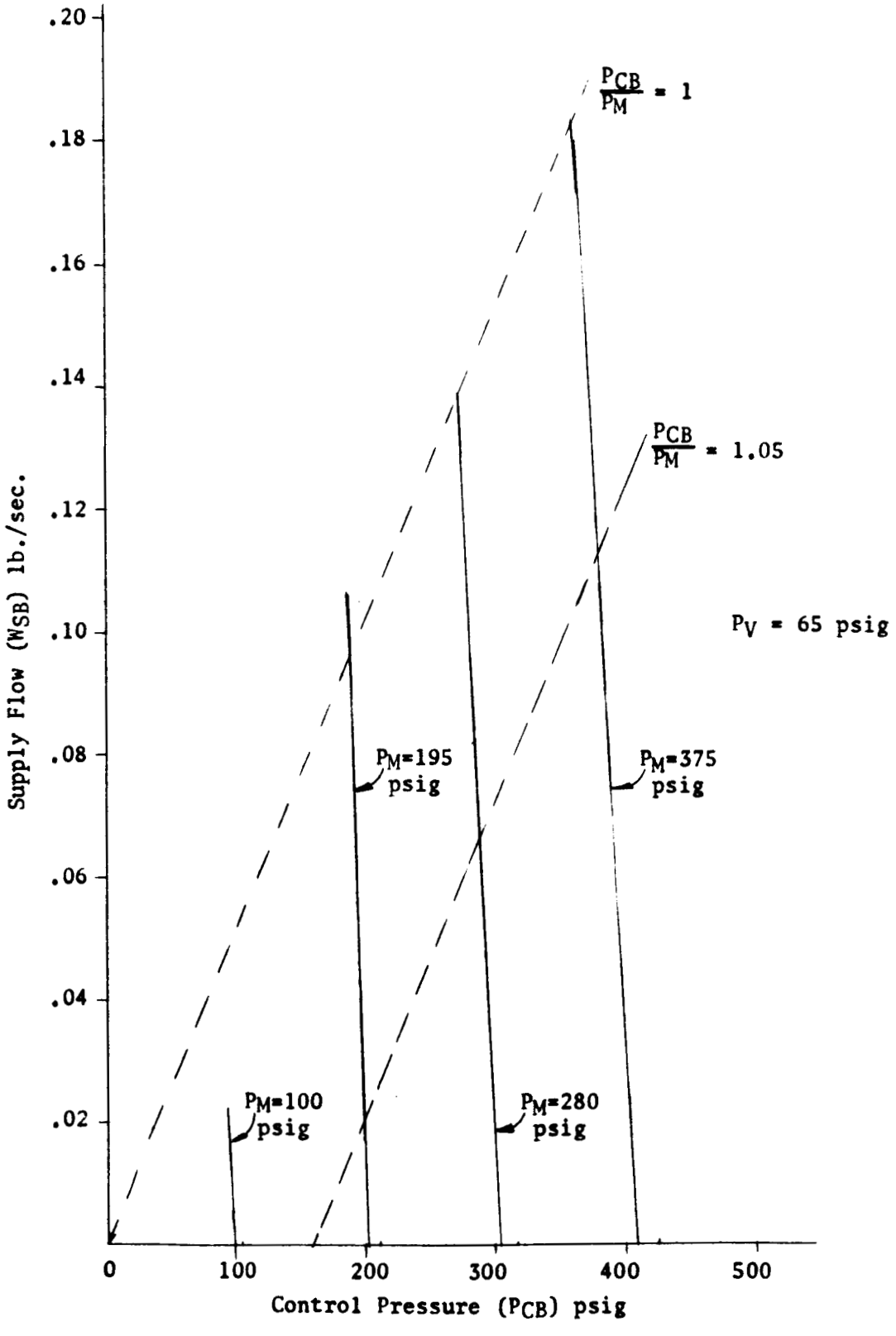

FIGURE 3-6 VALVE B FLOW VERSUS CONTROL PRESSURE

Figure 3-5 is a plot of the ratio of control pressure (P_{CB}) to supply pressure (which in this case is equal to P_M) against the load pressure P_M for complete turndown of valve B ($W_{SB} = 0$).

Figure 3-6 relates the amount of flow (W_{SB}) to the control pressure for various values of load pressure.

Figure 3-6 indicates a linear relationship over the range of interest, between the supply flow and the control pressure, when the ratio of P_{CB}/P_M is held constant. Also, the supply flow will decrease linearly with an increase in control pressure P_{CB} when the supply pressure is held constant.

The relationships presented in Figures 3-5 and 3-6 can be cross-plotted with Figure 3-4 to obtain the graph shown in Figure 3-7. This graph shows the distribution of flow from valve F for any pressure, P_M, and any control pressure ratio of valves F and B.

From Figure 3-7 it is possible to determine the magnitude of load flow available for a given load pressure. For example, point A on the graph indicates that the value of P_M/P_{SF} will be approximately .73 for control pressure ratios of $r_F = r_B = 1.06$ and zero load flow.

The range of operation of the combination of the two valves will be confined to the crosshatched area of the curve.

For practical reasons, the values of r_F and r_B will vary from 1 to approximately 1.10. It can be determined from Figure 3-7 that the minimum value for P_M for no load flow will be .2 P_{SF} (point B on graph).

The sizing of vortex valve P (the control for valve B) was determined experimentally. It was found that the maximum range of load pressure occurred when the area of the P_o tap of valve P was 80% to 90% of the control port area of valve B. Tests were then run to determine the optimum relationship between the P_o tap area and the exit or vent area. These test results are shown in Figure 3-8. Although reducing the vent hole of

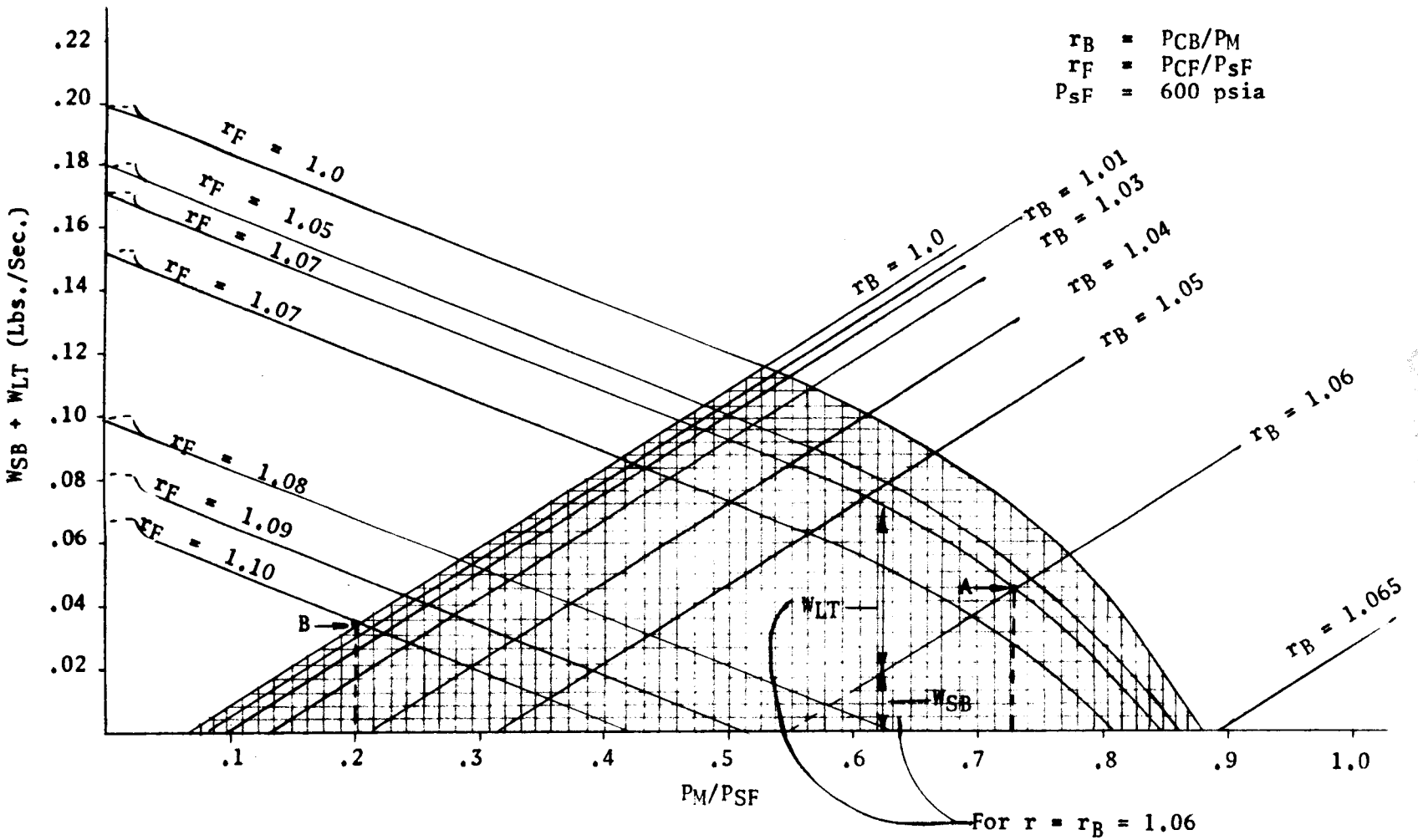

FIGURE 3-7 SERVOVALVE IMPEDANCE MATCHING

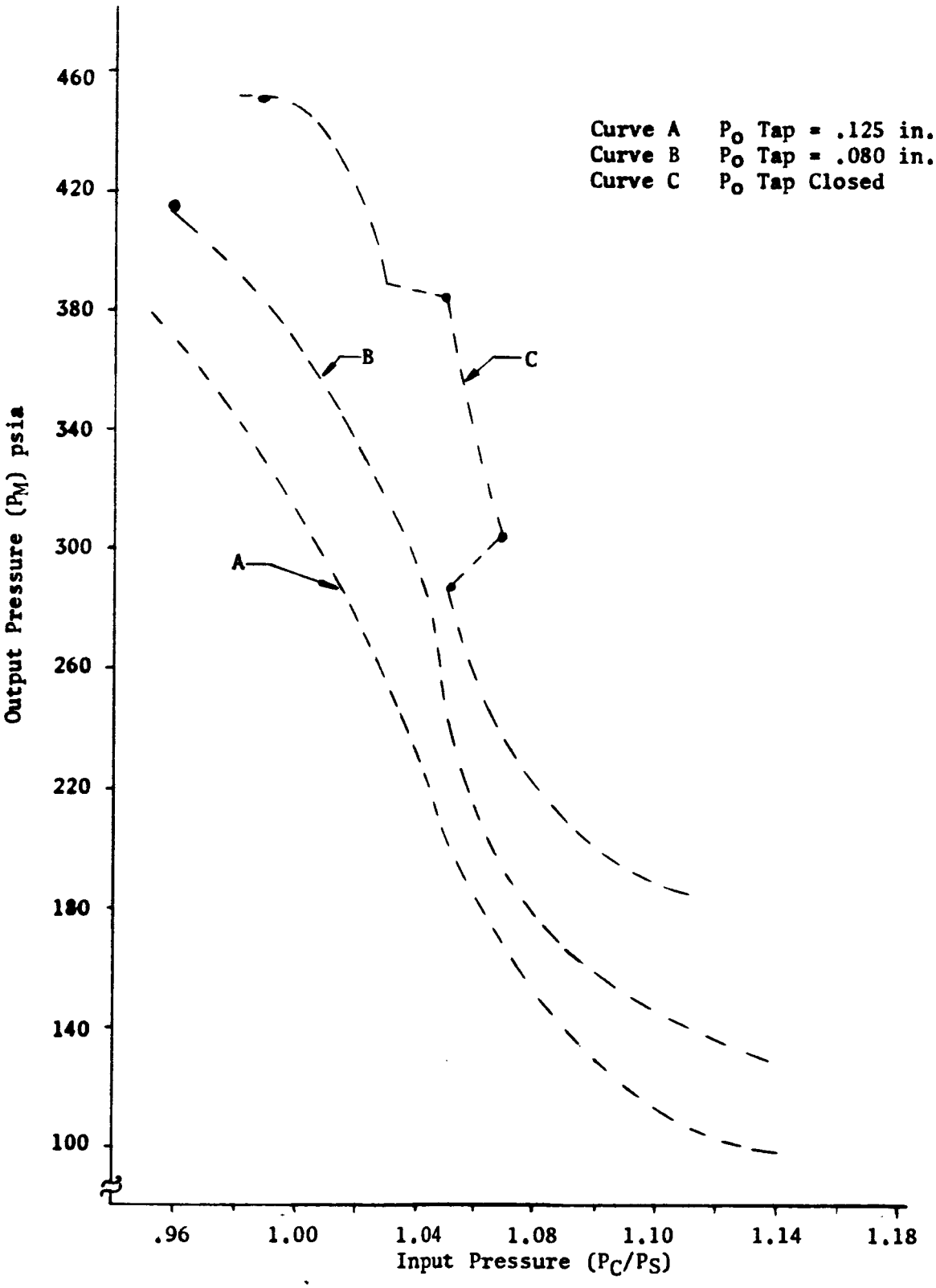

FIGURE 3-8 SERVOVALVE PRESSURE CHARACTERISTIC

valve P from .125 inch diameter to .080 inch increased the minimum load pressure, the range was not affected. It was decided, therefore, to use the smaller vent area in order to reduce the magnitude of the vented flow. If the vent area is reduced to zero, an unstable interaction occurs. The final dimensions of valve P are then as follows:

Chamber Depth	0.100 inch
Supply Port Width	0.250 inch
Exhaust Port Diameter	0.080 inch
P_O Tap Diameter	0.110 inch
Control Port Width	0.020 inch
Chamber Diameter	1.000 inch

Figure 3-9 shows the performance of the complete servovalve. The output motor pressure is plotted versus the ratio P_{CF}/P_{SF}.

With this type of servovalve, the quiescent pressure point, where both load pressures are equal, can be adjusted to suit the requirements of the load. This is an added advantage of this type of four-way bridge servovalve. Adjustment of the quiescent pressure point is made by changing the relative levels of the control pressures as shown in Figure 3-9.

The selection of the servovalve supply pressure was arbitrary. Initial analysis of the complete servovalve and amplifier indicated a potential supply pressure at the valve of 630 psia. Subsequent testing has shown that this value is feasible. For initial evaluation, the lower supply pressure was used.

Figure 3-9 shows that the maximum load pressure obtained is 79% of the valve supply pressure, with leakage flow simulated. This pressure level compares favorably with the performance obtained from a spool valve. The pressure gain of the servovalve (P_M/ P_C) is 3.5. Figure 3-10 is a photograph showing a partial assembly of one half the servovalve.

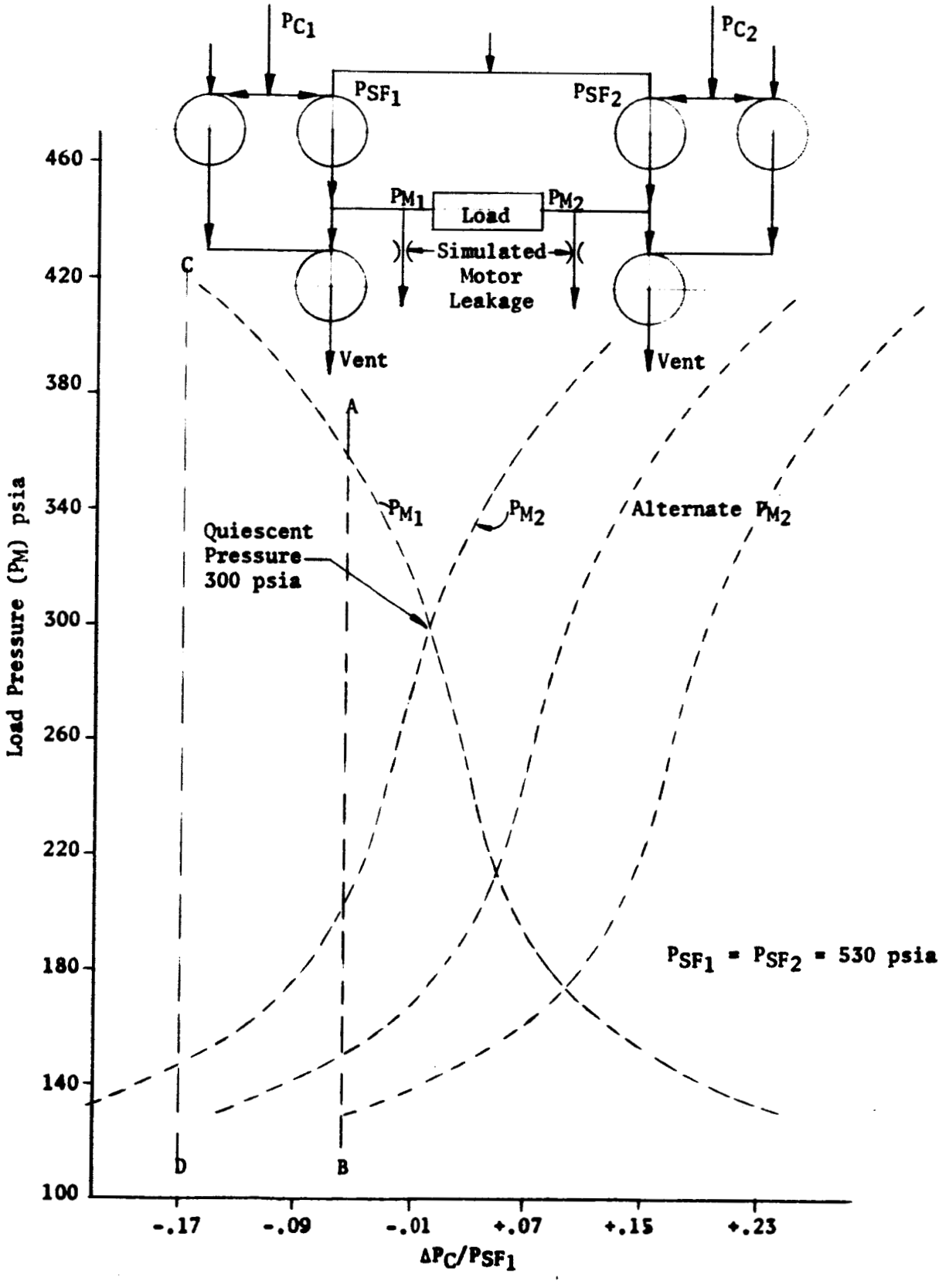

FIGURE 3-9 DIFFERENTIAL MOTOR PRESSURE VERSUS SERVOVALVE INPUT SIGNAL

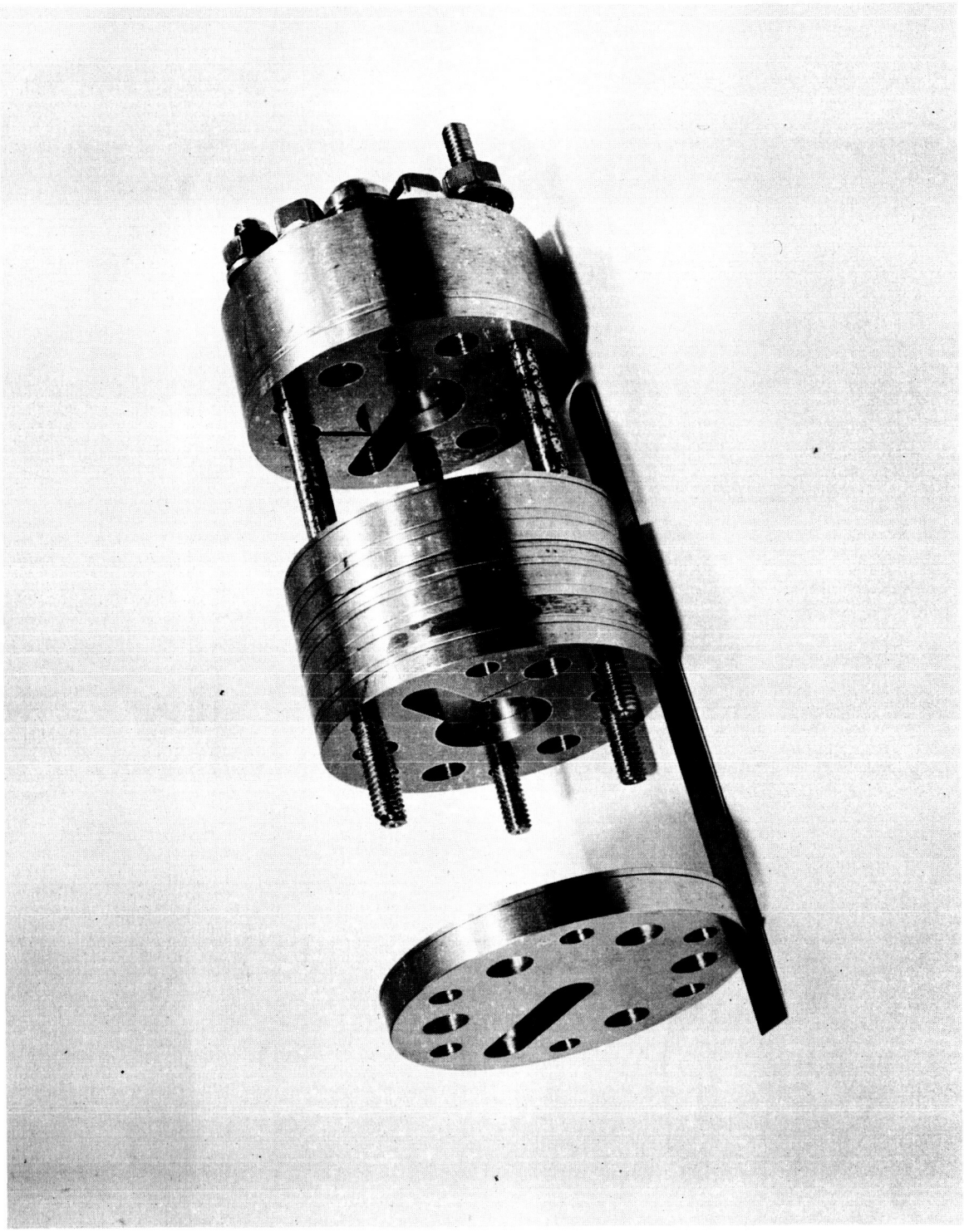

FIGURE 3-10 SERVOVALVE - PARTIAL ASSEMBLY

3.2 AMPLIFIER

Figure 3-11 is a schematic of part of the J-2 amplifier showing a three-stage amplifier using series connected double exhaust vortex valves.

The complete circuitry of the amplifier is shown in Figure 3-12. The output of the torque motor pilot stage is fed into the first stage of the amplifier in push-pull fashion. The valves are supplied in parallel from a common manifold.

Figure 3-13 shows the design of the gain adjustment bleeds. The gain of two of the stages can be lowered by reducing the effective outlet area of the vortex valves. This gain adjustment makes it possible to reduce unbalances caused by manufacturing tolerances.

The matching of the last stage of the amplifier with the servovalve was approached as follows. From Figure 3-8, for a fully closed servovalve (P_M minimum), P_C/P_{SF} = 1.15, and P_C/P_{SF} = .97 (minimum) for an open servovalve (P_M maximum).

The following design points were used:

$$P_{SF} = 530 \text{ psia}$$
$$P_{SP} = 540 \text{ psia}$$

Assuming the supply pressure to the amplifier output stage (L) is P_{SL} = 630 psia and a 3 to 1 flow turndown on valve L, we can plot P_{EL}/P_{EL} maximum = P_{EL}/P_{SL} versus W_{EL}/W_{EL} maximum as shown in Figure 3-14. Impedance matching with the control ports of valves P and F of the servovalve can be calculated.

Assume that for maximum turndown on valves P and F a ratio of $P_{CF}/P_{SF} = P_{CP}/P_{SP}$ = 1.10 is required.

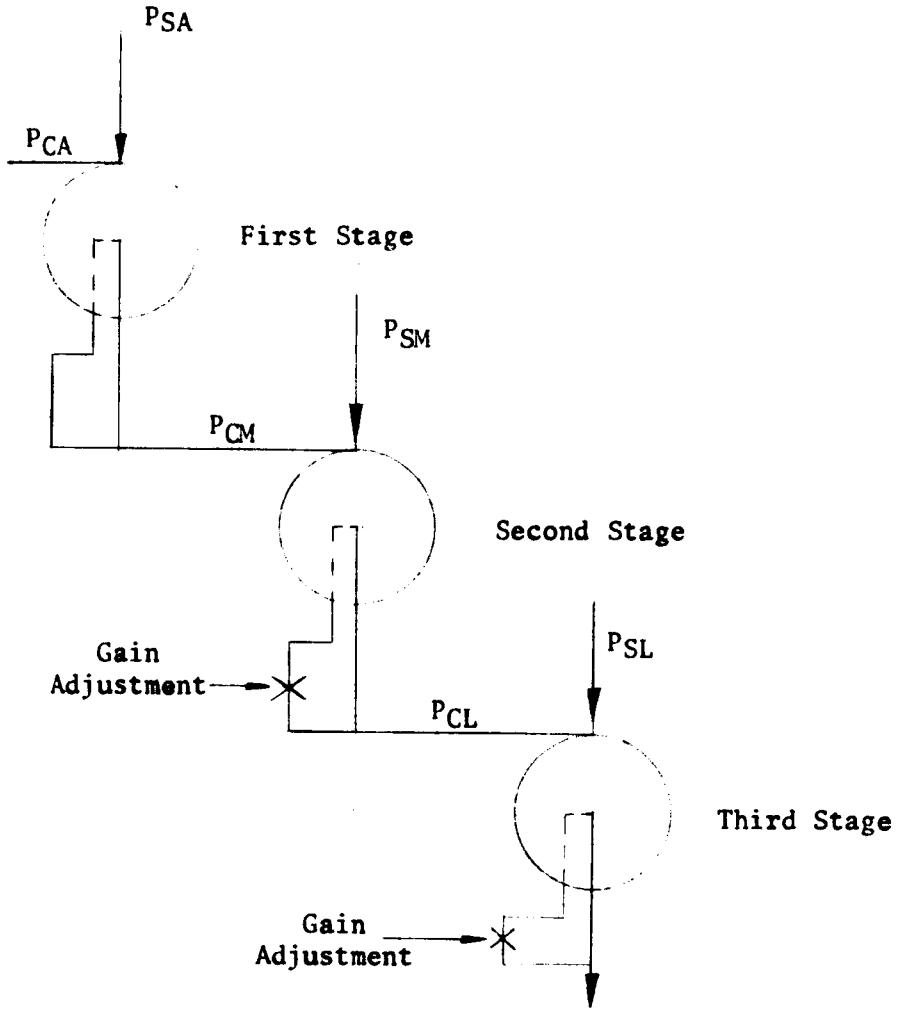

FIGURE 3-11 ONE SIDE OF AMPLIFIER SCHEMATIC

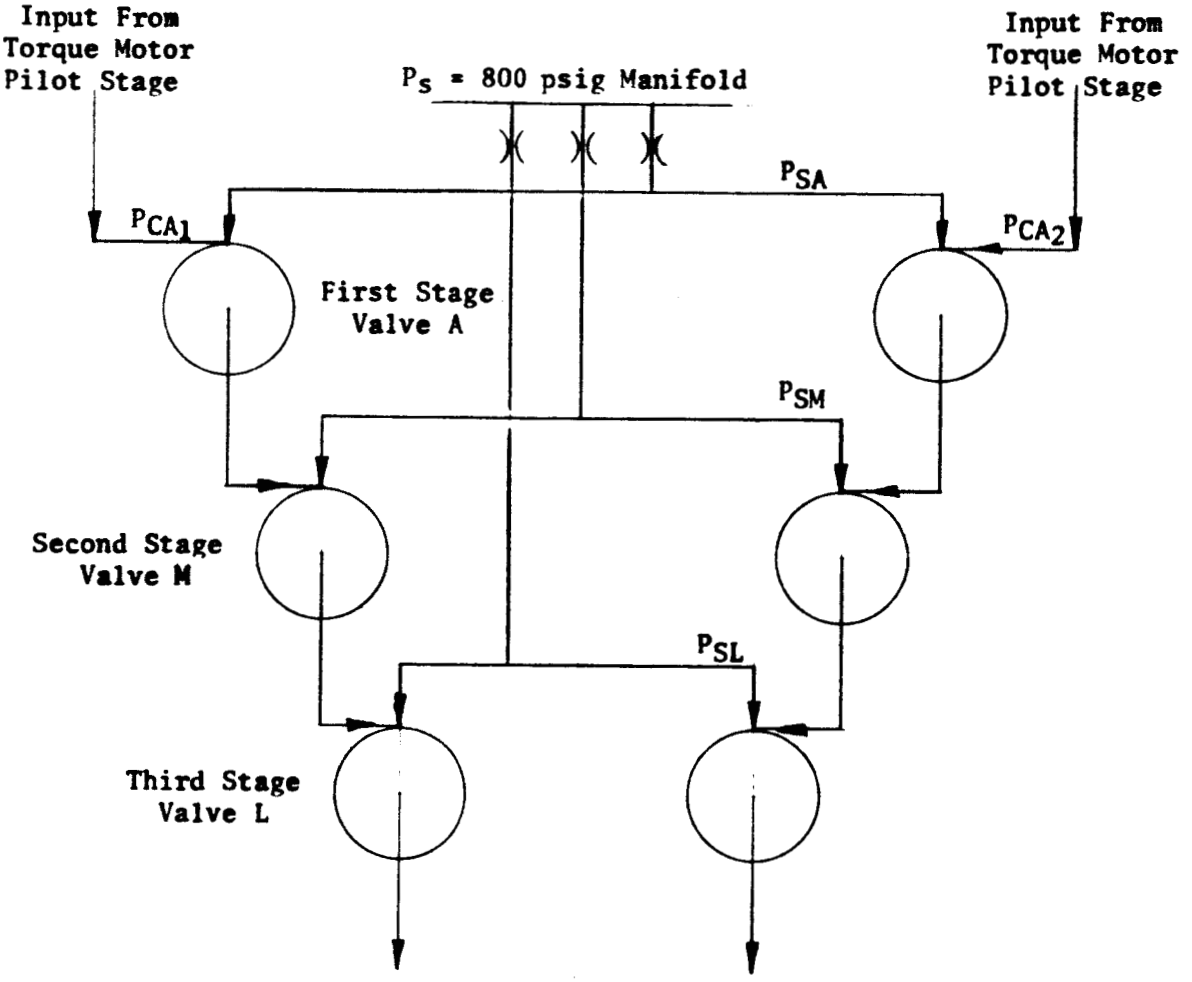

FIGURE 3-12 PUSH-PULL AMPLIFIER SCHEMATIC

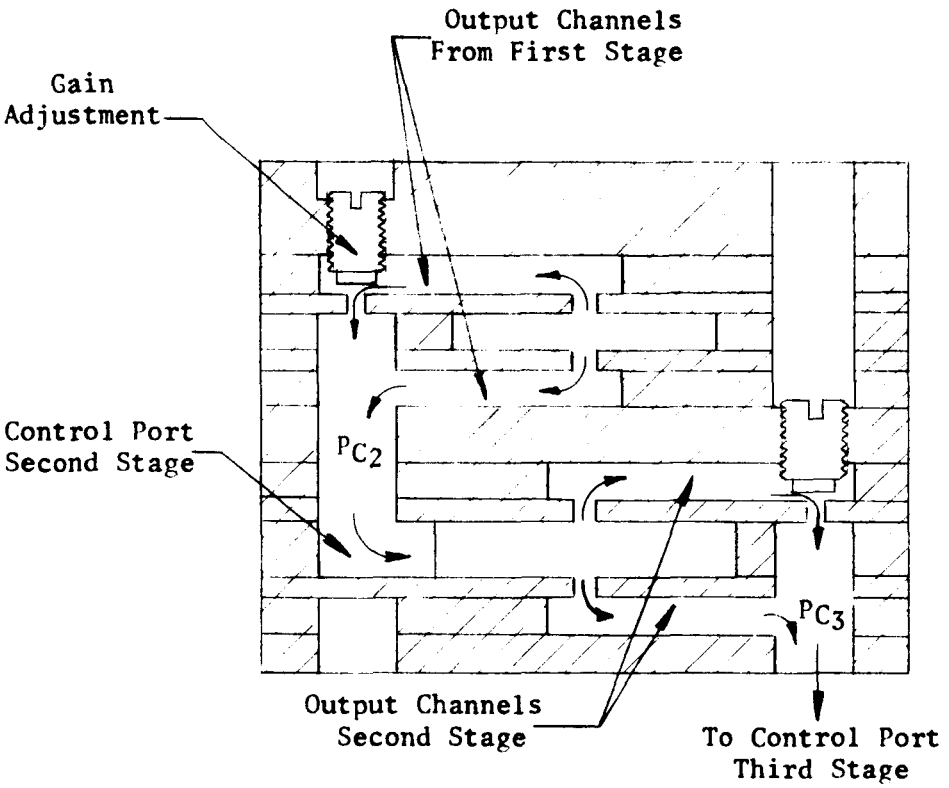

FIGURE 3-13 GAIN ADJUSTMENT OF AMPLIFIER STAGES

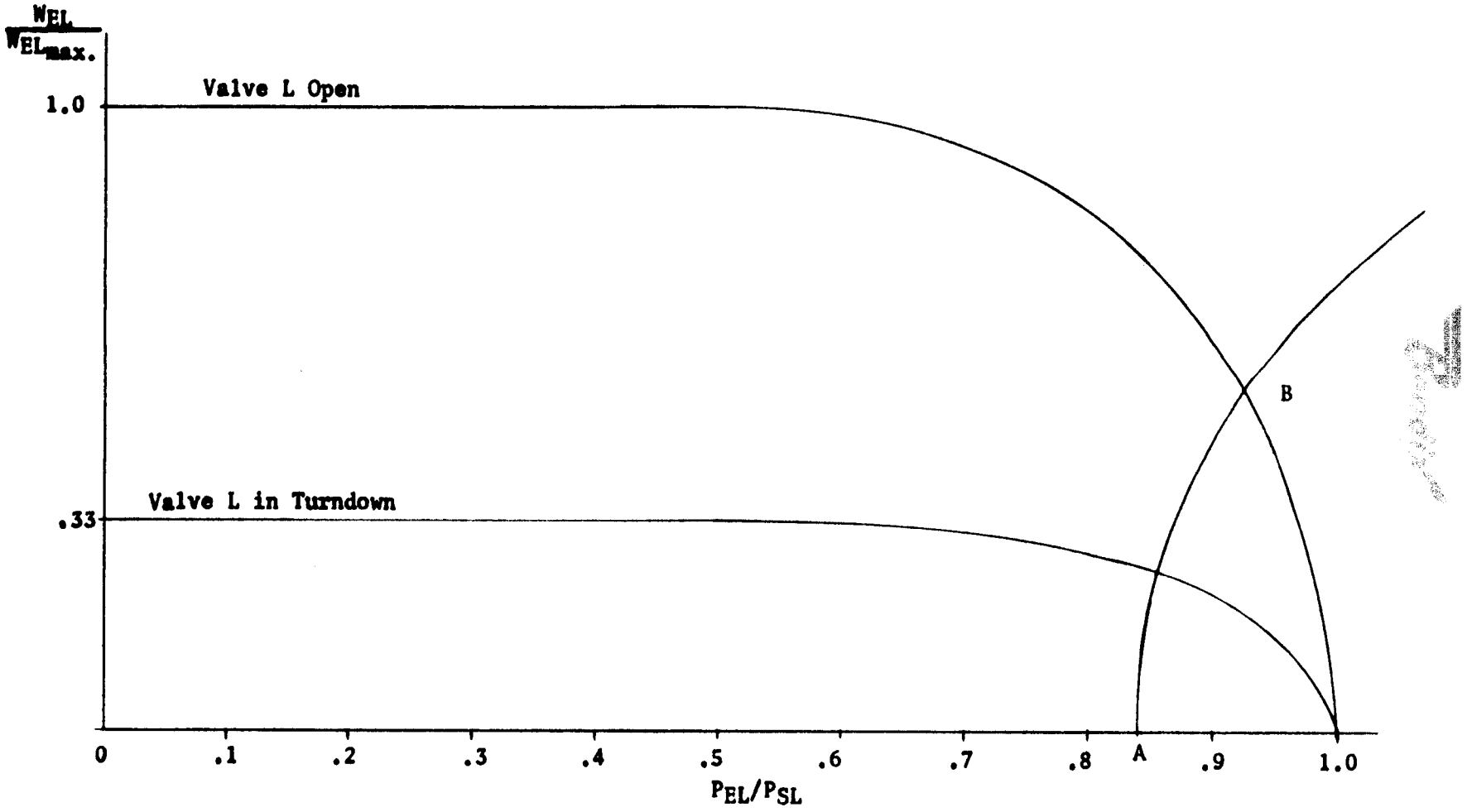

FIGURE 3-14 VALVE L LOAD CHARACTERISTIC

Assume: $P_{CF} = P_{CP} = P_C$

and $P_{SF} = P_{SP} = P_S = 530$ psia

$$\frac{P_S}{P_{SL}} = \frac{530}{630} = .841$$

At the point where $P_{SF} = P_{CP}$, no control flow is coming into valves P and F thus,

$$W_C = W_{EL} = 0$$

or $$\frac{W_{EL}}{W_{EL_{max.}}} = 0 \quad \text{(point A on Figure 3-14)}$$

For full turndown: $$\frac{P_C}{P_S} = 1.10$$

or $$\frac{P_C}{P_{SL}} = 1.10 \times .841 = .925$$

At $$\frac{P_{EL}}{P_{SL}} = .925$$

we find $$\frac{W_{EL}}{W_{EL_{max.}}} = .55 \quad \text{(point B on Figure 3-14)}$$

Points A and B are part of the line representing flow through the control ports of valves P and F. This line can now be completed using the subsonic flow equation. To establish the ratio of exit area of valve L to control port area of valves P and F, the equation of flow through the combined control port orifices is used.

$$W_C = W_{C_{max.}} \times P_C f_1\left(\frac{P_S}{P_C}\right) = .55\ P_{SL}\ W_{E_{max.}}$$

Where: P_C = 530 x 1.10 psia

P_{SL} = 630 psia

$$f_1\left(\frac{P_S}{P_C}\right) = f_1\left(\frac{.841}{.925}\right) = .59$$

$$W_{E_{max.}} = .99\ W_{C_{max.}}$$

Since for sonic flow conditions,

$$W_{E_{max.}} = K\ A_{EL}$$

$$W_{C_{max.}} = K\ A_C$$

Where: A_{EL} = area of exit of valve L

A_C = sum of areas of control ports of valves P and F

Then, $A_{EL} = .99\ A_C \neq A_C$

$$A_C = L_F C_F + T_P C_P = .006 \text{ in.}^2 = A_{EL}$$

Figure 3-15 indicates the output load pressure versus input pressure ratio P_{CL}/P_{SL} of the last stage of the amplifier. The test setup is shown in Figure 3-16.

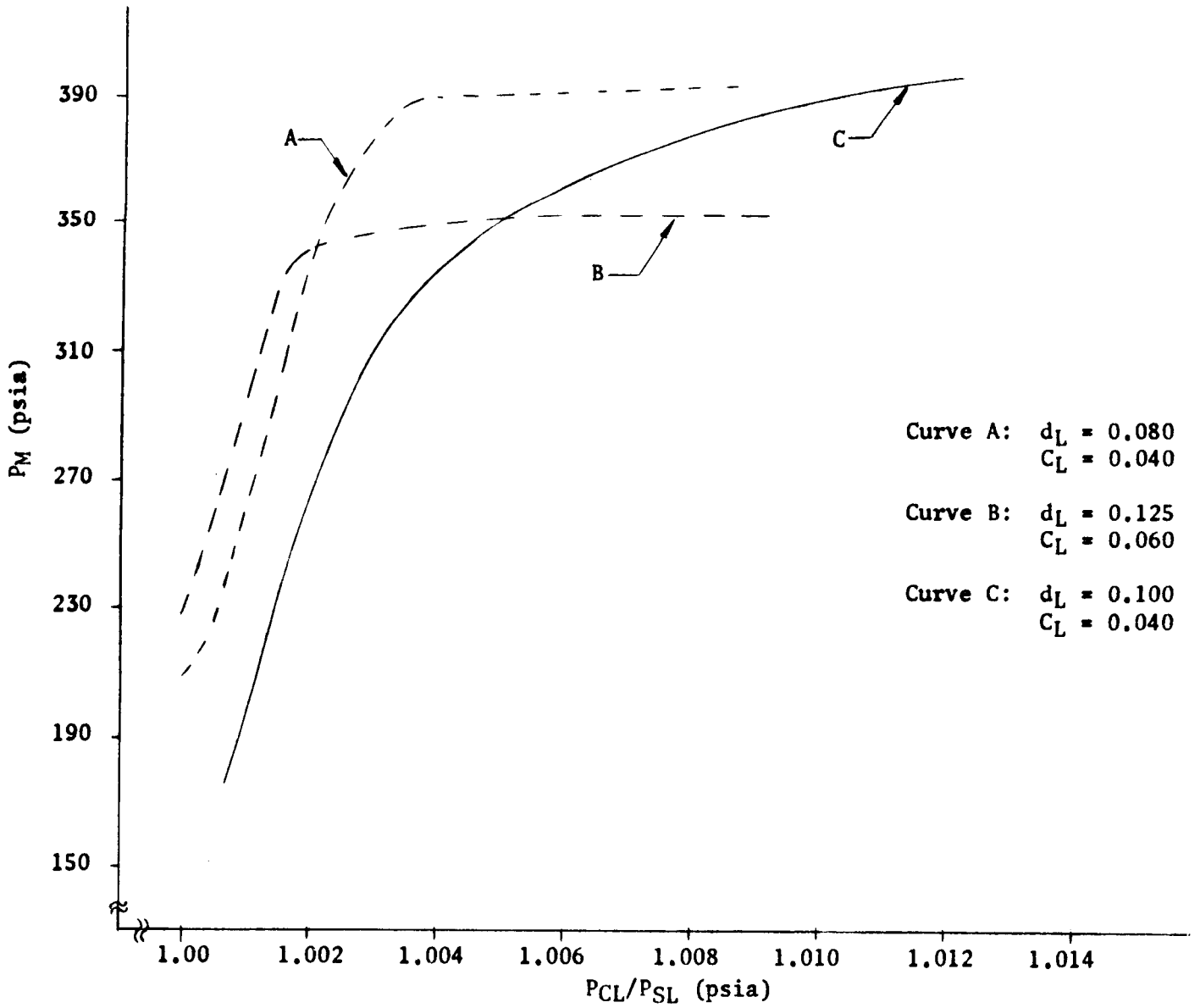

FIGURE 3-15 OUTPUT MOTOR PRESSURE VERSUS INPUT TO LAST STAGE OF AMPLIFIER

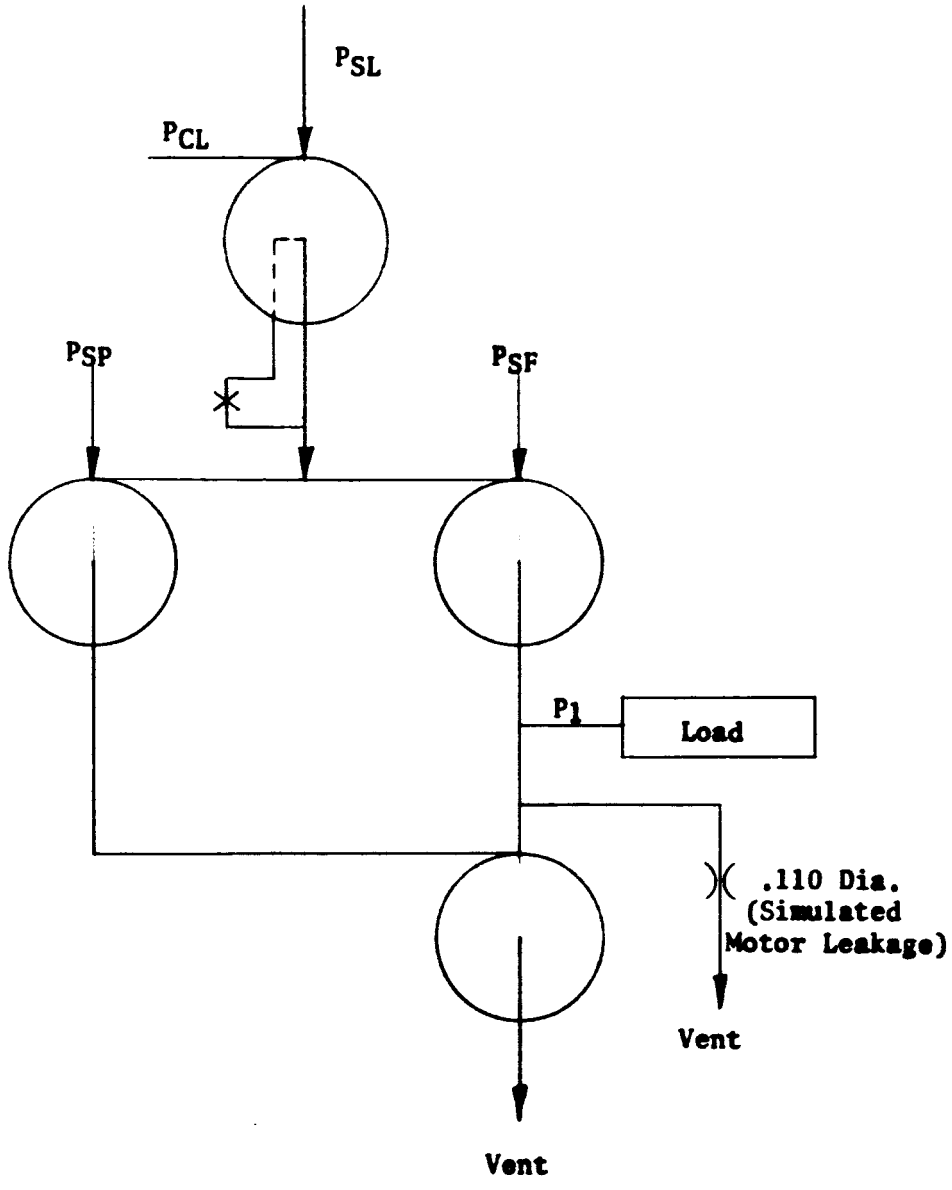

FIGURE 3-16 TEST CIRCUITRY

Curve A shows the test results of the combination of the servovalve and a valve L of the following dimensions:

d_L	=	Exit Diameter	.080 inch
D_L	=	Chamber Diameter	1.000 inch
L_L	=	Chamber Thickness	.100 inch
C_L	=	Control Port Width	.040 inch

Curve B shows test results when

d_L = .125 inch

and, C_L = .060 inch

Curve C shows the results obtained when

d_L = 0.100 inch

and, C_L = 0.040 inch

The configuration of curve C gives the largest range in load pressure differential although a lower stage gain results.

Figure 3-17 indicates the difference in performance of the two sides of the push-pull circuit.

A similar analytical procedure to that described above can be used to size the remaining stages of the amplifier. The sizes of the amplifier stages are summarized as follows:

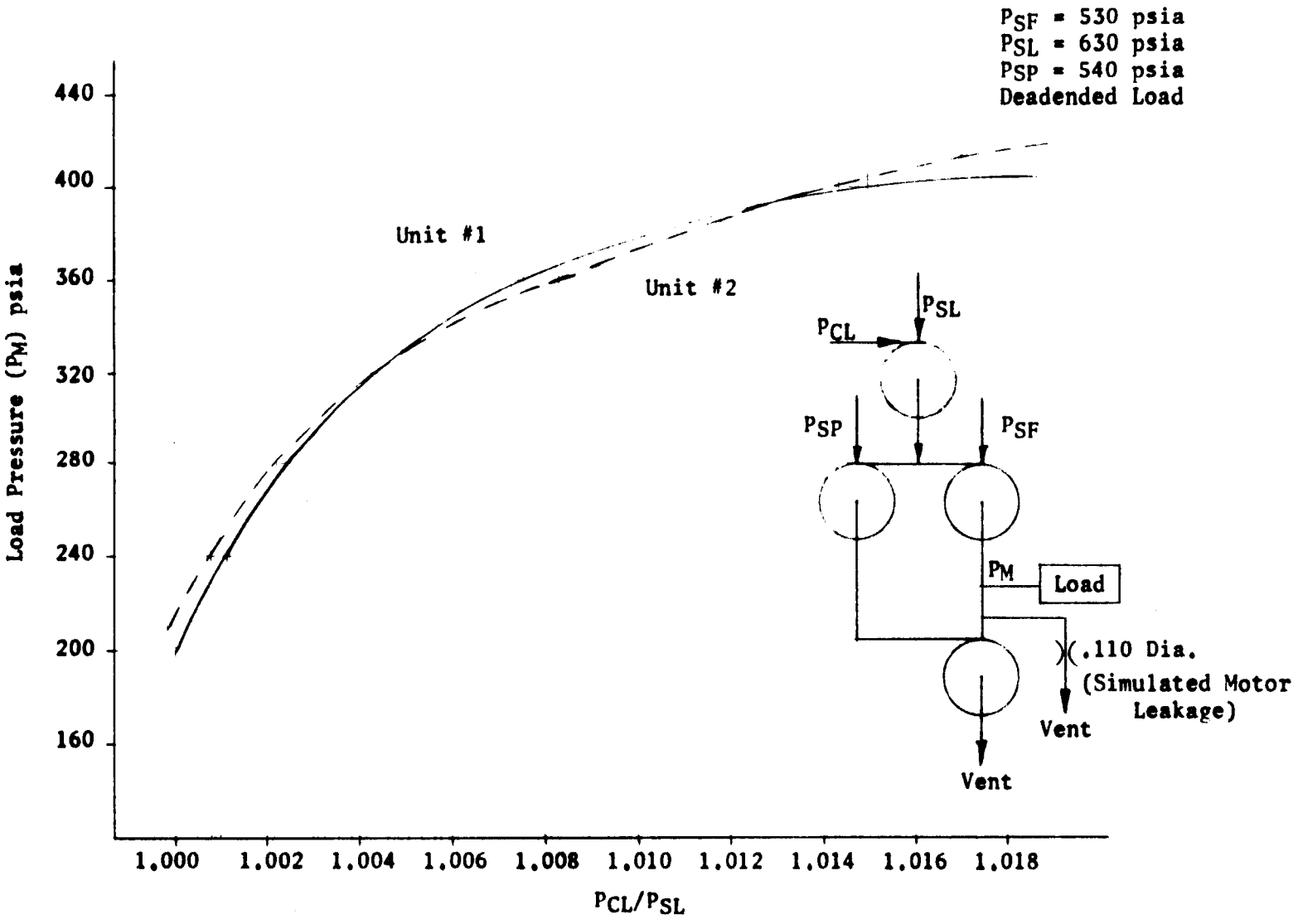

FIGURE 3-17 MATCHING OF PUSH-PULL SERVOVALVE

	Valve A (1st Stage)	Valve M (2nd Stage)	Valve L (3rd Stage)
Exit Port Diameter	0.048	0.065	0.088
P_o Tap Diameter	0.032	0.048	0.065
Chamber Diameter	0.400	0.510	0.710
Control Port Width	0.030	0.030	0.040
Supply Port Width	0.140	0.180	0.250
Chamber Depth	0.048	0.080	0.100

All three amplifier stages are double exhaust type (P_o tap plus exit) with gain adjustment in the P_o tap line of the second and third stages.

The complete amplifier and servovalve is shown schematically in Figure 3-18. The pressure level requirements of the various supply and control ports are indicated. The calibration of the system is shown in Figure 3-19. A gain of 1380 psi/psi was obtained for the amplifier-servovalve combination. Operation of the amplifier is stable and relatively noise-free. The control pressure level at the input is 670 psig giving a pressure drop across the complete amplifier of only 140 psi or 21%. The pressure drop is extremely low for the amplification obtained.

Figure 3-20 is a similar calibration of the amplifier-servovalve combination at one half the source pressure (i.e., 400 psig). Although the gain is slightly reduced (1200 psi/psi), the amplifier performance is not materially affected by the source pressure level.

The output flow versus load pressure characteristic is shown in Figure 3-21. Maximum flow recovery is .124 lb./sec. or 40% of the total supply flow of .308 lb./sec. The control flow, calculated from orifice pressure drop measurement, is .00035 lb./sec. The flow gain is then 354.

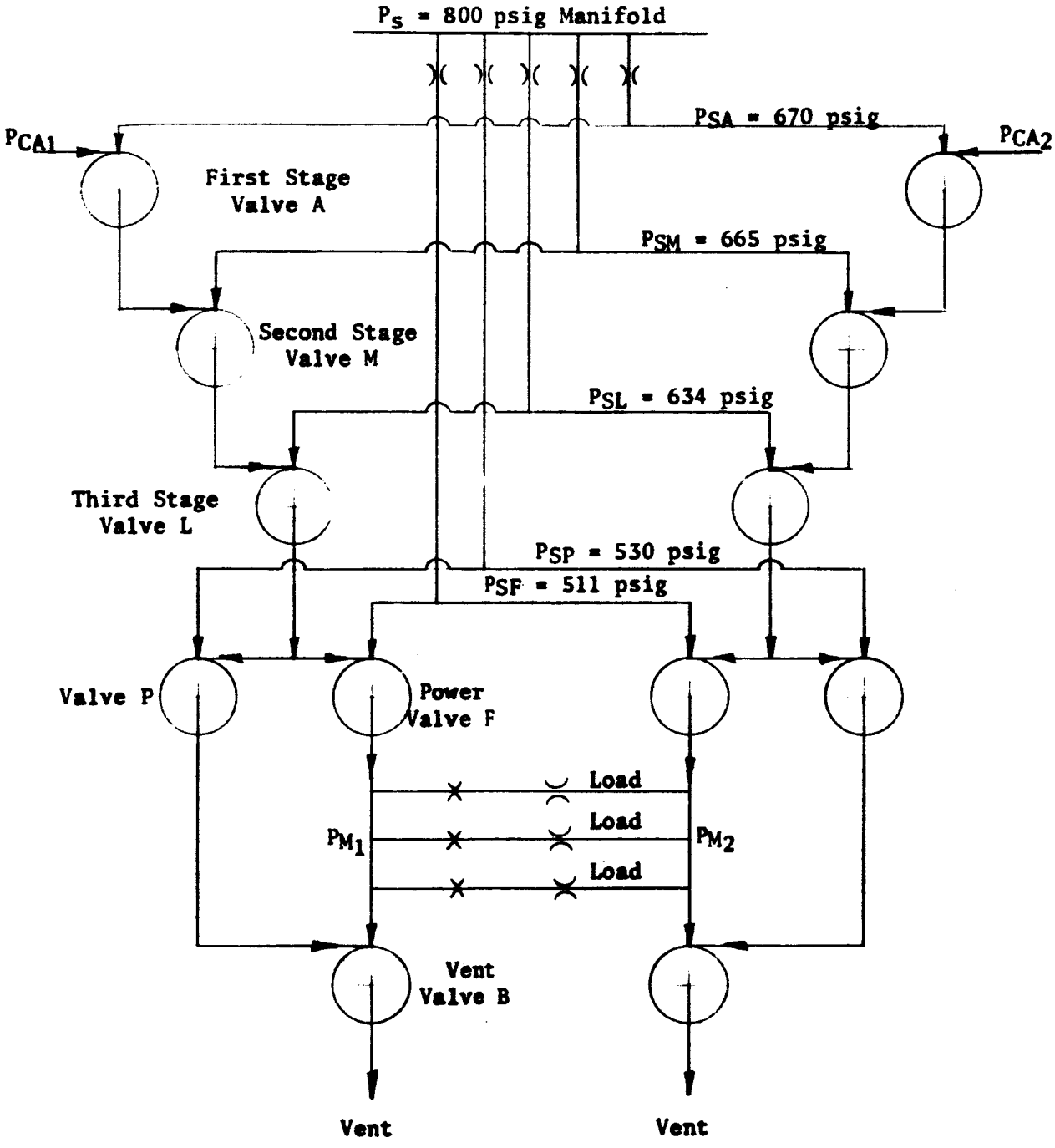

FIGURE 3-18 AMPLIFIER AND SERVOVALVE PRESSURE LEVELS

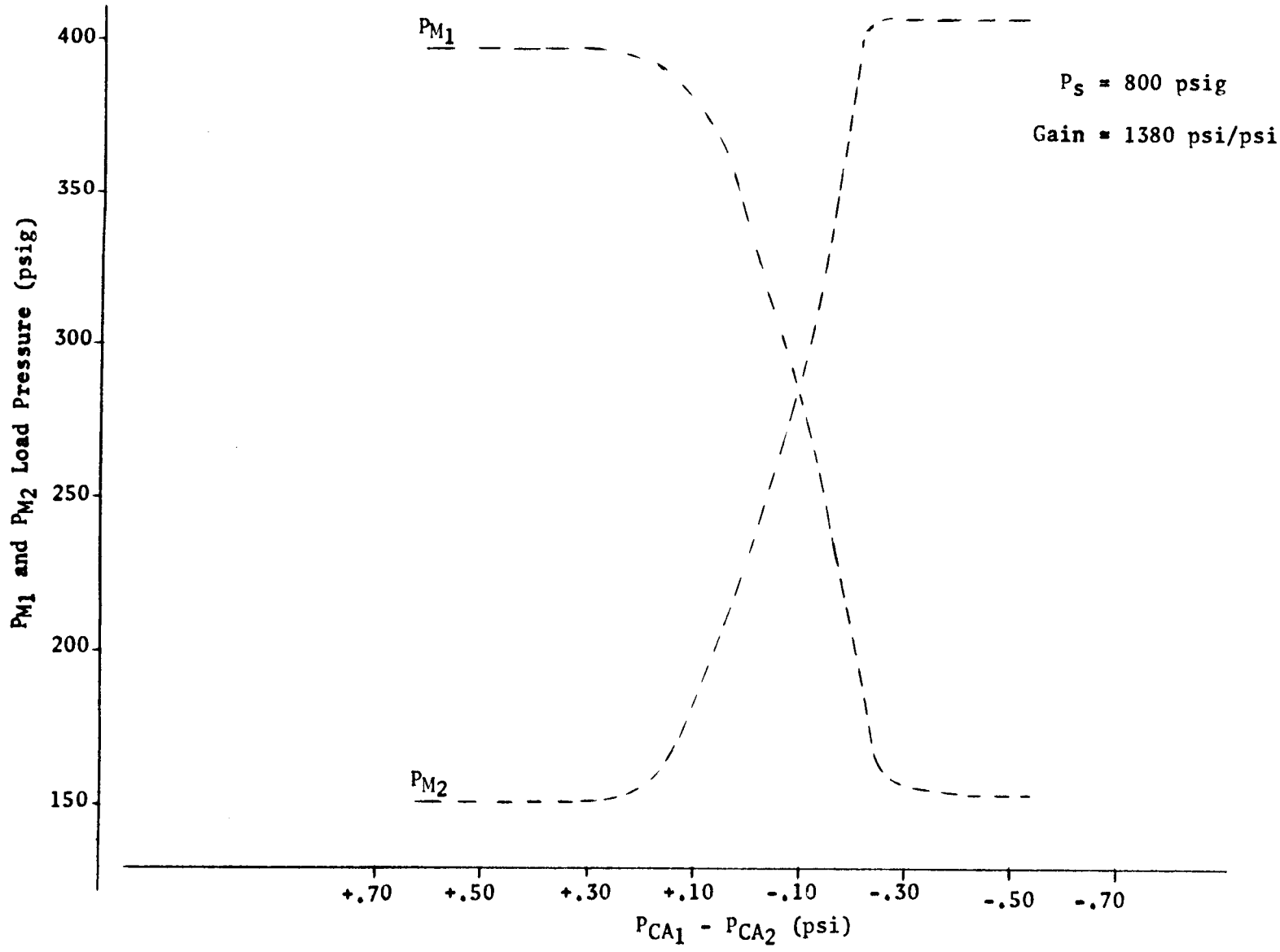

FIGURE 3-19 SERVOVALVE OUTPUT PRESSURE VERSUS AMPLIFIER INPUT PRESSURE AT 800 PSI

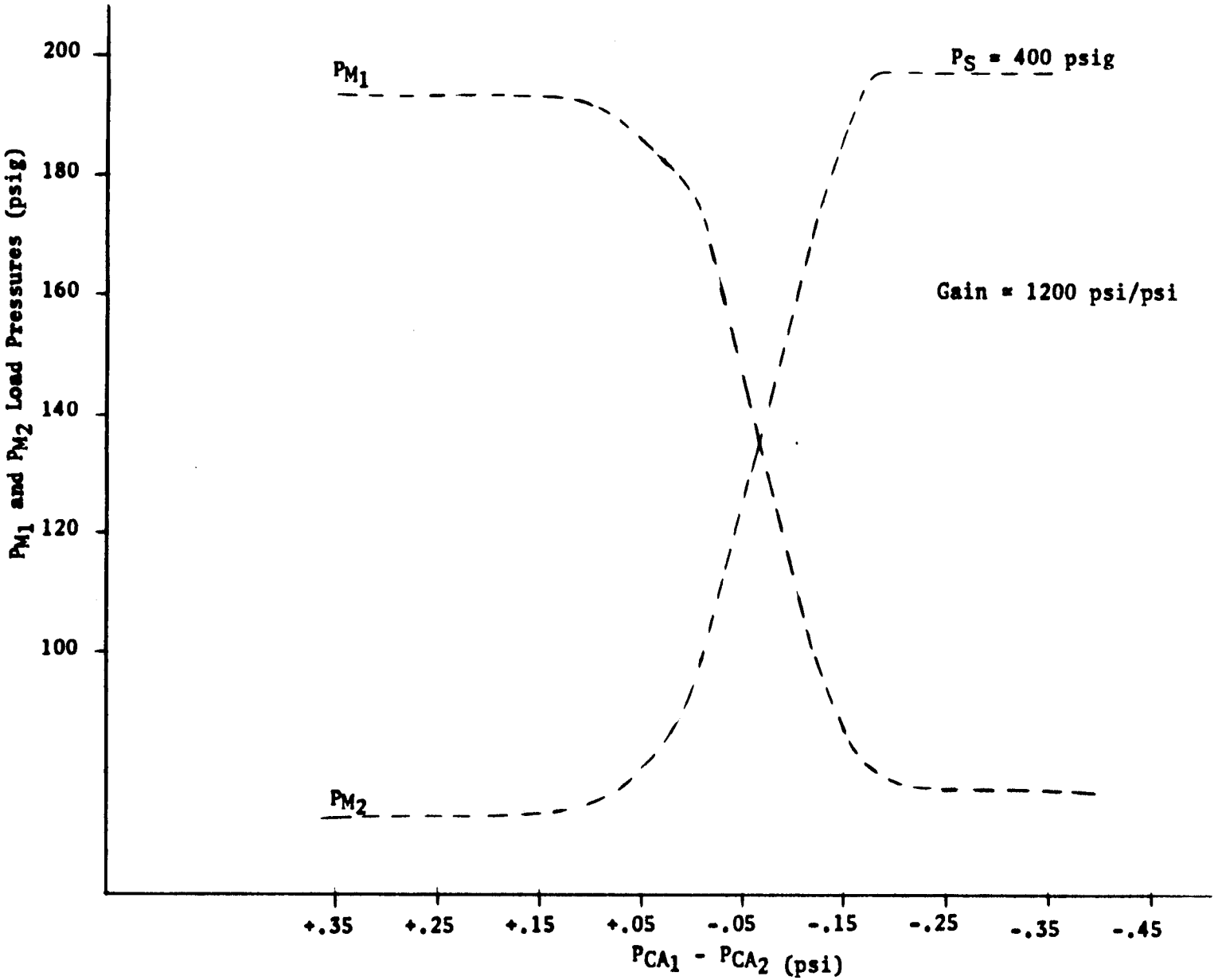

FIGURE 3-20 SERVOVALVE OUTPUT PRESSURE VERSUS AMPLIFIER INPUT PRESSURE AT 400 PSI

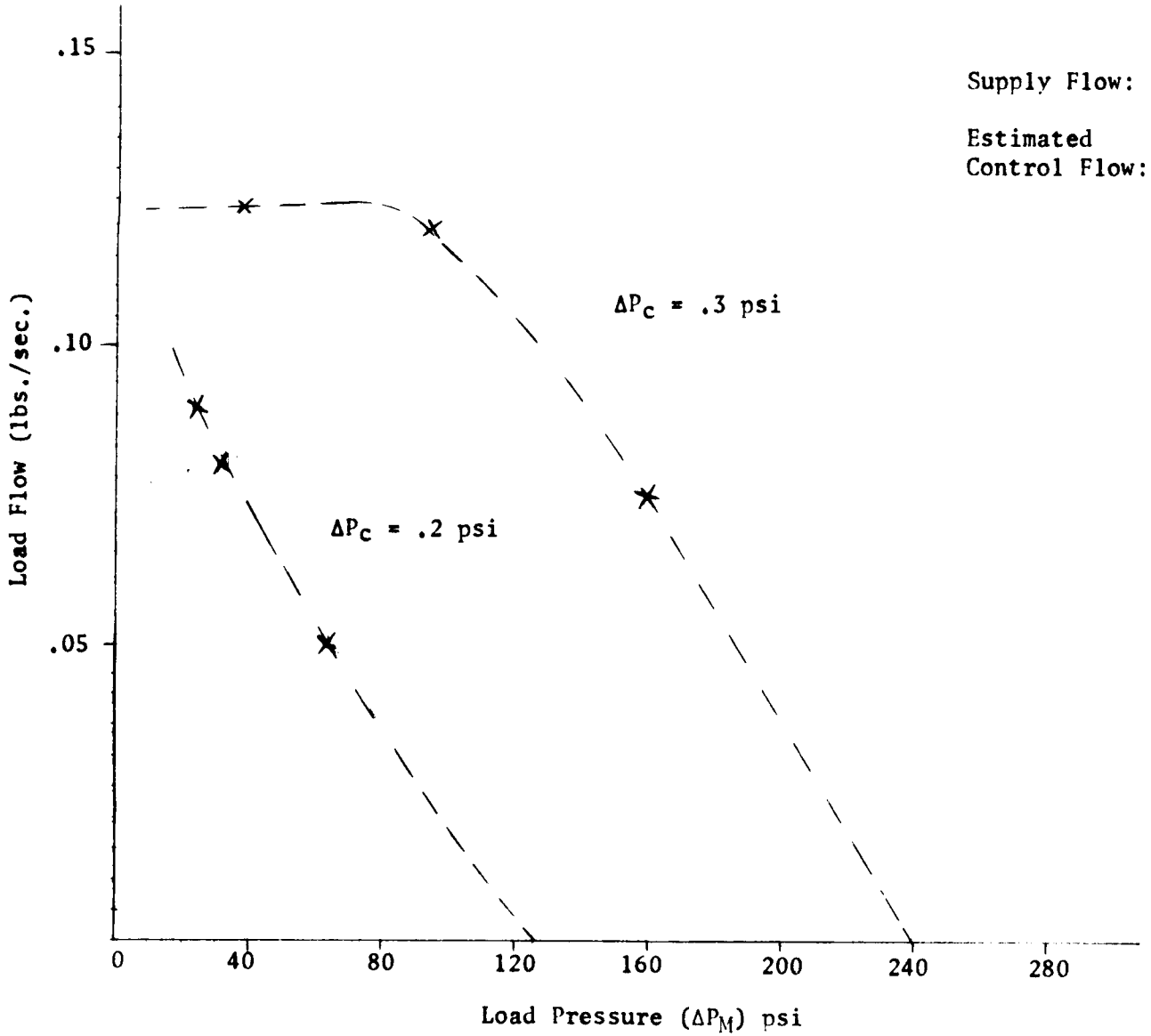

FIGURE 3-21 LOAD FLOW CHARACTERISTIC

3.3 INPUT TORQUE MOTOR STAGE

In order to provide a method of operating the amplifier and servovalve, it was decided to use a presently available torque motor. The torque motor for the J-2 gimbal actuator was therefore adapted to drive the amplifier. There are two possible means of connecting the torque motor to the input stage of the amplifier. These methods are shown schematically in Figure 3-22. Figure 3-22(a) shows a single orifice system in which the control flow is metered directly by the torque motor flapper. This method allows the maximum pressure level at the control ports. However, the flow forces cause a regenerative action on the flapper and a bistable action is likely to result. This is particularly true with the present amplifier, which requires a control pressure of 670 psi. The pressure drop across the flapper would then be 130 psi resulting in high flow forces.

Figure 3-22(b) shows the torque motor orifices used as bleeds for upstream fixed supply orifices. Of the total flow through the supply orifice, the flow not dumped to vent by the flapper (or the feedback devices) is available for control. Since the flow through the torque motor orifices is reversed, the pressure forces are degenerative and reduce the gain of the torque motor stage. For initial evaluation of the system performance, the torque motor configuration of Figure 3-22(b) was used.

Since the pressure variation to the input stage of the amplifier is small compared to the drop across the torque motor supply orifice, the orifice sizes can be calculated by assuming a constant supply flow and dividing this flow between the torque motor vent and the input stage control port. The torque motor bleed orifice was selected to allow a reasonable stroke while minimizing the flow forces. This gives an upstream supply orifice of .012 inch diameter.

A study of the torque motor used as the command signal transducer for a pure fluid amplifier indicates requirements which are appreciably different from the requirements for operation of a spool valve. Since the flapper is operating between two fixed orifices and is not self-centering, a short stroke, high force torque motor is required as opposed

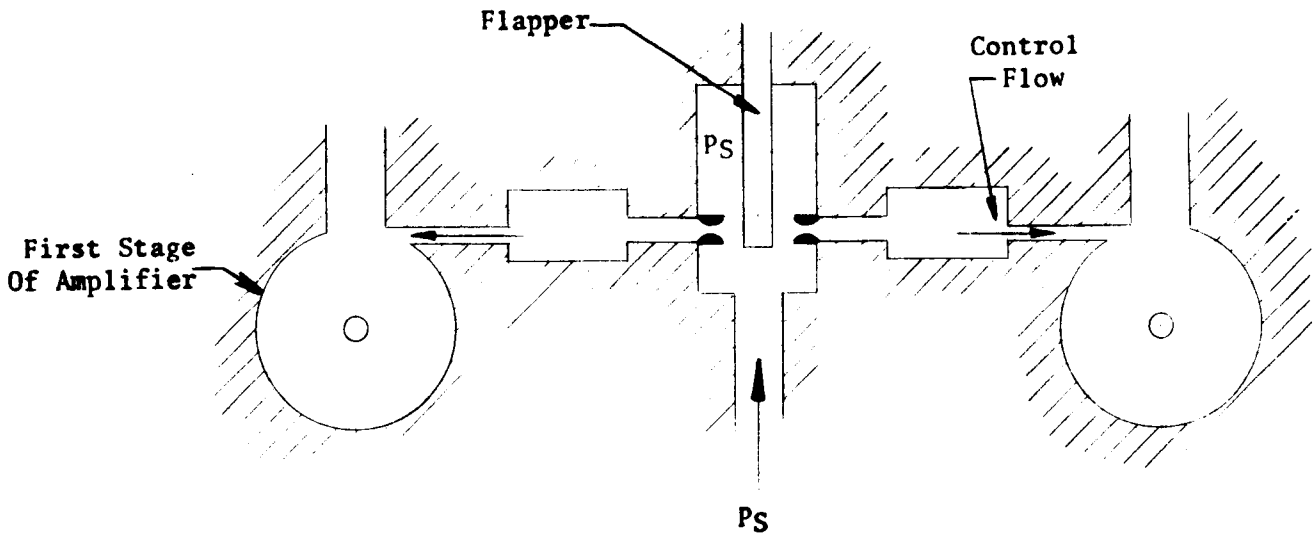

FIGURE 3-22(a) SCHEMATIC OF PILOT STAGE (FORWARD FLOW)

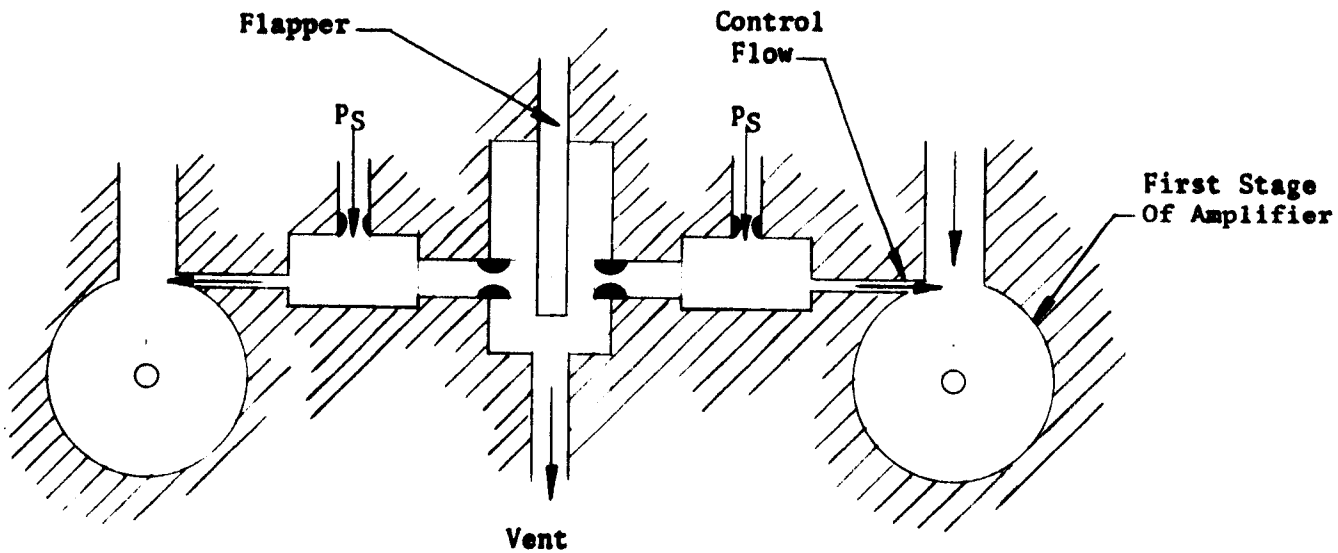

FIGURE 3-22(b) SCHEMATIC OF PILOT STAGE (REVERSE FLOW)

to the low force, long stroke required to move a spool valve. The stroke amplification of the torque tube and long flapper arm are therefore detrimental to the use of this torque motor in a pure fluid application. Suggested modifications to the input torque motor stage are discussed in more detail in Section 5.

3.4 RATE SENSOR

The method of operation of the rate sensor is described in Section 2.2.5 and shown schematically in Figure 2-10. Initial calibration of the speed transducer is shown in Figure 3-23. This figure indicates the effect of the bias level and direction in shifting the calibration. In the rate sensor, the bias is opposing the direction of rotation used for calibration. The output pressure (or flow) is then a straight line through the zero speed and is symmetrical for both directions of rotation.

A calibration of the complete rate sensor in conjunction with the amplifier-servovalve combination is given in Section 4.2.2.

The rate sensor was developed near the end of the contract period. At the time of manufacture of the sensor, the Pure Carbon Company Grade P-5-N bearing material, which is specified for this application, was not available. In order to obtain some performance data, a substitute (Morganite) carbon was used. This carbon is much softer than the specified material and the bearing life, particularly at 800 psi supply pressure, is not satisfactory. It is recommended that the correct carbon be used at the earliest opportunity. The radial grooves in the bearing thrust surface were found to be extremely helpful in prolonging bearing life. If the sensor torque requirement becomes excessive, the thrust bearing should be reground. A liberal coating of molybdenum disulphide (either powder or grease, but preferably powder) on all bearing surfaces will appreciably reduce the driving torque required.

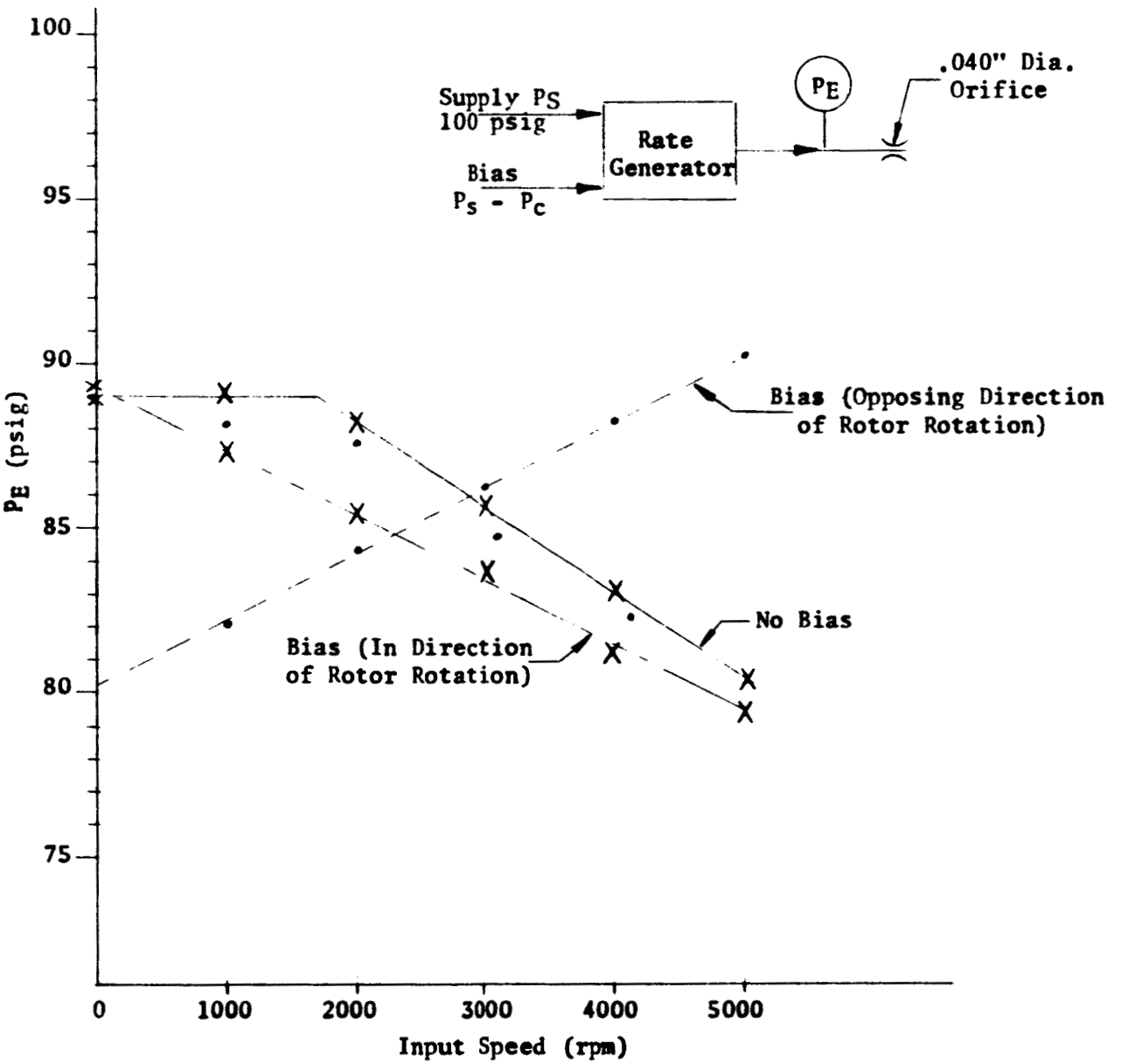

FIGURE 3-23 SPEED TRANSDUCER CALIBRATION

SECTION 4

SYSTEM ASSEMBLY AND TEST

4.1 ASSEMBLY PROCEDURE

The pure fluid amplifier is manufactured in a stacked steel plate construction. Each circular plate contains a vortex chamber, end plate or transfer slot. Each side of the amplifier and each side of the servovalve is assembled separately. Transfer blocks are provided at each end of the assembly and between the amplifier and servovalve assemblies. The complete assembly is shown in the photograph of Figure 4-1. The order in which the plates are stacked is shown in Bendix Drawing NPX-102-441. A light spray of "Krylon" lacquer on both sides of each plate will minimize plate leakage. The "Krylon" should be allowed to dry before assembly. On disassembly, the plates will tend to adhere together. They can be separated by soaking in any hydrocarbon solvent.

The torque motor is mounted on the top end of the first transfer block at the front of the amplifier section (see Figure 4-1). The gain adjustments are reached by removing the first transfer block and adjusting with a screwdriver. Three turns from the seated condition will provide maximum amplifier gain. All through bolts should be torqued to 200 inch-pounds.

The rate sensor assembly is shown in Bendix Drawing NPX-102-440. Before assembly, all surfaces of the carbon bearings should be liberally coated with molybdenum disulphide. The order in which the plates of the push-pull output circuit are stacked is shown in the above referenced drawing. The orientation of the plates is such that the grooved scribe mark on the edge of each plate forms a continuous line. These plates are lapped flat and do not require any spray coating. Bolt torque should not exceed 25 inch-pounds.

Care should be taken with all plates to avoid any scratches which result in a raised surface or provide a channel for inter-port leakage.

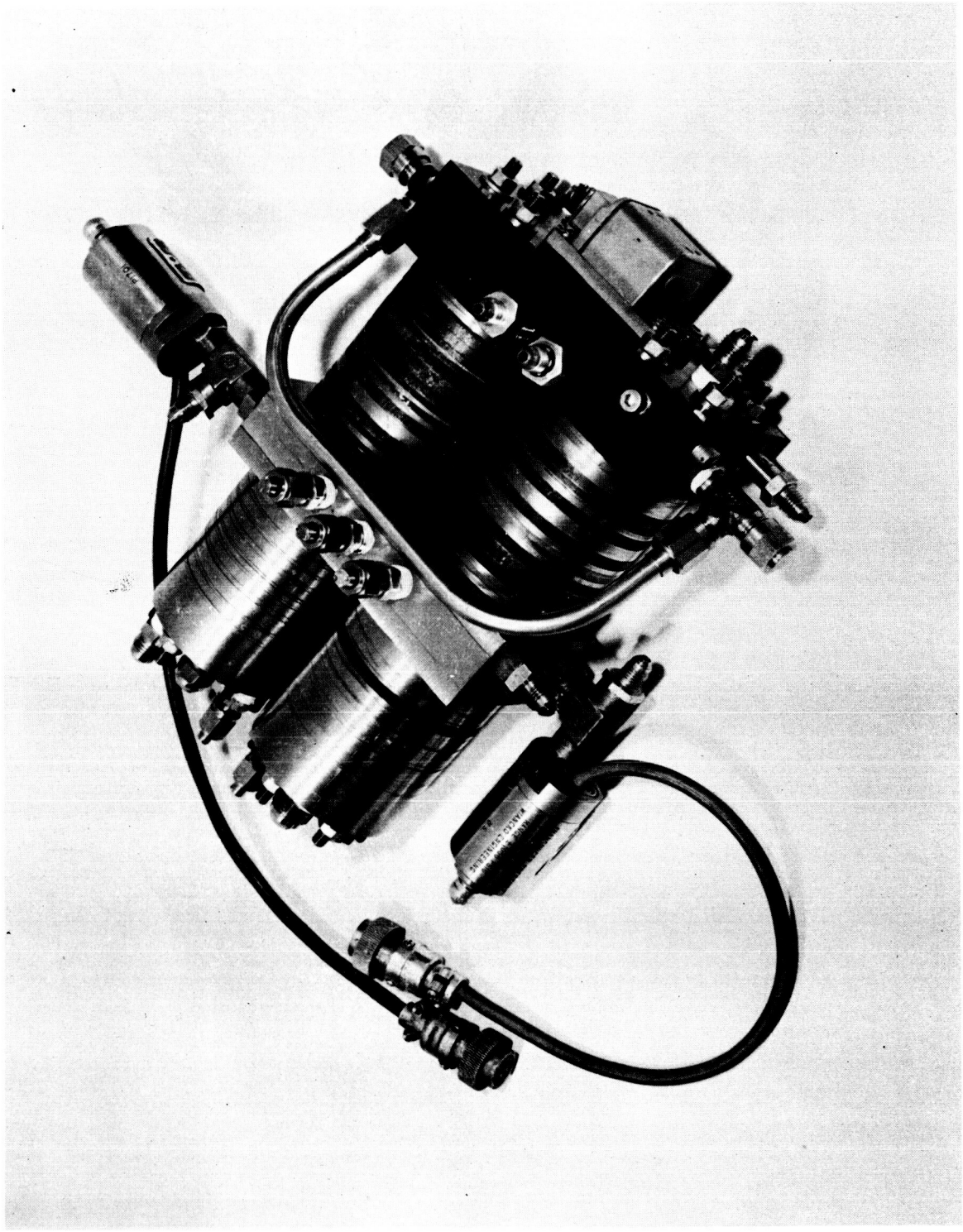

FIGURE 4-1 AMPLIFIER ASSEMBLY

A permanent seal between plates of both the amplifier and rate sensor can be obtained by silver bonding. Tests have shown that lapped surfaces, when plated with a .0005 inch thick layer of silver and heated for four hours under pressure in a 1000°F oven, will effect a leak-tight bond. The plates can be separated by reheating.

4.2 TEST PROCEDURE AND TEST RESULTS

4.2.1 Amplifier and Servovalve

The amplifier, servovalve, and rate sensor are shown in schematic assembly in Figure 4-2. The pressure taps in each transfer block of the amplifier and servovalve are indicated as well as the various fixed orifices. Except for the main supply ports (marked S) and the load output taps (P_{M_1} and P_{M_2}), all pressure taps should be deadended by means of plugs, gages or pressure transducers. The following pressures can be monitored:

$$P_{CA_1},\ P_{CA_2},\ P_{SA},\ P_{SM},\ P_{SL},\ P_{SP},\ P_{SF},\ P_{M_1},\ \text{and}\ P_{M_2}$$

The orifice diameters for the amplifier and servovalve are listed below in terms of standard drill sizes.

Amplifier

A_{SA} = #80 A_{SM} = #67 A_{SL} = #53

$A_{C_1} = A_{C_2}$ = #80 $A_{T_1} = A_{T_2}$ = #74

Servovalve

A_{SF} = #45 A_{SP} = #49

The clearance on the torque motor flapper is .0025 inch on each side.

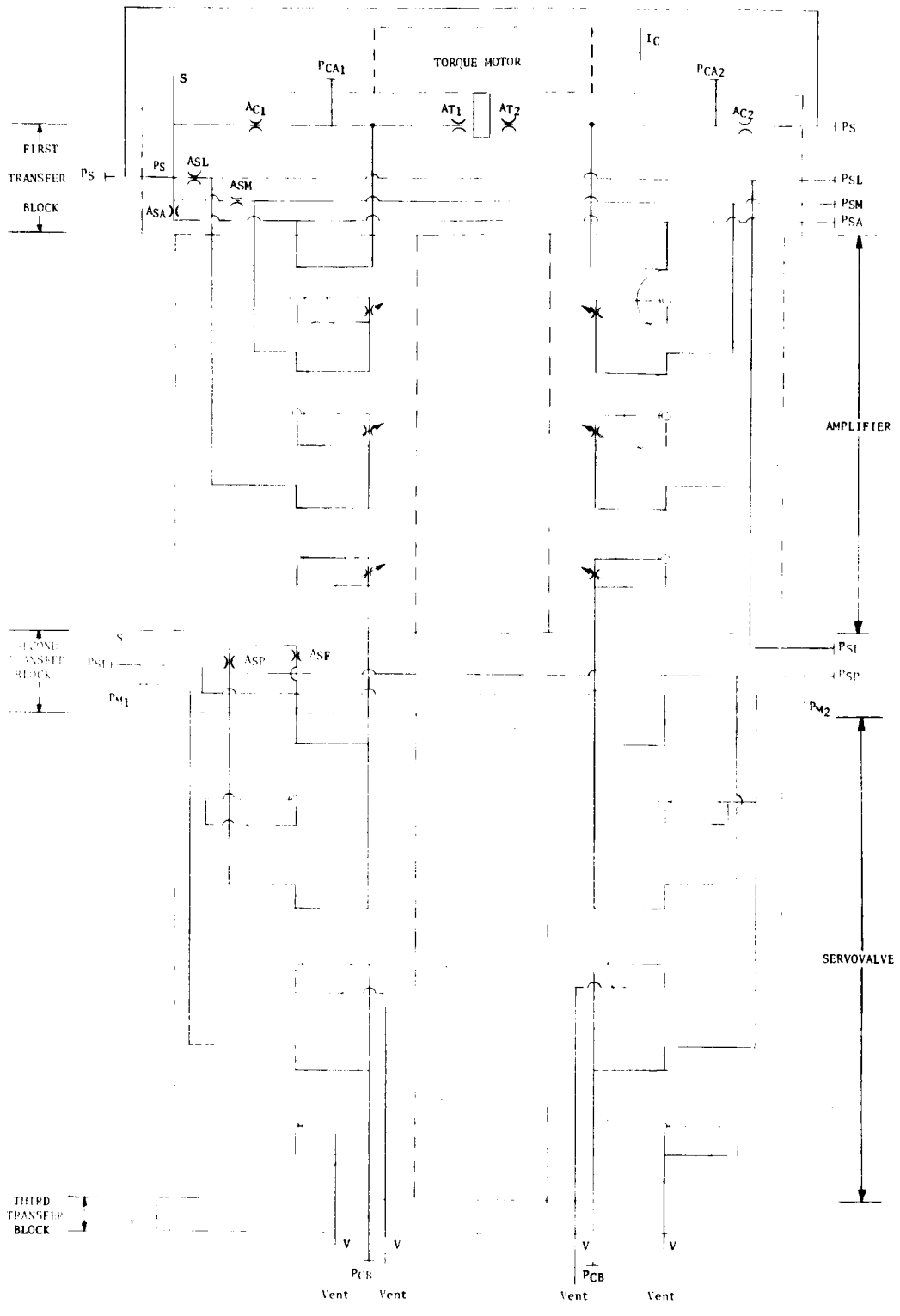

FIGURE 4-2(a) SYSTEM BLOCK LAYOUT

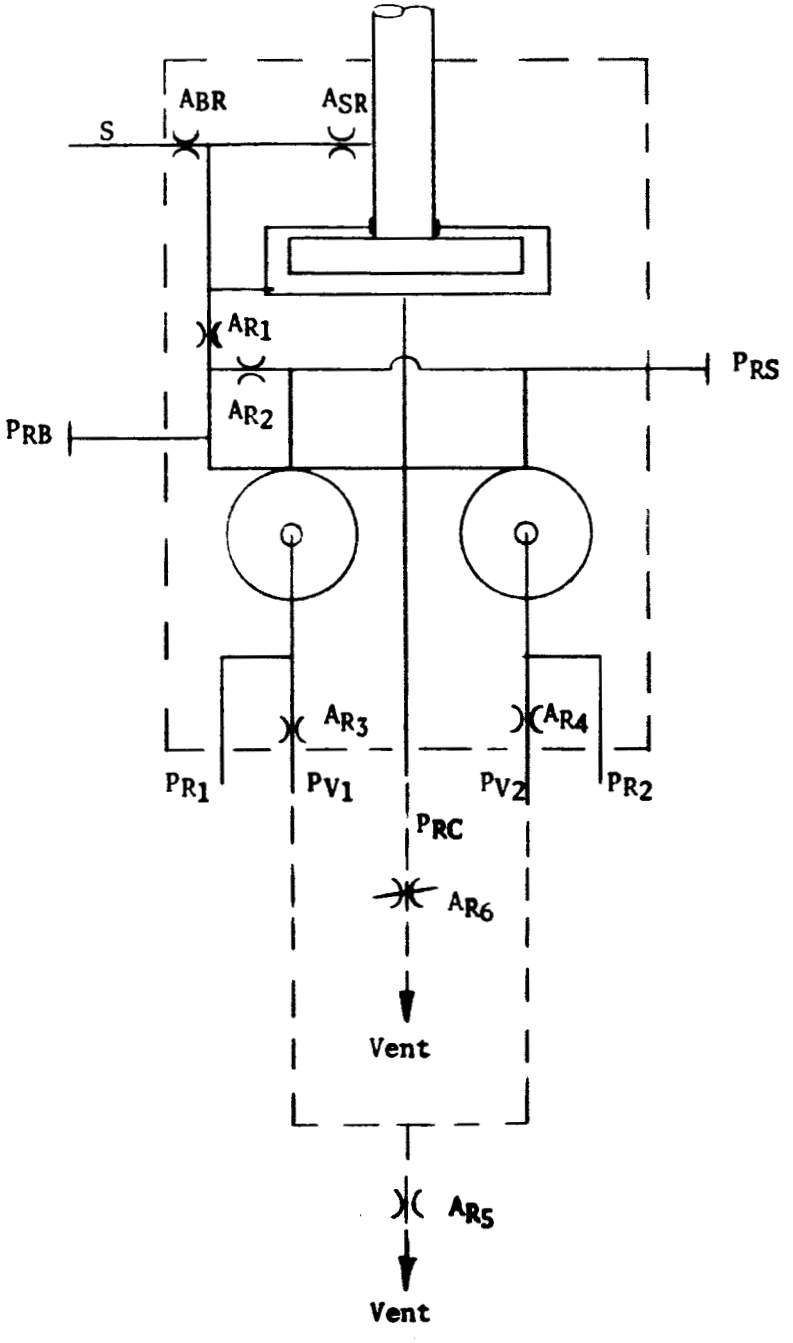

FIGURE 4-2(b) RATE SENSOR BLOCK LAYOUT

To operate the amplifier and servovalve, the connections marked S on both the first and second transfer plates are supplied from the regulated source pressure. The output load pressures (P_{M_1} and P_{M_2}) are attached across the desired load. The four vent connections in the third transfer plate should be opened to a minimum impedance. All other pressure taps must be deadended. The torque motor input can be supplied by a differential current amplifier and requires ±40 milliamperes and ±4000 millivolts.

For steady state calibration, a differential pressure gage calibrated in inches of kerosene was connected to measure $P_{CA_1} - P_{SA}$. A similar gage was connected across $P_{CA_2} - P_{SA}$. The deadended load pressures were measured with two 1000 psi gages. Torque motor differential current was measured across the output of the current amplifier. For transient analysis, the two input pressure differential gages were replaced by a single differential transducer measuring $P_{CA_2} - P_{CA_1}$. The load pressure gages were replaced by single ended pressure transducers.

The steady state calibration of the torque motor, amplifier and servovalve is shown in Figure 4-3. Approximately 15 milliamperes is required to saturate the servovalve output. No attempt was made at this time to null the torque motor. The low gain and large hysteresis of the torque motor stage demonstrates the unsuitability of this concept of electrical to pneumatic transducer.

Two transient response tests were performed using a sinusoidal differential current input. In the first test, the input current amplitude was maintained constant. In the second test, the input current amplitude was increased with increasing frequency in order to maintain a constant amplitude pressure differential into the first stage of the amplifier. The Bode plot shown in Figure 4-4 was derived from these test results. Figure 4-4(a) shows the amplitude ratios versus frequency of the system with and without the torque motor stage. Figure 4-4(b) is the corresponding phase shift between the input and output. Examination of the frequency response results indicates that the amplifier and servovalve appear to perform as a single order lag system with transportation delay. The break frequency appears to be approximately 3 cps. The addition of the torque motor stage adds a second single order lag to the system which breaks at approximately the same frequency.

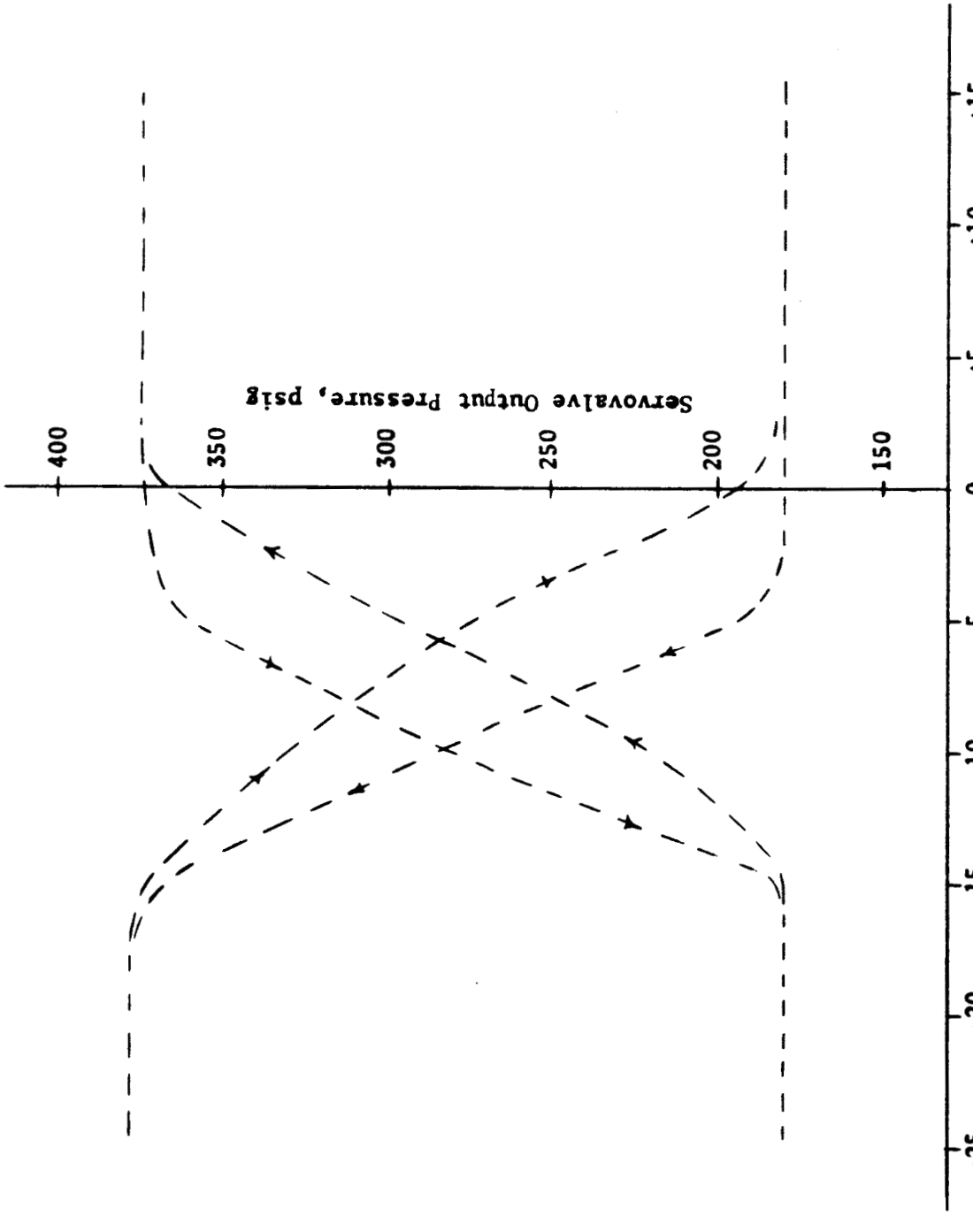

FIGURE 4-3 SYSTEM CALIBRATION

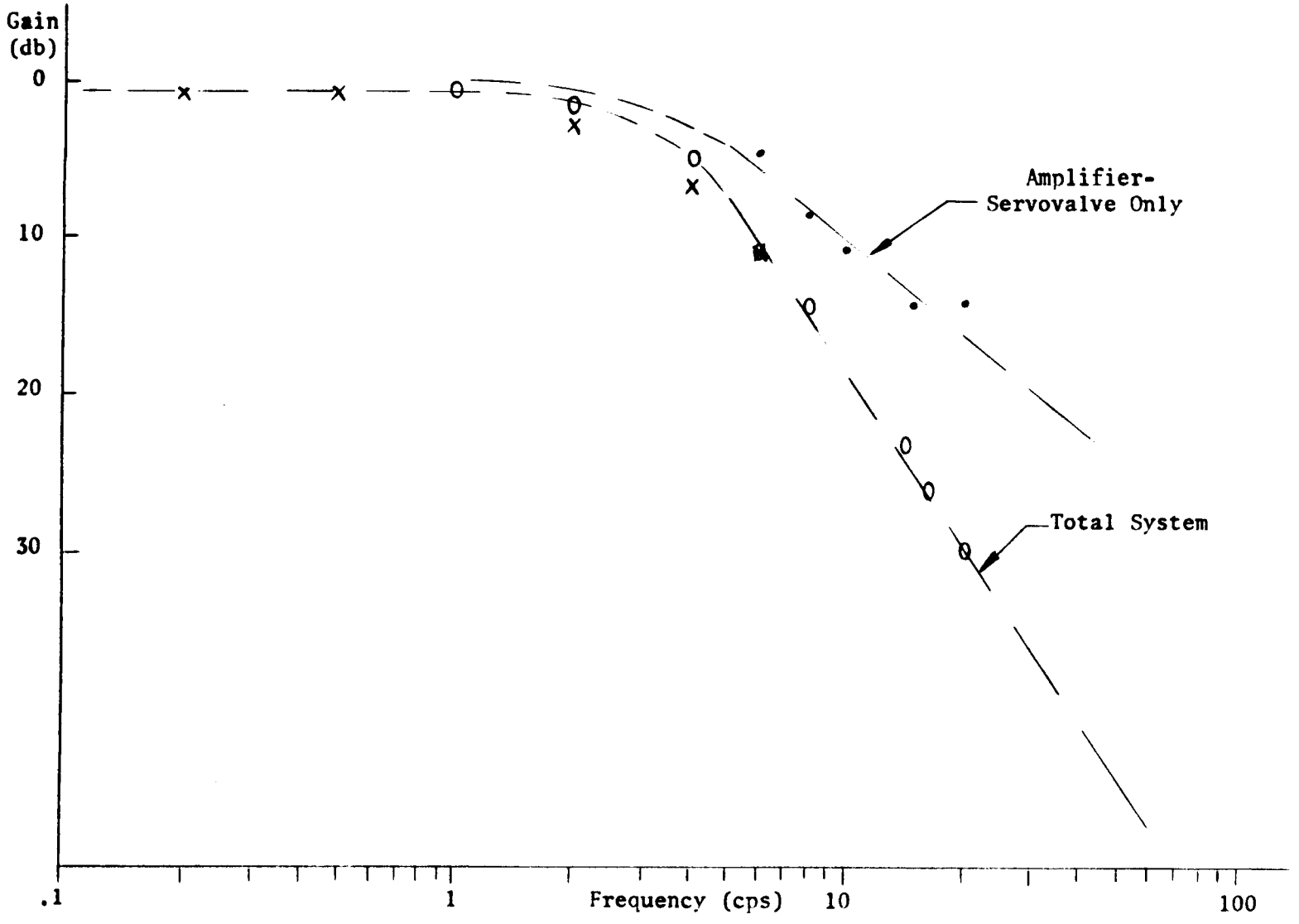

FIGURE 4-4(a) SYSTEM FREQUENCY RESPONSE - GAIN VERSUS FREQUENCY

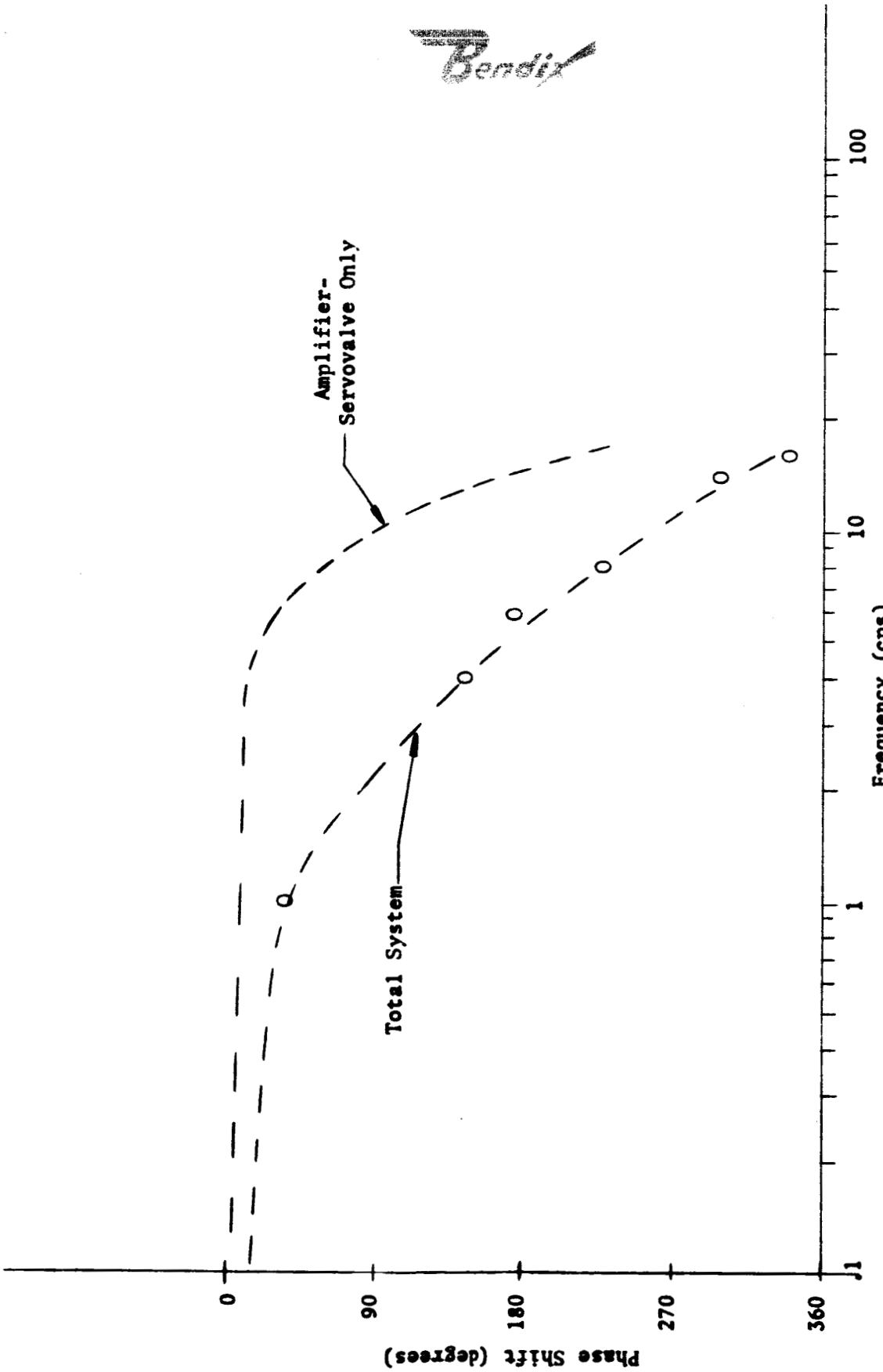

FIGURE 4-4(b) SYSTEM FREQUENCY RESPONSE - PHASE ANGLE VERSUS FREQUENCY

An examination of the phase shift characteristics shown in Figure 4-4(b) indicates the importance of close coupling of stages in a prototype system. The effect of transport delay causes a rapid increase in phase shift, particularly above 10 cps. The effect of the distance between the torque motor and the amplifier first stage is also apparent.

It is felt that both the frequency response and phase shift characteristics can be materially improved by rearranging the amplifier configuration. Other performance improvements are discussed in detail in Section 5.

Figures 4-5(a) and 4-5(b) are sample tracings from the Sanborn recorder used to obtain the frequency response data. The torque motor hysteresis is apparent in the pressure differential characteristics. The noise content (shown in Figure 4-5(a) in the input pressure differential appears to be at a frequency above 160 cps and is not discernable in the servovalve output. It is believed that this noise is generated by the extremely small control source orifice (A_{C_1}). The use of a much smaller source pressure to control pressure differential, with a correspondingly larger orifice, will aid materially in providing a quieter input signal.

4.2.2 Rate Sensor

The rate sensor input can be added to the torque motor input by connecting output pressure P_{R_1} of the rate sensor to pressure tap P_{CA_1} on the first transfer block. Similarly, P_{R_2} is connected to P_{CA_2}. The vent connections P_{V_1} and P_{V_2} should be connected together and vented through A_{R_5} as indicated by the dotted lines in Figure 4-2. The center tap, marked P_{RC}, is vented through a variable valve A_{R_6}. The purpose of the center variable bleed is to permit adjustment of the rate sensor null point. The adjustment of A_{R_6} is extremely sensitive and should not be

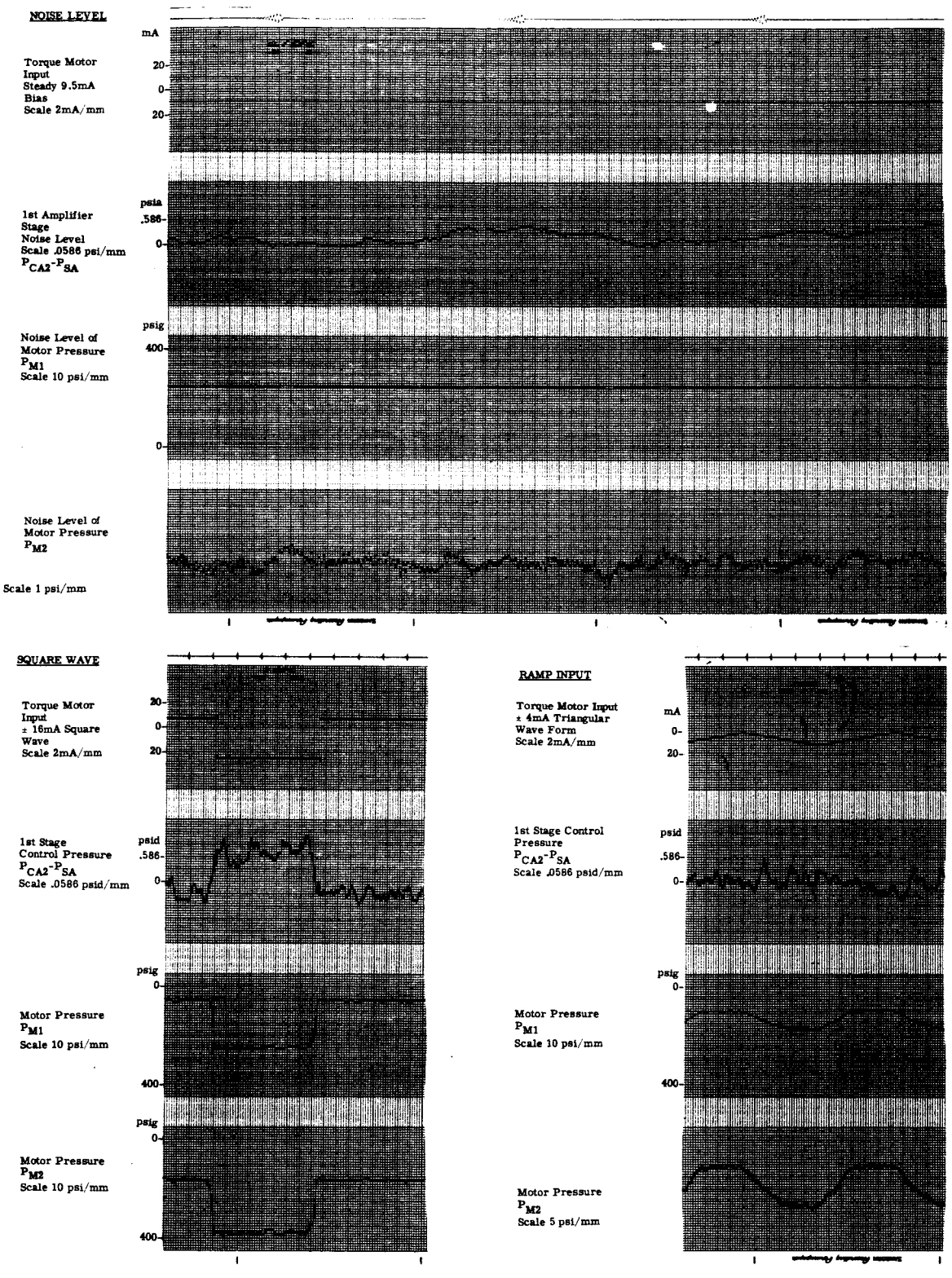

FIGURE 4-5(a) PRESSURE WAVEFORM RECORDINGS

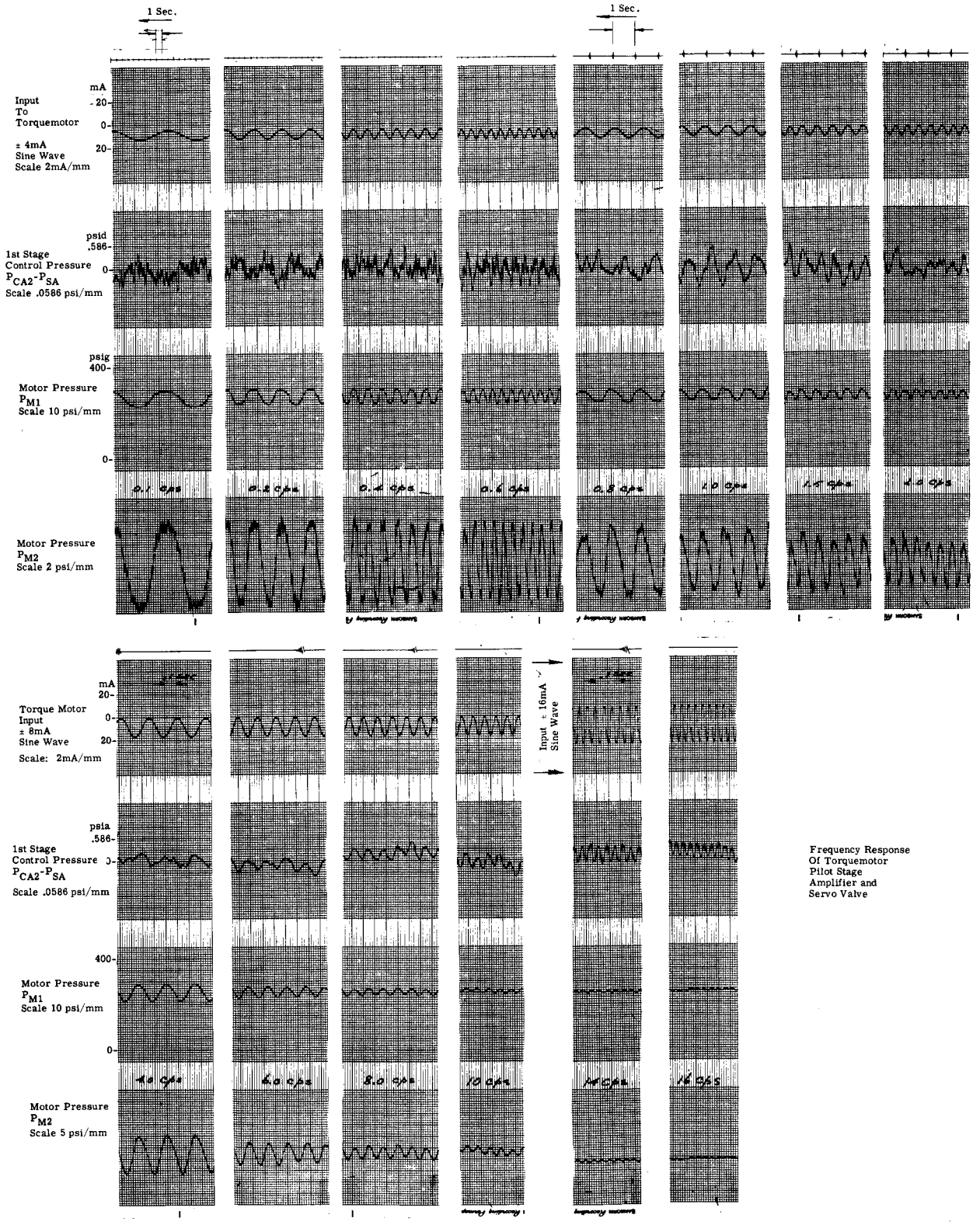

Frequency Response
Of Torquemotor
Pilot Stage
Amplifier and
Servo Valve

FIGURE 4-5(b) TRANSIENT RESPONSE RECORDINGS

opened wider than the equivalent of a #80 bleed. The rate sensor is supplied from the source pressure through the port marked S. The sizing of the fixed orifices in the rate sensor is as follows:

A_{BR} = #73	A_{R3} = #67
A_{SR} = #65	A_{R4} = #67
A_{R1} = #60	A_{R5} = #80 (not supplied)
A_{R2} = #50	A_{R6} = variable (not supplied)

A calibration of the load pressure output against speed input to the rate sensor is shown in Figure 4-6. This calibration was run with a source pressure of 400 psig. Some running was done with a source pressure of 800 psig, although no data was taken due to the thrust bearing problems discussed in Section 3.4. The gain of the unit appeared to be approximately doubled at the higher pressure level. The gain obtained would be 1.0 psi/rpm. This compares with a required gain from the computer study of .366 psi/rpm, or a factor of three times the required gain. The rate sensor is therefore a higher gain device than is required for the application. Rather than attempt to modify the sensor to reduce gain, it is recommended that the rate sensor signal be added at the second stage of amplification by summing with the output of the first stage.

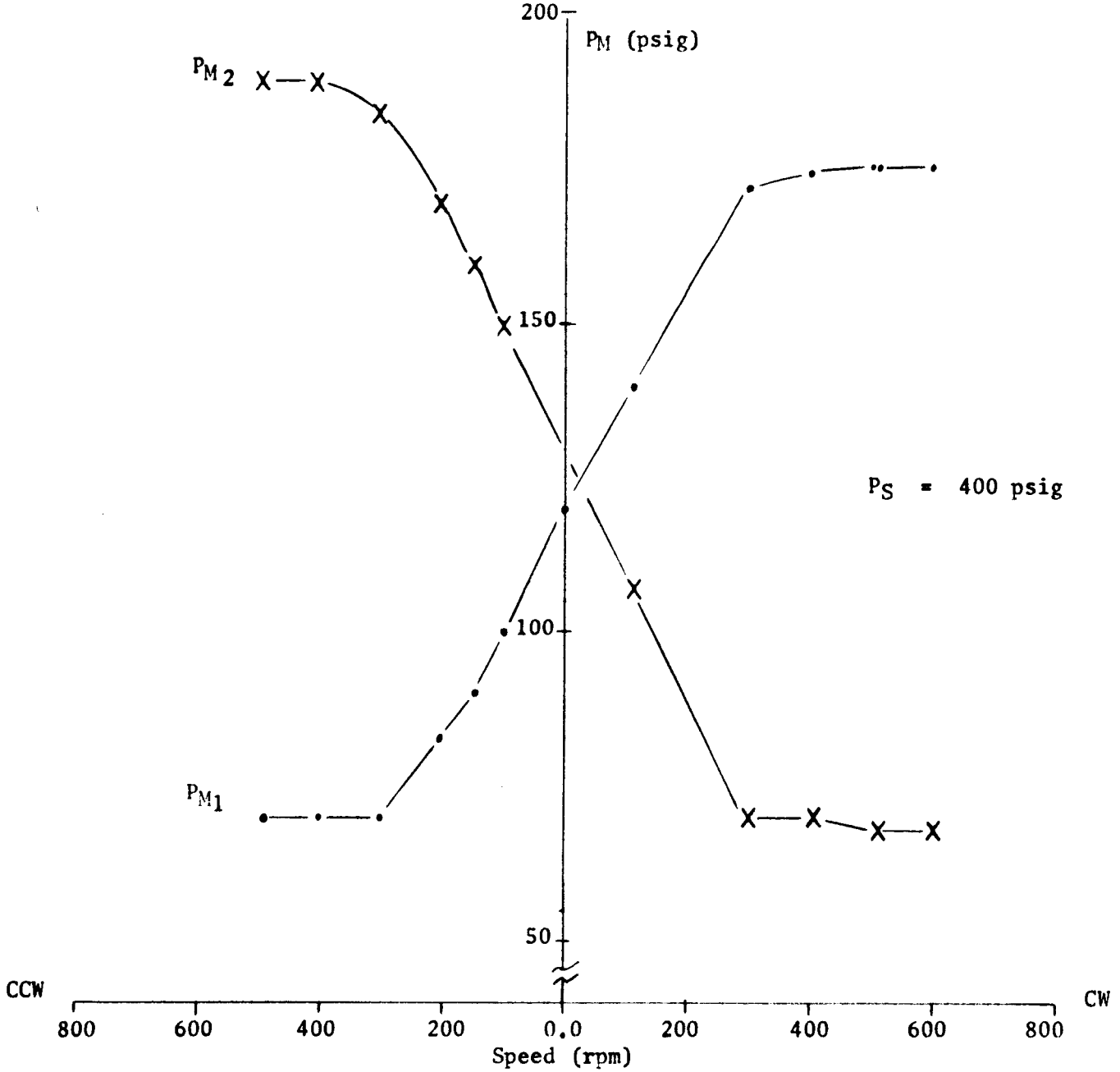

FIGURE 4-6 RATE SENSOR AND AMPLIFIER CALIBRATION

SECTION 5

CONCLUSIONS AND RECOMMENDATIONS

5.1 SUMMARY AND CONCLUSIONS

The major characteristics of the amplifier and servovalve system are listed in Table I. The successful operation of the amplifier is a milestone in the application of pure fluid devices to servosystem control. The system represents the use of pure fluid devices to obtain a high gain device operating at high pressure levels and controlling large quantities of flow. The four-way bridge servovalve demonstrates the feasibility of employing vortex valves to control the forward and reverse flow requirements of a positive displacement load.

The amplifier and servovalve were designed and built to obtain the maximum facility for interchange and replacement of parts. In order to obtain this flexibility and the ability to monitor intermediate pressures, relatively long interconnections and volume capacitances were unavoidable. These capacitances become noticeable in dynamic response testing. Once the breadboard system has been optimized, a redesign is necessary to eliminate all unnecessary passages. It is expected that major improvements can be made in the frequency response by a more optimum arrangement of the components.

The maximum pressure differential available to the load is dictated by the total pressure drop requirements of the amplifier section. An examination of the supply pressure levels to the amplifier stages (see Figure 3-18) shows the following:

ΔP Last Stage of Amplification = 104 psi

ΔP Middle Stage of Amplification = 31 psi

ΔP First Stage of Amplification = 5 psi

TABLE I

PERFORMANCE DATA

System Pressure Gain	1380
Servovalve Pressure Gain	3.5
Amplifier Stage Pressure Gain	7.3
System Flow Gain	354
Maximum Load Pressure	410 psig
Maximum Load Pressure Differential	260 psi
Maximum Load Flow	.124 lb./sec.
System Break Frequency	3.0 cps
Phase Angle at Break Frequency	10 degrees
Phase Angle at 10 cps	90 degrees
Maximum Supply Flow	.308 lb./sec.
Maximum Control Flow	.00035 lb./sec.
Rate Feedback Pressure Gain	1.0 psi/rpm

A curve of number of stages of amplification versus pressure drop required would indicate that a fourth or more amplifier stages could be added without appreciably increasing the overall pressure drop in the amplifier. Therefore, the gain of the amplifier can be increased without penalizing the maximum available load pressure appreciably.

In order to obtain the maximum possible load pressure and flow, the control pressure to the input of the first stage should be as near the source pressure as is practical. The present control pressure level is approximately 671 psi out of an available 800 psi source. This large drop immediately penalizes the performance in two ways.

(1) The entire amplifier pressure level is lowered, resulting in a lower available load pressure.

(2) The extremely small orifice from the source pressure to control pressure (.012 inch diameter) results in a large R-C network at the input which penalizes the dynamic performance and generates an undesirable noise level.

Both the static and dynamic performance characteristics of the amplifier and servovalve can be materially improved by increasing the supply pressure level to the amplifier stages.

Breadboard tests on the staging of the vortex amplifiers has indicated that optimum pressure gain per stage is obtained if the stage supply pressures are in series with the source pressure rather than in parallel. This method is more difficult to set up initially, but allows the entire system level to be controlled by varying the first stage supply restrictor only. By this means, pressure gain per stage should increase to around 9 from the present 7.3. The overall pressure gain of 1860 psi/psi should, therefore, be obtainable without employing additional stages.

The third valve in each side of the four-way bridge (valve P) was used, as described in Section 3.1, to obtain the control signal for the vent valve B. The vented flow from valve P materially reduces the overall flow recovery of the system. It is felt that with further optimization of the servovalve configuration, this valve can be eliminated from the system and the control pressure obtained from the P_o tap of valve F.

Since the output flow from a vortex valve cannot be reduced to zero, there exists a minimum control flow into a second stage. This minimum flow causes a partial turndown of the second (and consecutive) stage resulting in an increase in the required stage pressure drop. This turndown can be minimized by applying a bias flow to the valve equal to and canceling the effect of the minimum control flow. The same effect can be obtained by bringing the supply flow into the chamber through a slanted port. Such a modification would reduce the required amplifier pressure drop and provide more pressure differential at the load.

The torque motor from the present actuator system was used as the electrical to pneumatic input signal transducer. The experimental results of this torque motor as employed in a pure fluid amplifier indicate the need for a redesign to make the transducer more compatible with the amplifier requirements. Consideration should be given to a rotary type transducer with the flapper attached rigidly to the armature. The stroke amplification obtained by a torque tube arrangement is both undesirable and detrimental to the overall performance of a pure fluid system. In this application, a "dry coil" torque motor is not required.

Although mechanical bearing problems prohibited extensive testing of the rate sensor, the minimum gain obtained from the device exceeded the requirements as determined by the analog computer simulation. The gain can be further increased by reducing the back pressure on the speed transducer. The gain can be reduced by reducing the size of the supply orifice A_{SR}, by reducing the diameter of the button, or by reducing button speed by addition of a gear train at the transducer input. It is felt that it would be more desirable to sum the rate signal in the second stage of amplification than to attempt a gain reduction.

5.2 RECOMMENDATIONS FOR FUTURE WORK

In order to obtain the ultimate objective of the program which is to incorporate the pure fluid amplifier and compensation in a complete electropneumatic actuator system, it is recommended that further development be considered in three phases.

Phase I - The present amplifier system should be optimized. This can be done with a minimum amount of hardware fabrication. As discussed above, optimization should include:

(a) Increasing the supply pressure levels to the amplifier stages.

(b) Use series taps to provide the stage supply pressures.

(c) Bias the amplifier stages by modifying the supply port configuration.

(d) Optimize or eliminate valve P.

(e) Incorporate the positive load feedback.

(f) Evaluate the effect of position feedback.

Phase II - When the optimum sizing of the system has been obtained, a redesign and rebuild of the amplifier and servovalve should be performed to obtain the minimum package size and minimum length of the interstage connections. A different concept in torque motor should be designed, fabricated and tested.

Phase III - When the dynamic performance of the packaged unit is known, computer simulation of the entire system is recommended. The pure fluid components can then be incorporated with an electropneumatic actuator and the entire system evaluated in the actual operating environment.

APPENDIX A

ANALOG COMPUTER STUDY

OF

VARIOUS COMPENSATION CONFIGURATIONS FOR THE J-2 ACTUATOR

An analog computer study was conducted to gain some insight as to the most simple and yet adequate means of compensating the J-2 actuator when used in conjunction with fluid interaction devices as the vehicle for pressure amplification.

The present electropneumatic Model NV-B1 control system transient response was simulated for correlation purposes. The correlation was not as close as was desired, and was due primarily to the lack of information on the load fixture dynamic configuration. The actual load fixture appeared to resonate at approximately 4 cps which would correspond to a structural spring rate of 73,600 lbs./in. for an inertia of 1400 slugs. Computer information was obtained using this data and compared to the actual data. The initial rise of the transient had a double slope in each case, the damped oscillation frequency was approximately the same in each case, and the settling times were comparable. The first undershoot was not as severe on the computer traces as in the actual case.

Shown in Figure 1 is the computer block diagram. The block diagram configuration, exclusive of Figures 1a through 1f, was common to all systems evaluated. During the initial correlation study the structural spring rate K_3 was set at 73,600 lbs./in., and from then on, it was left at 391,000 lbs./in. The motor pressure speed characteristic Kp and the motor compressibility time constant τ_3 were changed to the values noted according to whether nitrogen or hydrogen gas was used as the servo medium. All systems were evaluated for a load friction force of 7,300 and 1,460 pounds.

Experimental evidence has shown that the motor friction torque was high at low motor speeds, and was reduced considerably when the motor vanes were in a state of agitation. Because of the complexity involved in simulating this condition, the motor friction torque was reduced to zero for transient response tests and over the frequency range of 2 to 10 cps for the frequency response tests. At frequencies of 0.5 and 1 cps the friction torque was set at 40 in. lbs.

Shown in Figures 1a through 1f are the actuator configurations and their corresponding coefficients upstream of the pneumatic vane motor for each of the systems evaluated. System Number 0 shown in Figure 1a is the present electropneumatic control system. The transient response

correlation data is shown in Figure 2 and the transient response of the same system with a structural spring rate of 391,000 lbs./in. and with nitrogen and hydrogen gas for the servo medium is shown in Figures 3 and 4 respectively.

The criteria for establishing the performance of the overall control system for each of the systems shown in Figures 1b through 1f was based on maintaining a static resolution equal to or slightly better than that of the present actuator shown in Figure 1a, maintaining the overall system stability for a 5:1 variation in load friction, and limiting the attenuation at 8 cps to no more than 3 db.

The input to each of the systems was current to a permanent magnet torque motor, whose output displacement was limited to ±0.014 inch for an input current of ±40 milliamperes which corresponds to ±2.91 inches displacement of the actuator output shaft. For convenience, the actuator feedback displacement was mixed at the torque motor input.

Because this is a preliminary study and the dynamics and possible configuration of the fluid interacting device was not known, the transfer function of the device was assumed to consist of gain only.

The transient response of each of the systems for load friction forces of 7,300 and 1,460 pounds are shown in Figures 5 through 10 and the corresponding frequency responses are shown in Figures 12 through 16.

The transient response of each of the systems is well within reason, and the corresponding frequency responses are similar to each other and are not as flat as one would like to see. The peak amplitude ratios occur between 5 and 7 cps, and vary in magnitude from 4 to 6 db relative to that at 0.5 cps. Since all of the systems have this characteristic, it appears that each system may have to have additional compensation to reduce the actuator stiffness in this frequency range. The phase shift at 1 cps is in the order of 22 to 31 degrees for all systems.

Since there is no particular system with outstanding performance characteristics, the system to consider would have to be the one with the least complexity and the smallest package size as related to development time available.

The generation of a sizable velocity signal is considered feasible within the development time available, and because large lags generally require considerable volume. System 3 shown in Figure 1d appears promising, but the high forward gain required and the possibility that additional attenuation of the actuator stiffness beyond 2 or 3 cps may be necessary makes System 4 shown in Figure 1e the most desirable.

The coefficients corresponding to operation with hydrogen gas as the servo medium were set and the transient and frequency responses of System 4 were taken and are shown in Figure 9 and 16 respectively.

An additional spring rate of 700,000 lbs./in. corresponding to the spring rate of the snubber was added to the block diagram and the operation of the actuator was checked for steps into and away from the snubber as shown in Figure 11.

			TRANSIENT RESPONSE ①			FREQUENCY RESPONSE ④		
SYSTEM	SERVO MEDIUM	LOAD FRICTION (POUNDS)	RISE TIME ② (SEC.)	OVER-SHOOT (INCHES)	SETTLING TIME ③ (SEC.)	AMPLITUDE RATIO @ 1 C.P.S. (DB)	PHASE SHIFT @ 1 C.P.S. (DEG.)	MAX. AMPLITUDE RATIO & FREQ. (DB & C.P.S.)
1	N_2	7,300	0.06	0.005	0.31	-4.4	-29	+1.6 @ 5
		1,460	0.06	0.040	0.26	-0.4	-9	+4.7 @ 6
2	N_2	7,300	0.046	0.00	0.08	-4.3	-29	+0.85 @ 4.5
		1,460	0.04	0.083	0.16	-0.3	-7	+4.2 @ 6
3	N_2	7,300	0.042	0.00	0.07	-4.8	-21	+0.2 @ 5
		1,460	0.05	0.017	0.17	-0.9	-7	+4.0 @ 7
4	N_2	7,300	0.06	0.00	0.065	-4.4	-25	+0.1 @ 4.6
		1,460	0.04	0.018	0.18	-0.6	-9	+6.1 @ 7
4	H_2	7,300	0.048	0.00	0.07	-4.8	-31	+2.4 @ 6.4
		1,460	0.036	0.038	0.25	-1.0	-10	+5.3 @ 7
5	N_2	7,300	0.08	0.00	0.085	-6.0	-29	+1.1 @ 5.5
		1,460	0.04	0.027	0.19	-1.2	-7	+4.7 @ 6.5

NOTES:

① STEP INPUT OF 0.087 INCHES.
② TIME TO TRAVEL FROM 0.00419 TO 0.0783 INCHES.
③ TIME TO SETTLE TO WITHIN 0.00174 AND 0.00435 INCHES OF REQUESTED SET POINT.
④ SINE WAVE INPUT OF ±0.05 INCHES AMPLITUDE.

TABLE 1 SUMMARY OF ANALOG COMPUTER RESULTS

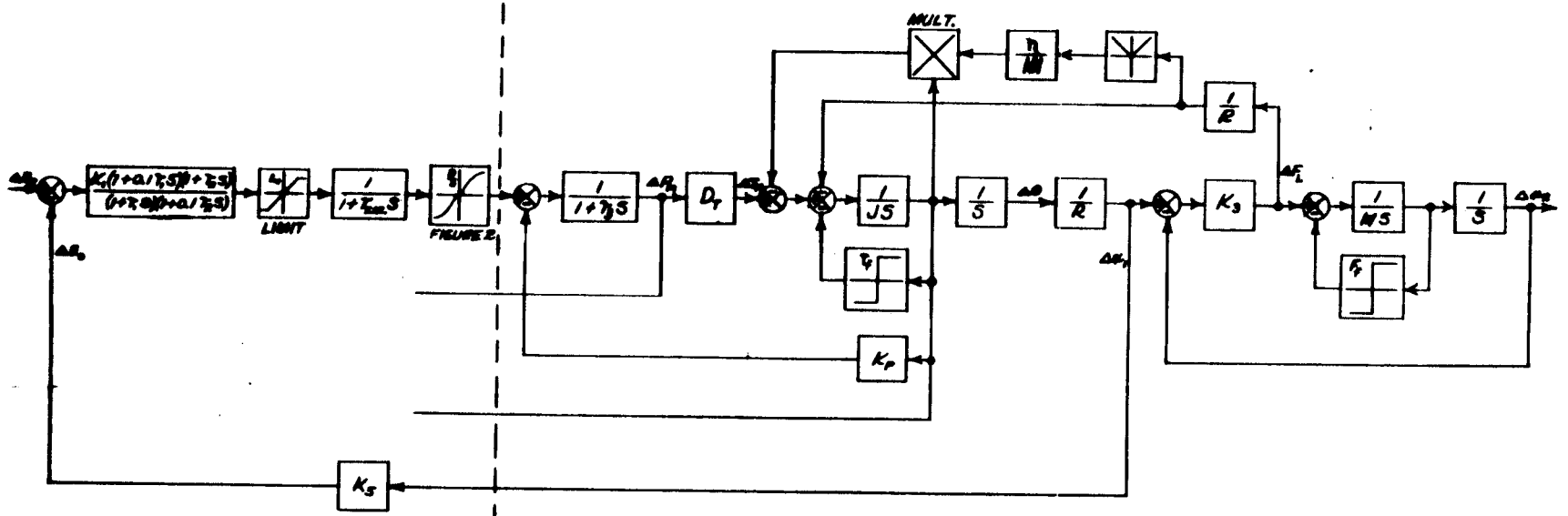

K_1 = ELECTRONIC AMPLIFIER GAIN = 70 MA/VOLT
T_1 = COMPENSATION LEAD OR LAG = 1.0 SEC.
T_2 = COMPENSATION LEAD OR LAG = 0.079 SEC.
T_{SVA} = TORQUE MOTOR AND VALVE LAG = 0.0045 SEC.
K_B = ACTUATOR FDBK GAIN = 17.18 VOLTS/IN.
L_1 = TORQUE MOTOR CURRENT LIMIT = 40 MA.

FIGURE 1a SYSTEM NO. 0

COEFFICIENTS COMMON TO SYSTEMS 1 THROUGH 5

$K_{T.M.}$ = TORQUE MOTOR GAIN = 0.35×10^{-3} IN/MA.
K_B = ACTUATOR FDBK GAIN = 27.4 MA/IN.
L_2 = TORQUE MOTOR LIMIT = 0.014 IN.
L_3 = STALL PRESSURE LIMIT = 400 PSI.

MOTOR, TRANSMISSION, AND LOAD COEFFICIENTS

D_T = MOTOR TORQUE DISPLACEMENT = 0.3 IN^3/RAD
R = TRANSMISSION RATIO = 221 RAD/IN.
J = MOTOR PLUS TRANSMISSION INERTIA = 3.07×10^{-3} IN. LB. SEC^2
M = LOAD INERTIA = 16.7 LB. SEC^2/IN.
K_3 = LOAD STRUCTURAL SPRING RATE = 73,600 OR 391,000 LB/IN.
η = TRANSMISSION EFFICIENCY = 0.7
K_P = MOTOR PRESSURE SPEED CHARACTERISTIC = 0.9 PSI/RAD/SEC. FOR H_2 OR 0.45 FOR H_2
F_f = LOAD FRICTION FORCE = 7,300 OR 1,460 LBS.
T_f = MOTOR FRICTION TORQUE = 40 IN. LBS.
T_3 = MOTOR COMPRESSIBILITY TIME CONSTANT = 0.005 SEC. FOR H_2 AND 0.003 FOR H_2

FIGURE 1 COMPUTER BLOCK DIAGRAMS

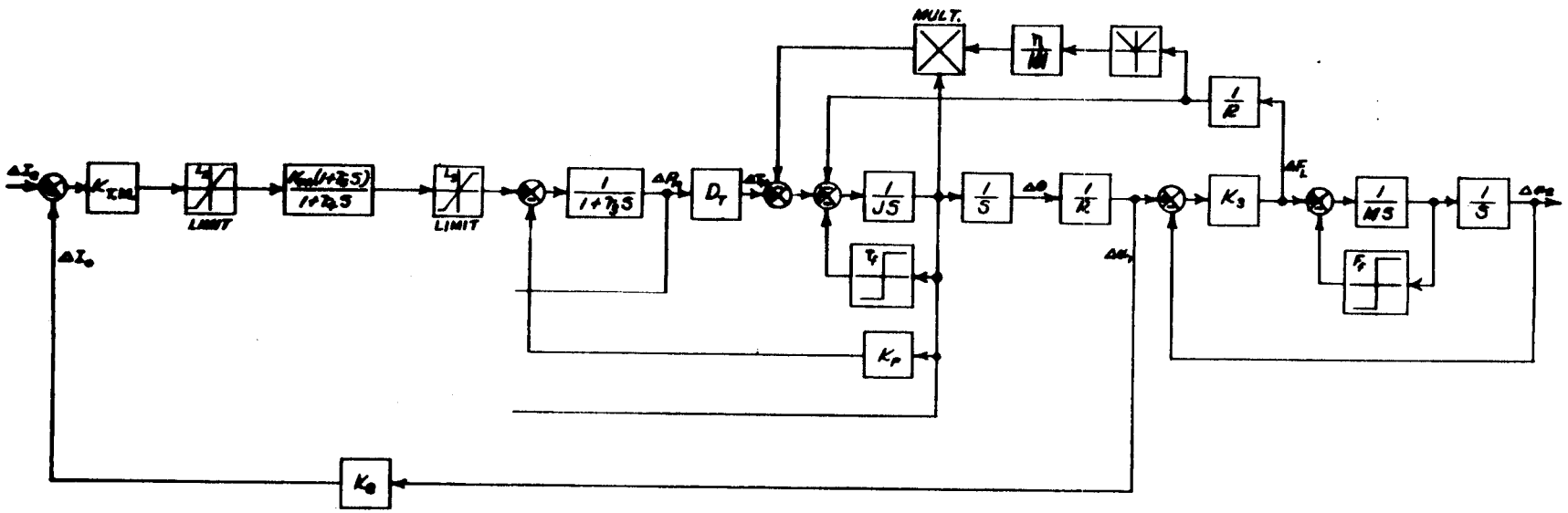

K_{FA} = FLUID AMPLIFIER GAIN = 4×10^6 P.S.I./IN.
τ_c = COMPENSATION LAG = 0.2 SEC.
τ_g = COMPENSATION LEAD = 0.08 SEC.

FIGURE 1b SYSTEM NO. 1

COEFFICIENTS COMMON TO SYSTEMS 1 THROUGH 5

$K_{T.M.}$ = TORQUE MOTOR GAIN = 0.35×10^{-3} IN./MA.
K_θ = ACTUATOR FDBK GAIN = 27.4 MA/IN.
L_2 = TORQUE MOTOR LIMIT = 0.014 IN.
L_3 = STALL PRESSURE LIMIT = 4000 P.S.I.

MOTOR, TRANSMISSION, AND LOAD COEFFICIENTS

D_T = MOTOR TORQUE DISPLACEMENT = 0.5 IN^3/RAD
R = TRANSMISSION RATIO = 221 RAD./IN.
J = MOTOR PLUS TRANSMISSION INERTIA = 3.07×10^{-3} IN. LB. SEC^2
M = LOAD INERTIA = 116.7 LB. SEC^2/IN.
K_3 = LOAD STRUCTURAL SPRING RATE = 73,000 OR 391,000 LB./IN.
η = TRANSMISSION EFFICIENCY = 0.7
K_p = MOTOR PRESSURE SPEED CHARACTERISTIC = 0.9 $\frac{P.S.I.}{RAD./SEC.}$ FOR M_2 OR 0.45 FOR M_2
F_f = LOAD FRICTION FORCE = 1,300 OR 1,460 LBS.
T_f = MOTOR FRICTION TORQUE = 40 IN. LBS.
τ_f = MOTOR COMPRESSIBILITY TIME CONSTANT = 0.005 SEC. FOR M_2 AND 0.003 FOR M_2

FIGURE 1 COMPUTER BLOCK DIAGRAM

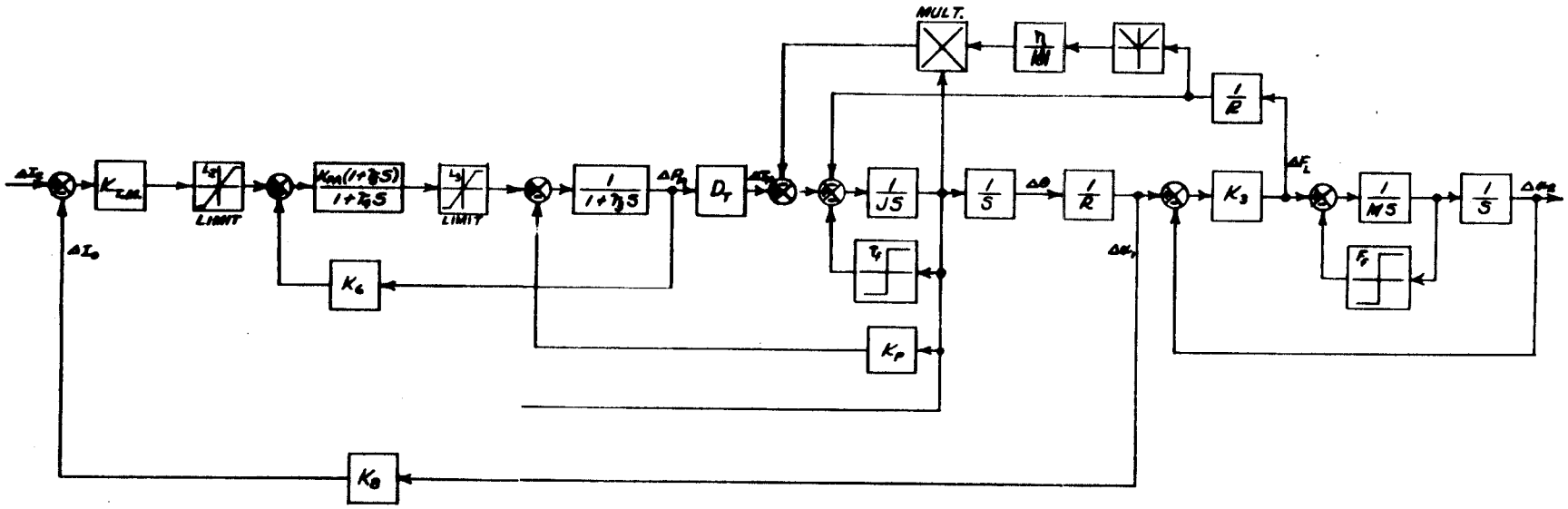

K_{FA} = FLUID AMPLIFIER GAIN = 2×10^6 RS.I./IN.
K_4 = POS. PRESSURE FDBK GAIN = 0.25×10^{-6} IN./RS.I.
T_1 = COMPENSATION LAG = 0.15 SEC.
T_2 = COMPENSATION LEAD = 0.08 SEC.

FIGURE 1C SYSTEM NO. 2

COEFFICIENTS COMMON TO SYSTEMS 1 THROUGH 5

$K_{T.M.}$ = TORQUE MOTOR GAIN = 0.35×10^{-3} IN./MA.
K_B = ACTUATOR FDBK GAIN = 27.4 MA/IN.
L_2 = TORQUE MOTOR LIMIT = 0.014 IN.
L_3 = STALL PRESSURE LIMIT = 4000 PSI.

MOTOR, TRANSMISSION, AND LOAD COEFFICIENTS

D_T = MOTOR TORQUE DISPLACEMENT = 0.5 IN^3/RAD.
R = TRANSMISSION RATIO = 221 RAD./IN.
J = MOTOR PLUS TRANSMISSION INERTIA = 3.07×10^{-3} IN. LB. SEC^2
M = LOAD INERTIA = 116.7 LB. SEC^2/IN.
K_3 = LOAD STRUCTURAL SPRING RATE = 73,000 OR 391,000 LB./IN.
η = TRANSMISSION EFFICIENCY = 0.7
K_P = MOTOR PRESSURE SPEED CHARACTERISTIC = 0.9 PSI/RAD/SEC. FOR N_2 OR 0.45 FOR H_2
F_f = LOAD FRICTION FORCE = 730 OR 1,460 LBS.
T_f = MOTOR FRICTION TORQUE = 40 IN. LBS.
T_3 = MOTOR COMPRESSIBILITY TIME CONSTANT = 0.005 SEC. FOR N_2 AND 0.003 FOR H_2

FIGURE 1 COMPUTER BLOCK DIAGRAMS

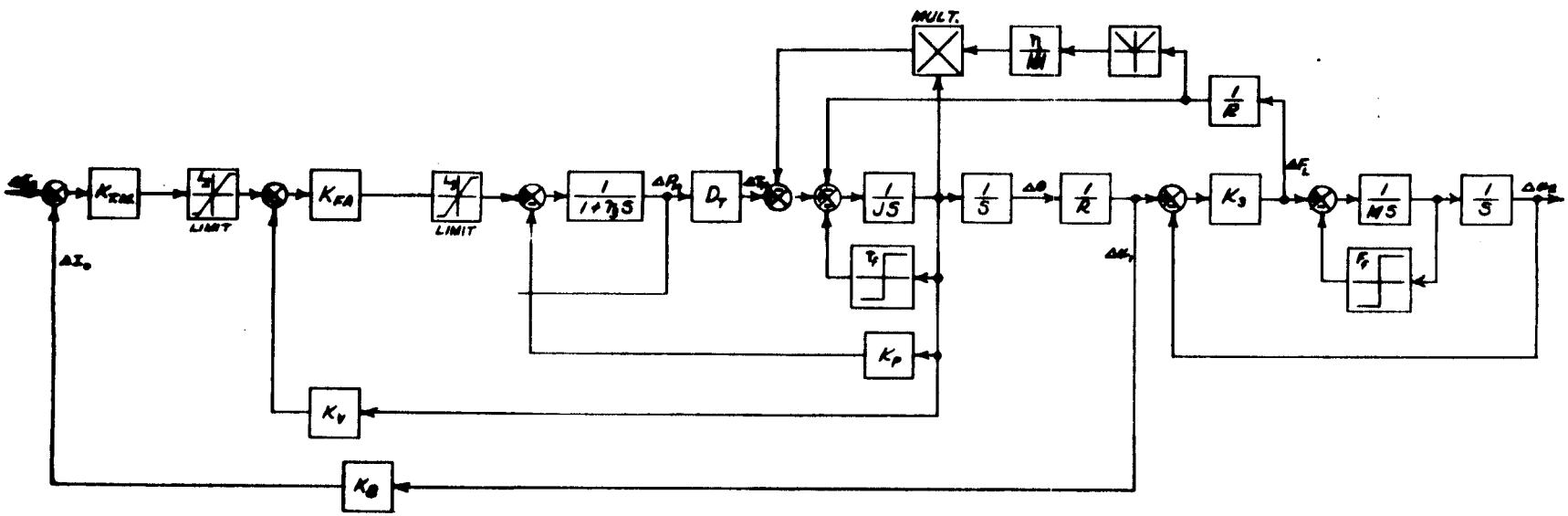

K_{FA} = FLUID AMPLIFIER GAIN = 4×10^6 P.S.I./IN.

K_v = MOTOR VELOCITY FDBK GAIN = 0.43 RAD./SEC.

FIGURE 1d SYSTEM NO. 3

COEFFICIENTS COMMON TO SYSTEMS 1 THROUGH 5

$K_{T.A.}$ = TORQUE MOTOR GAIN = 0.35×10^{-3} IN./MA.

K_B = ACTUATOR FDBK GAIN = 27.4 MA/IN.

L_B = TORQUE MOTOR LIMIT = 0.014 IN.

L_3 = STALL PRESSURE LIMIT = 400 P.S.I.

MOTOR, TRANSMISSION, AND LOAD COEFFICIENTS

D_T = MOTOR TORQUE DISPLACEMENT = 0.5 IN.^{3}/RAD.

R = TRANSMISSION RATIO = 221 RAD./IN.

J = MOTOR PLUS TRANSMISSION INERTIA = 3.07×10^{-3} IN. LB. SEC.^{2}

M = LOAD INERTIA = 116.7 LB. SEC.^{2}/IN.

K_3 = LOAD STRUCTURAL SPRING RATE = 73,000 OR 391,000 LB./IN.

η = TRANSMISSION EFFICIENCY = 0.7

K_p = MOTOR PRESSURE SPEED CHARACTERISTIC = 0.9 $\frac{P.S.I.}{RAD./SEC}$ FOR N_2 OR 0.45 FOR H_2

F_f = LOAD FRICTION FORCE = 7,300 OR 1,460 LBS.

T_f = MOTOR FRICTION TORQUE = 40 IN. LBS.

T_3 = MOTOR COMPRESSIBILITY TIME CONSTANT = 0.005 SEC. FOR N_2 AND 0.003 FOR H_2

FIGURE 1 COMPUTER BLOCK DIAGRAMS

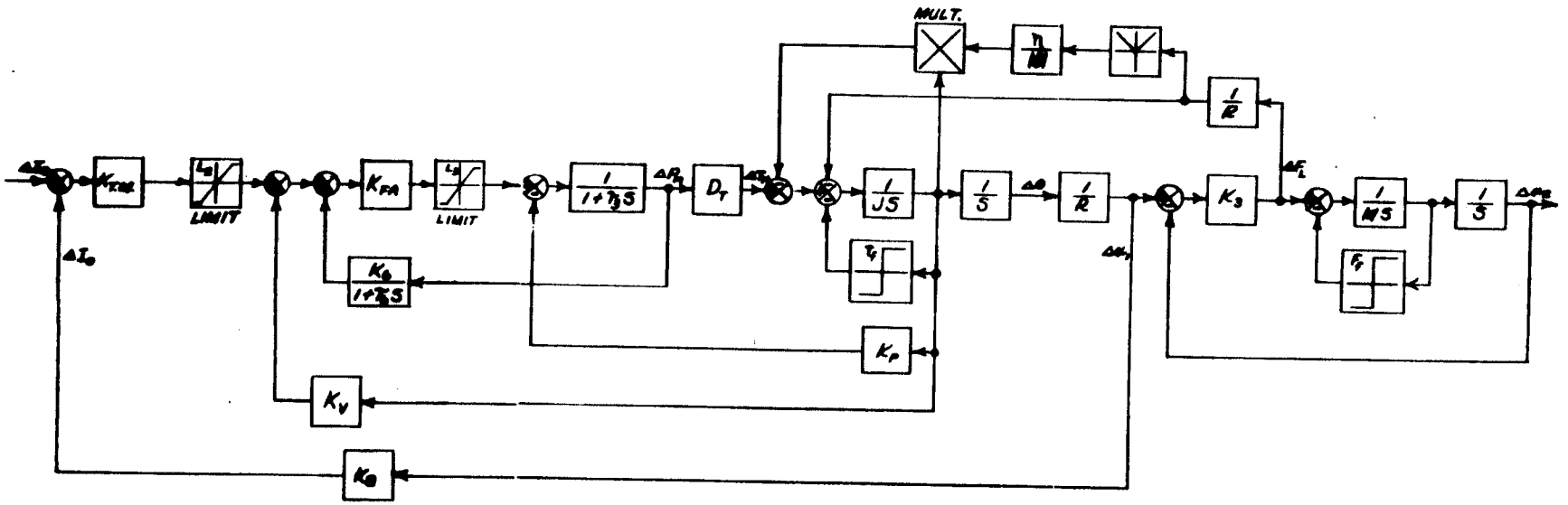

K_{FA} = FLAPPER AMPLIFIER GAIN = 2×10^6 R.S.I./IN.

K_f = FUEL PRESSURE FDBK GAIN = 0.23×10^{-6} IN./R.S.I.

K_v = SERVO VELOCITY FDBK GAIN = 0.38×10^{-6} IN./RAD./SEC.

T_3 = COMPENSATION LAG = 0.04 SEC.

FIGURE 10 SYSTEM NO. 4

COEFFICIENTS COMMON TO SYSTEMS 1 THROUGH 5

K_{TM} = TORQUE MOTOR GAIN = 0.35×10^{-3} IN./MA.

K_a = ACTUATOR FDBK GAIN = 27.4 MA/IN.

L_2 = TORQUE MOTOR LIMIT = 0.014 IN.

L_3 = STALL PRESSURE LIMIT = 400 P.S.I.

MOTOR, TRANSMISSION, AND LOAD COEFFICIENTS

D_T = MOTOR TORQUE DISPLACEMENT = 0.5 IN^3/RAD

R = TRANSMISSION RATIO = 221 RAD./IN.

J = MOTOR PLUS TRANSMISSION INERTIA = 3.07×10^{-3} IN. LB. SEC^2

M = LOAD INERTIA = 116.7 LB. SEC^2/IN.

K_3 = LOAD STRUCTURAL SPRING RATE = 73,000 OR 391,000 LB./IN.

η = TRANSMISSION EFFICIENCY = 0.7

K_p = MOTOR PRESSURE SPEED CHARACTERISTIC = 0.9 $\frac{P.S.I.}{RAD./SEC.}$ FOR H_2 OR 0.45 FOR H_2

F_f = LOAD FRICTION FORCE = 7,300 OR 1,460 LBS.

T_f = MOTOR FRICTION TORQUE = 40 IN. LBS.

T_3 = MOTOR COMPRESSIBILITY TIME CONSTANT = 0.005 SEC. FOR H_2 AND 0.003 FOR H_2

FIGURE 1 COMPUTER BLOCK DIAGRAMS

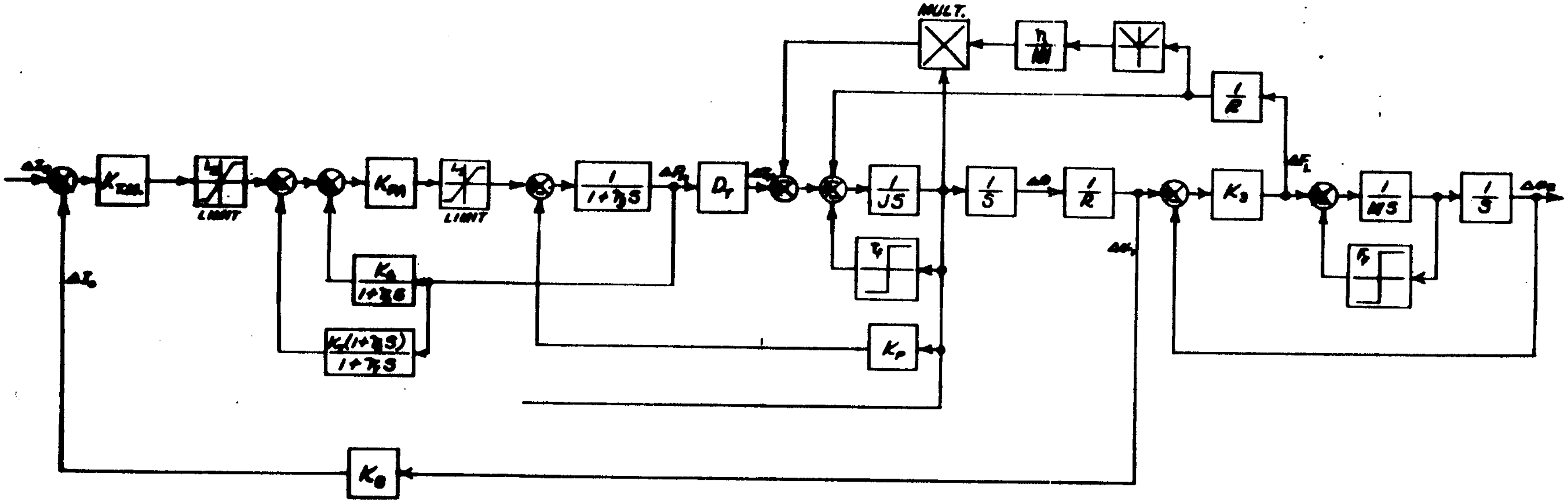

K_{FA} = FLUID AMPLIFIER GAIN = 4×10^{6} P.S.I./MA.
K_4 = POS. PRESSURE FDBK GAIN = 10^{-6} IN./P.S.I.
K_5 = NEG. PRESSURE FDBK GAIN = 10^{-6} IN./P.S.I.
τ_1 = COMPENSATION LAG = 0.33 SEC.
τ_2 = COMPENSATION LAG = 0.05 SEC.
τ_3 = COMPENSATION LEAD = 0.019 SEC.

FIGURE 1F SYSTEM NO. 5

COEFFICIENTS COMMON TO SYSTEMS 1 THROUGH 5

$K_{T.M.}$ = TORQUE MOTOR GAIN = 0.35×10^{-3} IN./MA.
K_θ = ACTUATOR FDBK GAIN = 27.4 MA/IN.
L_2 = TORQUE MOTOR LIMIT = 0.014 IN.
L_3 = STALL PRESSURE LIMIT = 400 PSI.

MOTOR, TRANSMISSION, AND LOAD COEFFICIENTS

D_T = MOTOR TORQUE DISPLACEMENT = 0.5 IN^3/RAD.
R = TRANSMISSION RATIO = 221 RAD/IN.
J = MOTOR PLUS TRANSMISSION INERTIA = 3.07×10^{-3} IN. LB. SEC.^{2}
M = LOAD INERTIA = 16.7 LB. SEC.^{2}/IN.
K_s = LOAD STRUCTURAL SPRING RATE = 73,600 OR 391,000 LB/IN.
η = TRANSMISSION EFFICIENCY = 0.7
K_P = MOTOR PRESSURE SPEED CHARACTERISTIC = 0.9 $\frac{P.S.I.}{RAD/SEC.}$ FOR H_2 OR 0.45 FOR H_2
F_f = LOAD FRICTION FORCE = 7,300 OR 1,460 LBS.
T_f = MOTOR FRICTION TORQUE = 40 IN. LBS.
τ_B = MOTOR COMPRESSIBILITY TIME CONSTANT = 0.005 SEC. FOR H_2 AND 0.003 FOR H_2

FIGURE 1 COMPUTER BLOCK DIAGRAMS

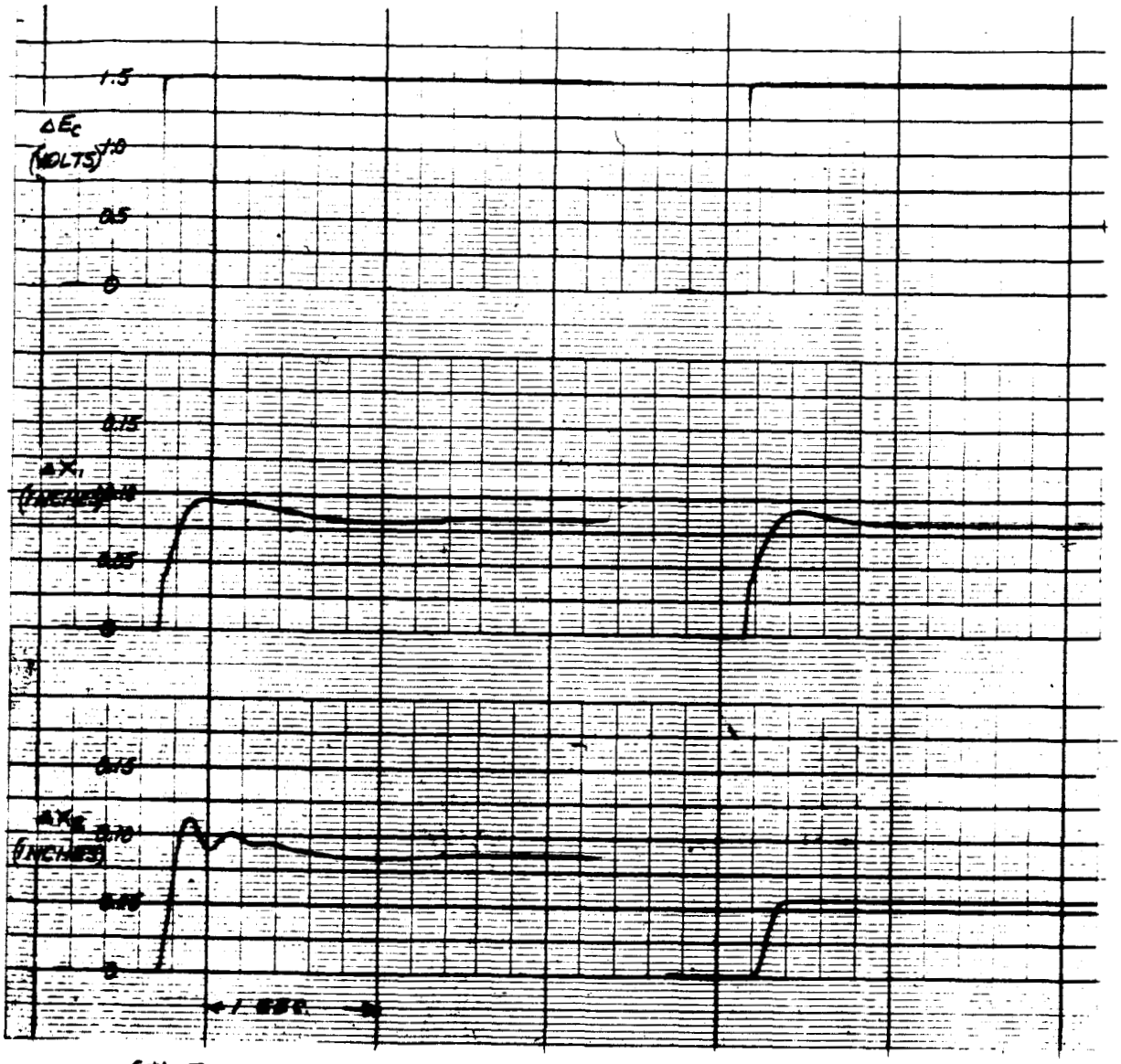

(a) F_f = 0 LB.

(b) F_f = 3,400 LB.

K_3 = 74,000 LB./IN.

NITROGEN

FIGURE 2 SYSTEM NO. 0 TRANSIENT RESPONSE

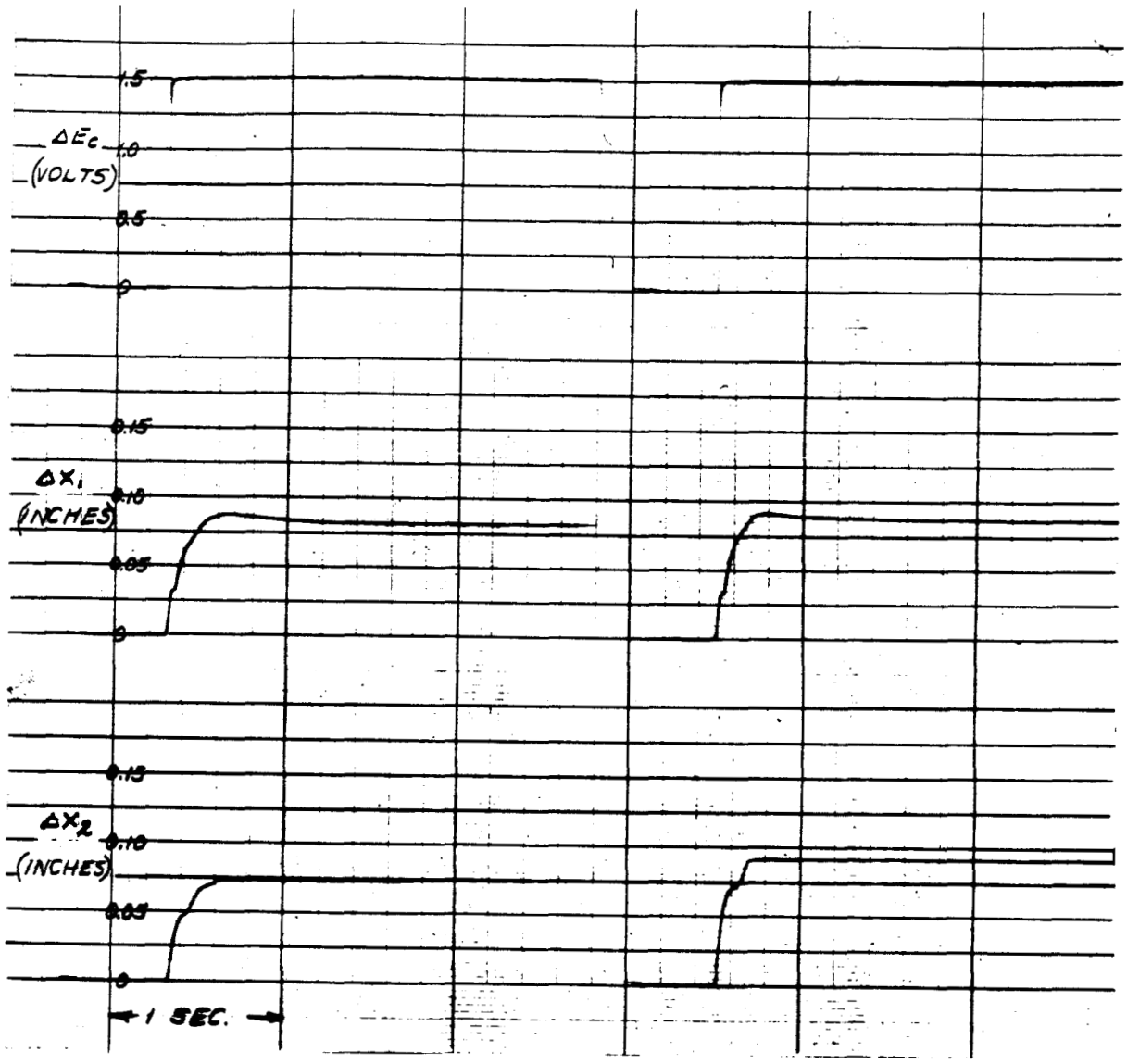

(a) F_f = 7300 LB.

(b) F_f = 1460 LB.

K_3 = 391000 LB./IN.

NITROGEN

FIGURE 3 SYSTEM NO. 0 TRANSIENT RESPONSE

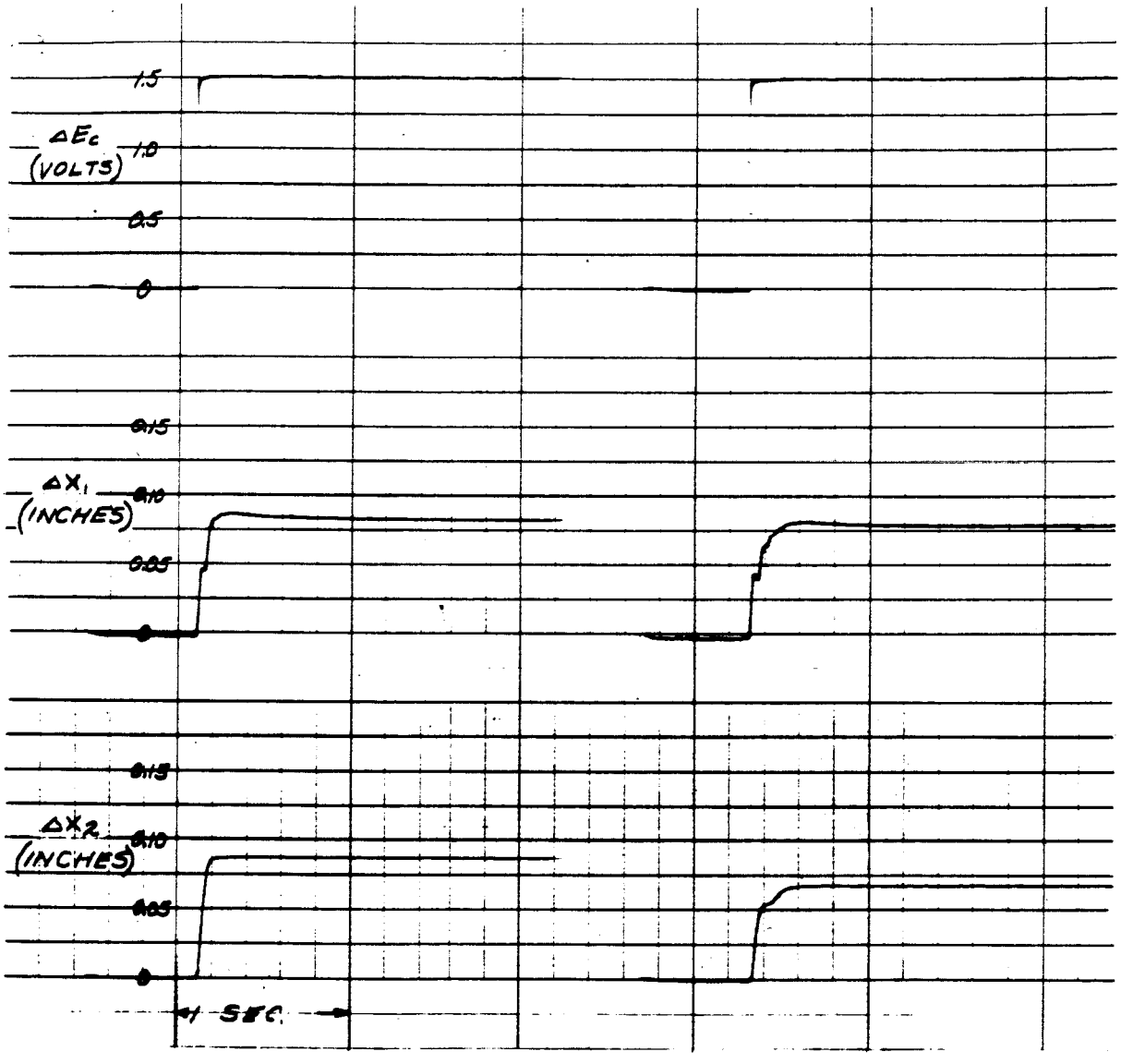

(a) F_t = 1,460 LB.

(b) F_t' = 7,300 LB.

K_3 = 391,000 LB./IN.

HYDROGEN

FIGURE 4 SYSTEM NO. 0 TRANSIENT RESPONSE

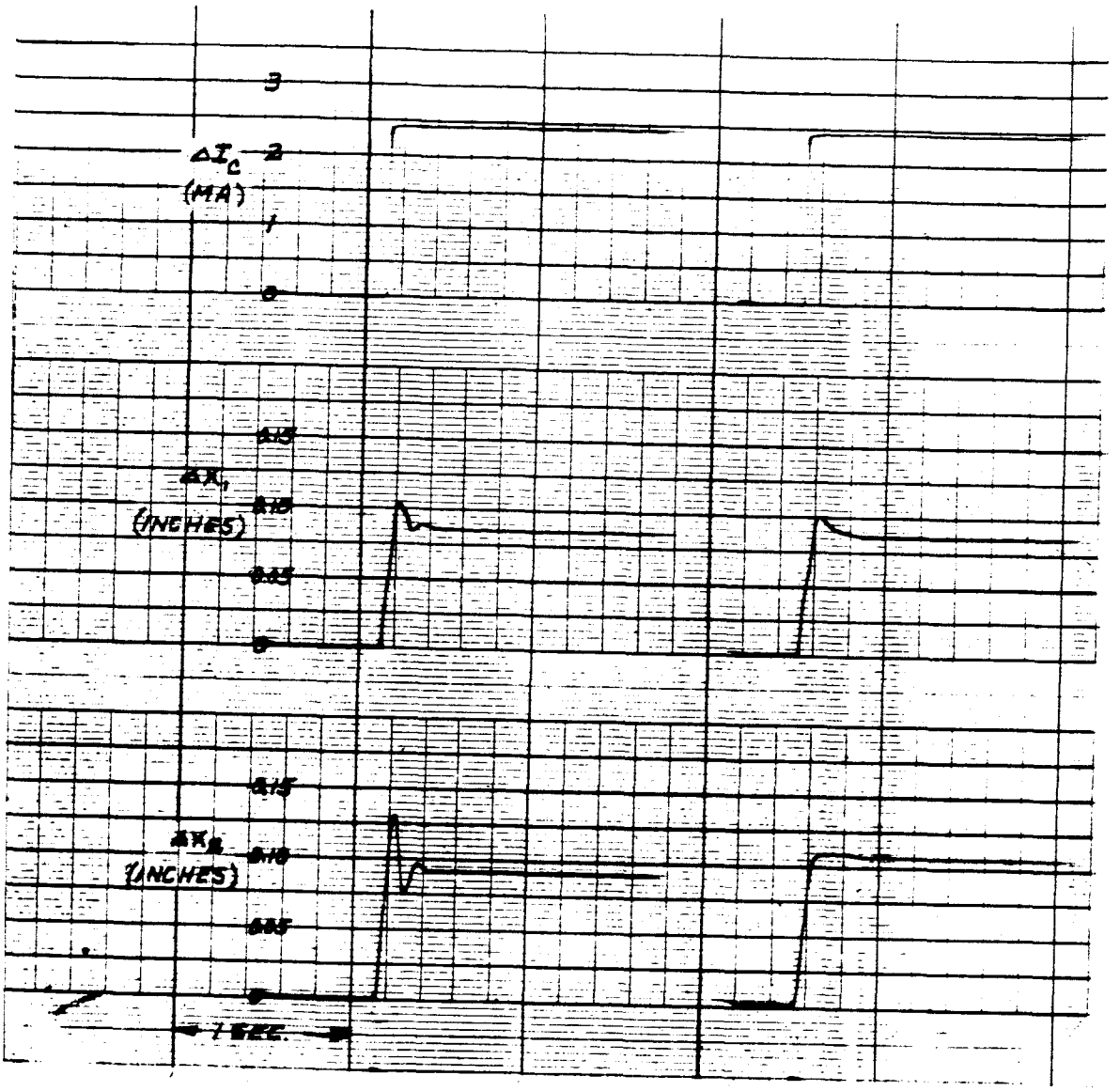

(a) F_f = 1,460 LB. (b) F_f = 7,300 LB.

K_3 = 391,000 LB./IN.

NITROGEN

FIGURE 5 SYSTEM NO. 1 TRANSIENT RESPONSE

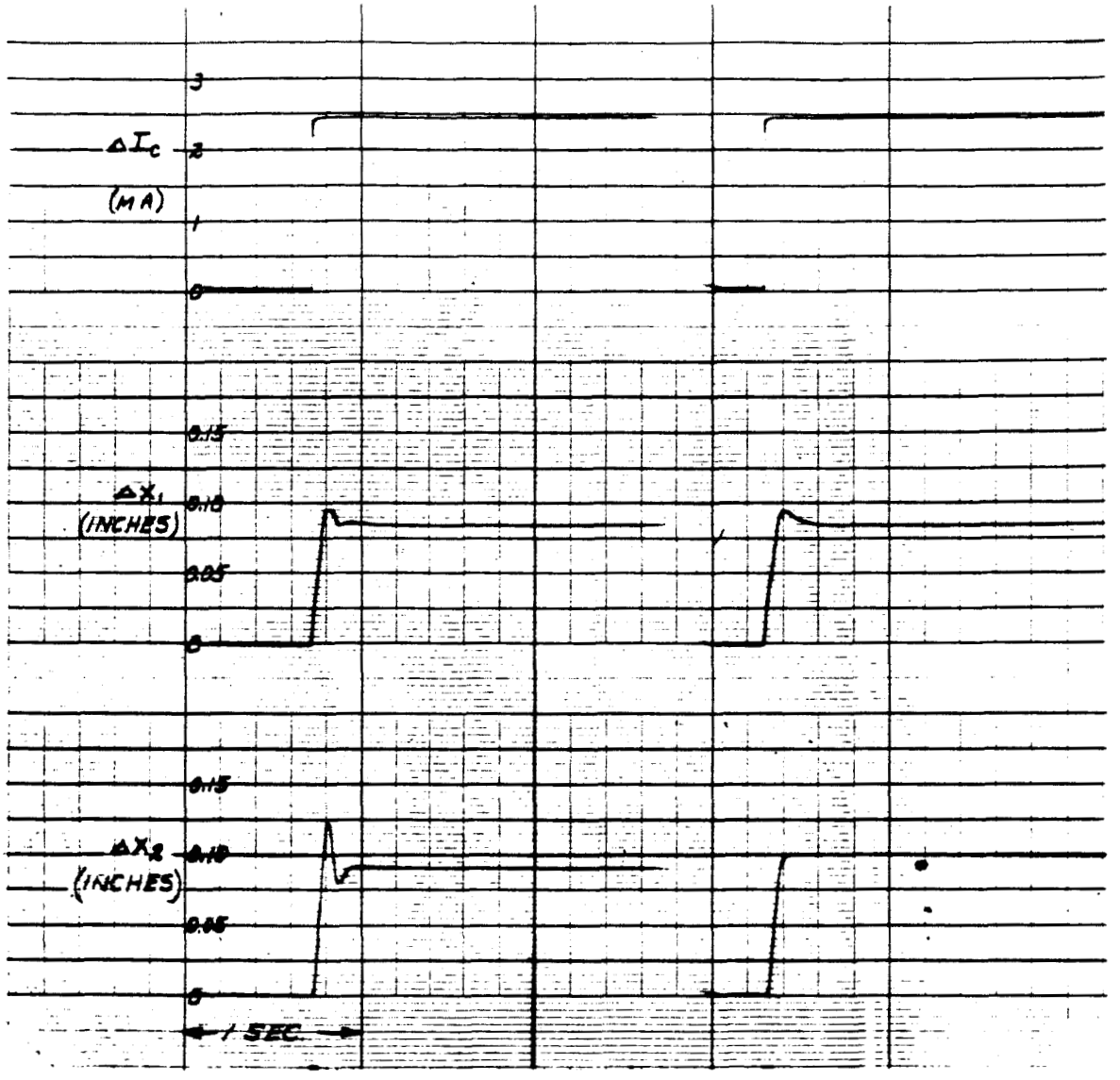

(a) F_f = 1,460 LB. (b) F_f = 7,300 LB.

K_3 = 391,000 LB./IN.

NITROGEN

FIGURE 6 SYSTEM NO.2 TRANSIENT RESPONSE

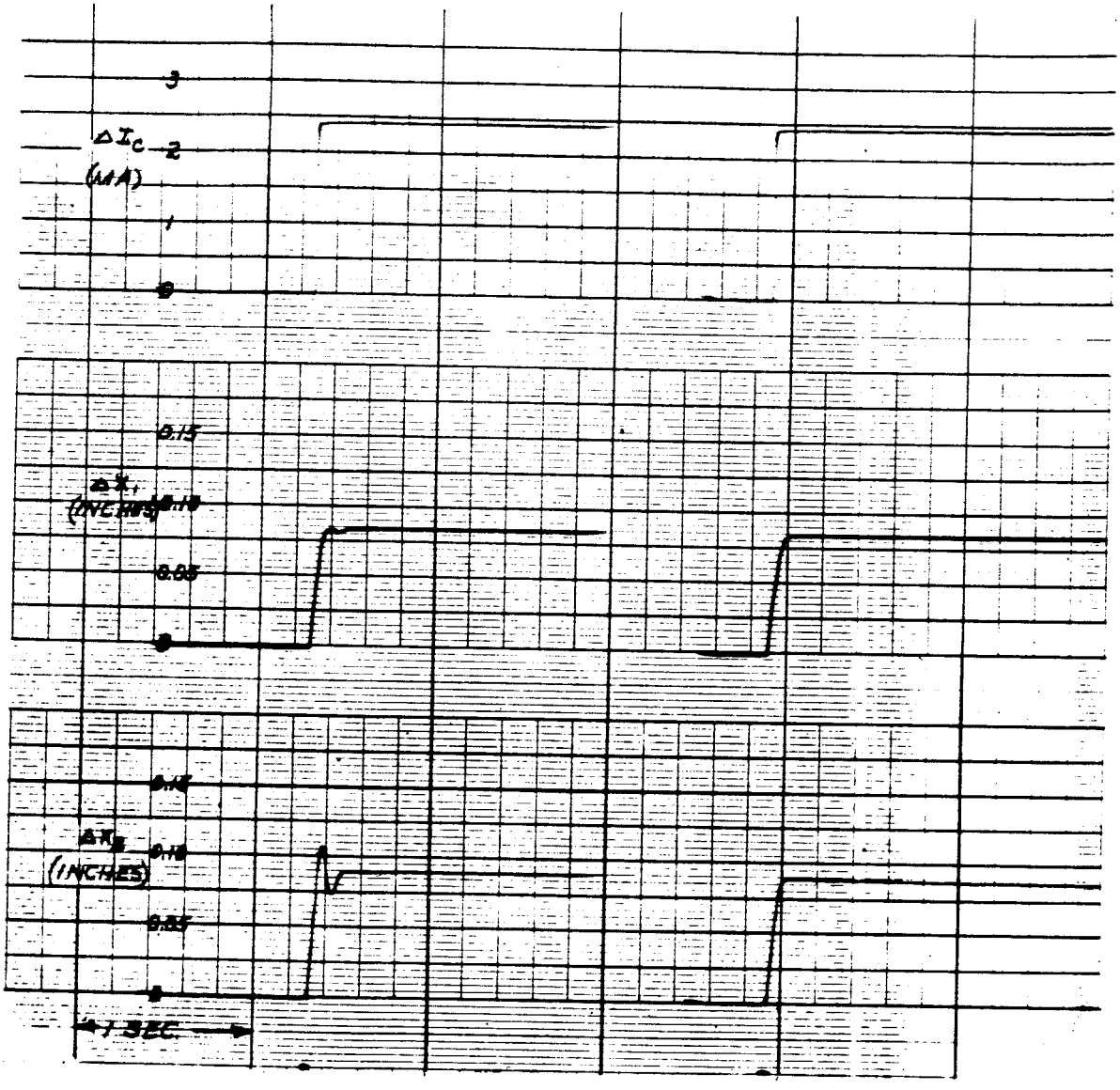

(a) F_f = 1,460 LB. (b) F_f = 7,300 LB.

K_3 = 391,000 LB./IN.

NITROGEN

FIGURE 7 SYSTEM NO. 3 TRANSIENT RESPONSE

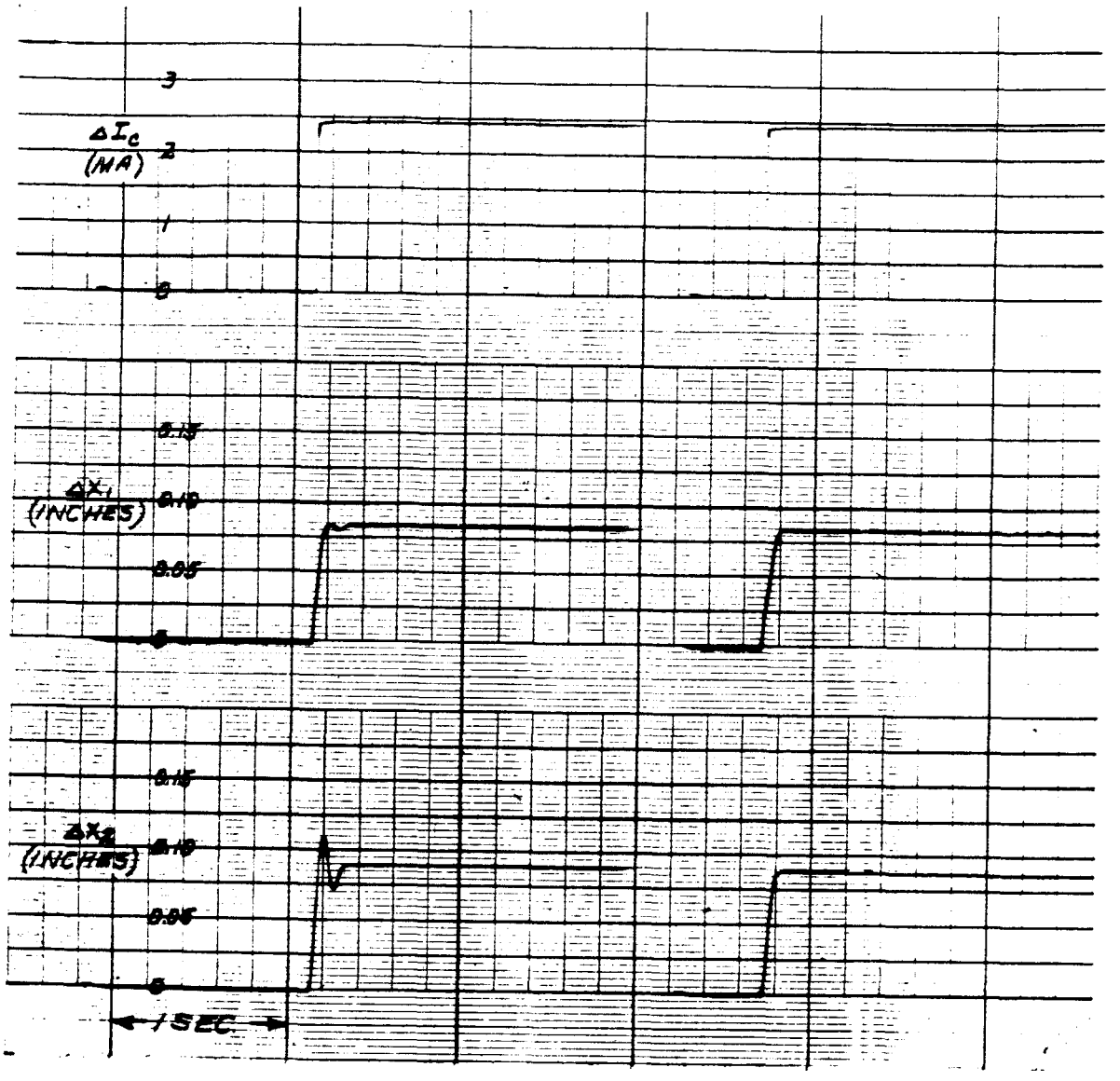

(a) F_f = 1,460 LB.

(b) F_f = 7,300 LB.

K_3 = 391,000 LB./IN.

NITROGEN

FIGURE 8 SYSTEM NO. 4 TRANSIENT RESPONSE

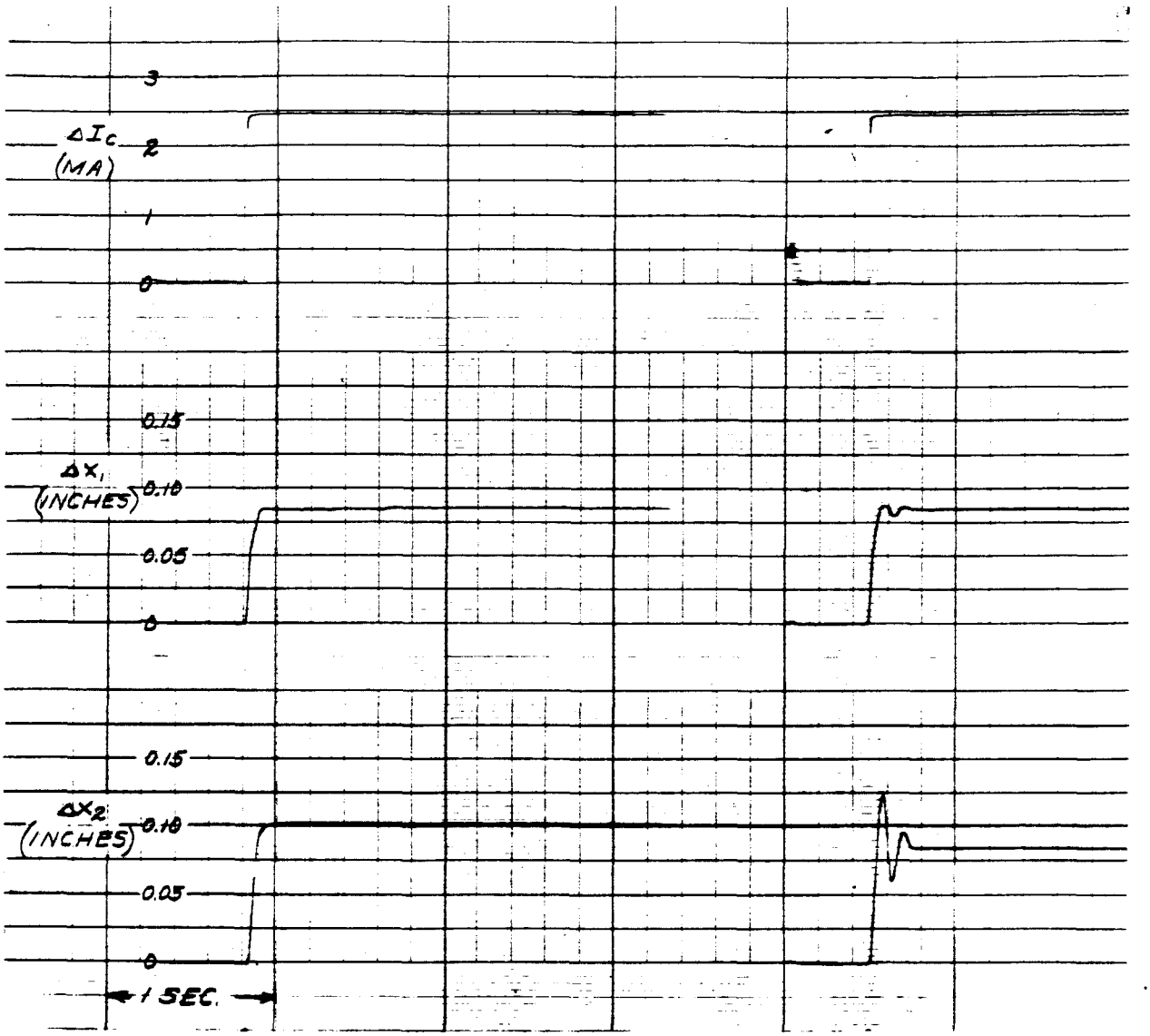

(a) F_f = 7,300 LB. (b) F_f = 1,460 LB.

K_3 = 391,000 LB./IN.

HYDROGEN

FIGURE 9 SYSTEM NO. 4 TRANSIENT RESPONSE

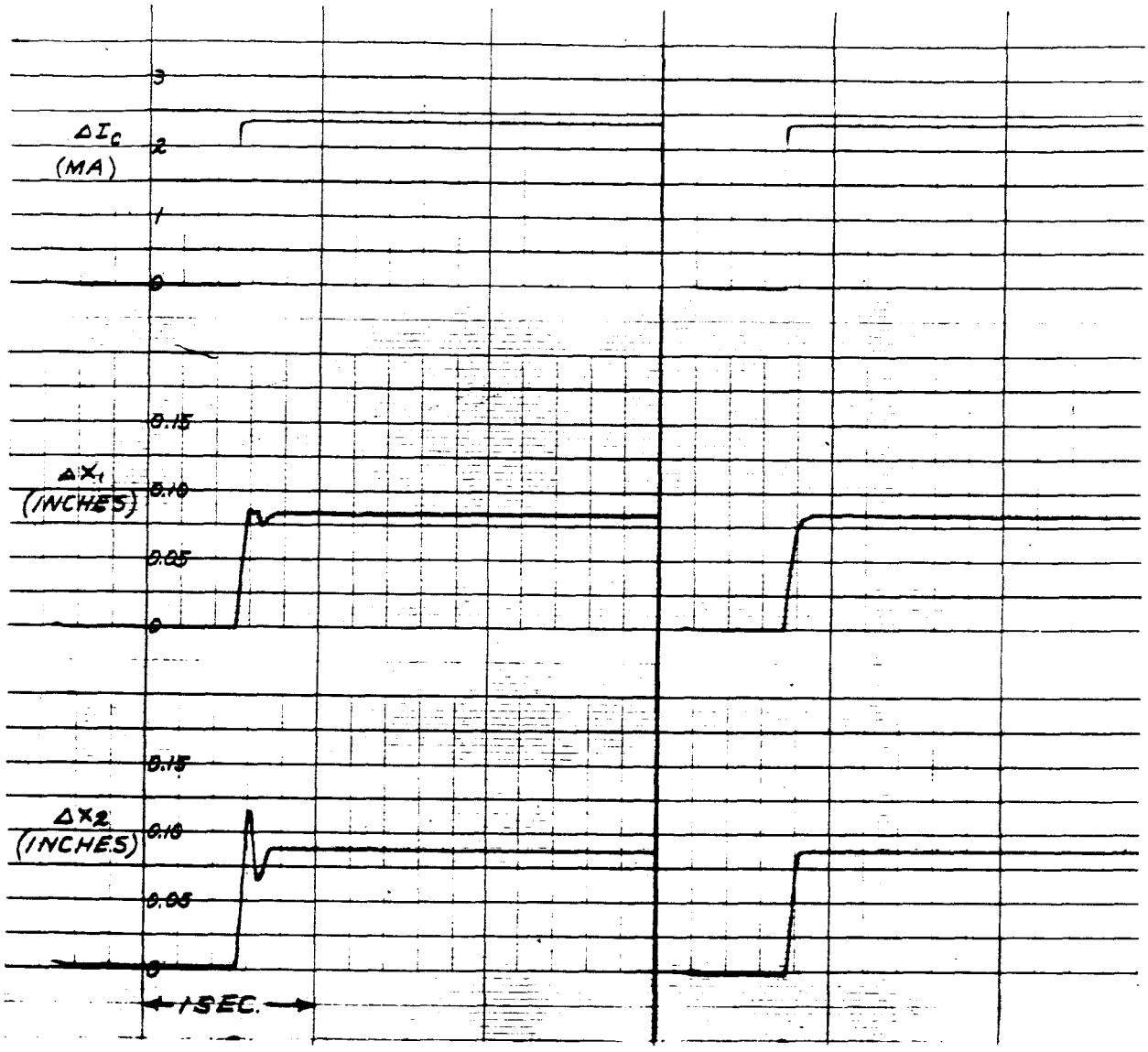

(a) F_f = 1,460 LB.

(b) F_f = 7,300 LB.

K_3 = 391,000 LB./IN.

NITROGEN

FIGURE 10 SYSTEM NO. 5 TRANSIENT RESPONSE

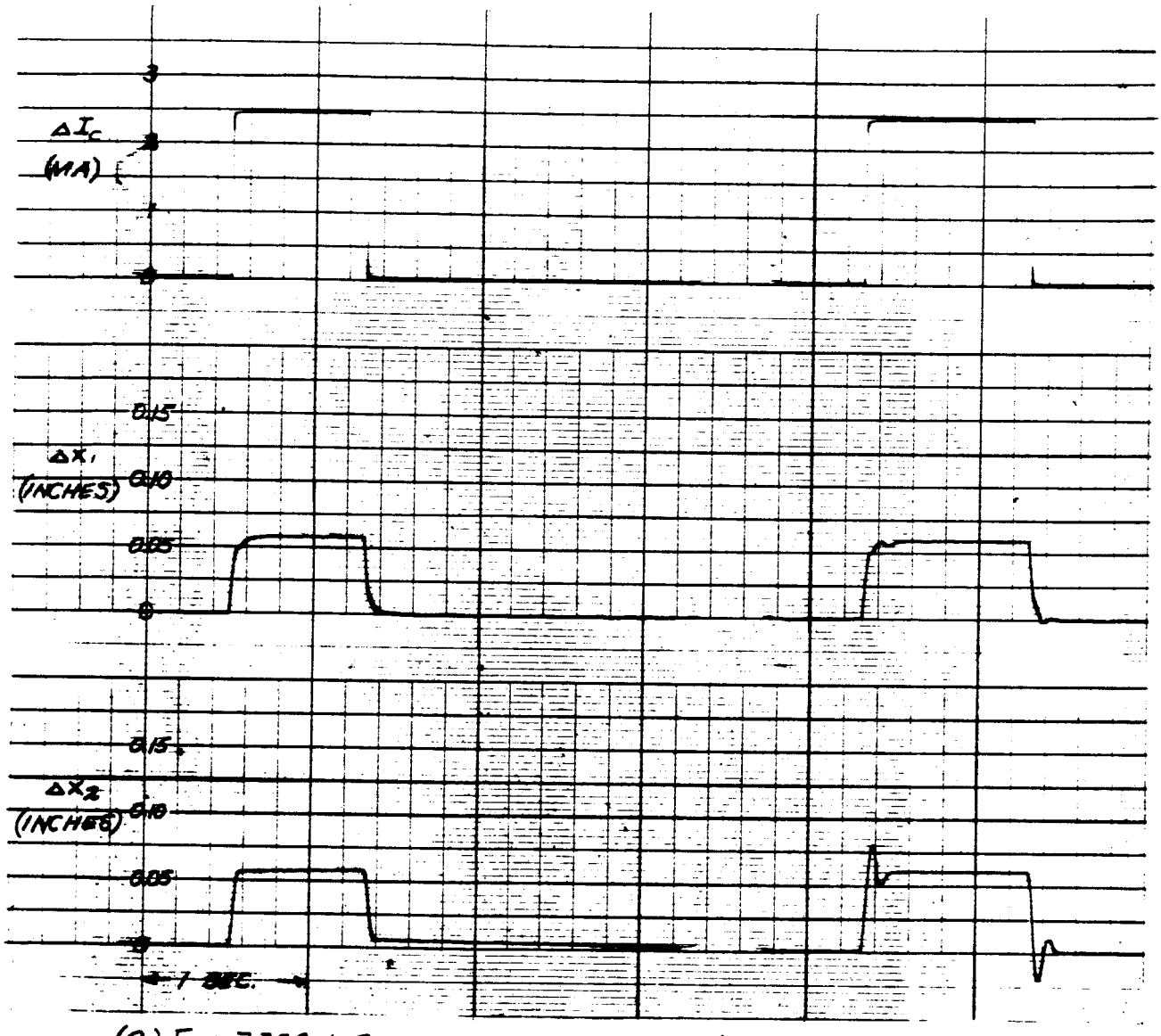

(a) F_f = 7,300 LB.

(b) F_f = 1,460 LB.

K_3 = 391,000 LB./IN.

K_S = 700,000 LB./IN. (SNUBBER)

X_1 LIMIT AT 0.05 IN.

NITROGEN

SYSTEM NO. 4

FIGURE 11 TRANSIENT INTO AND AWAY FROM SNUBBERS

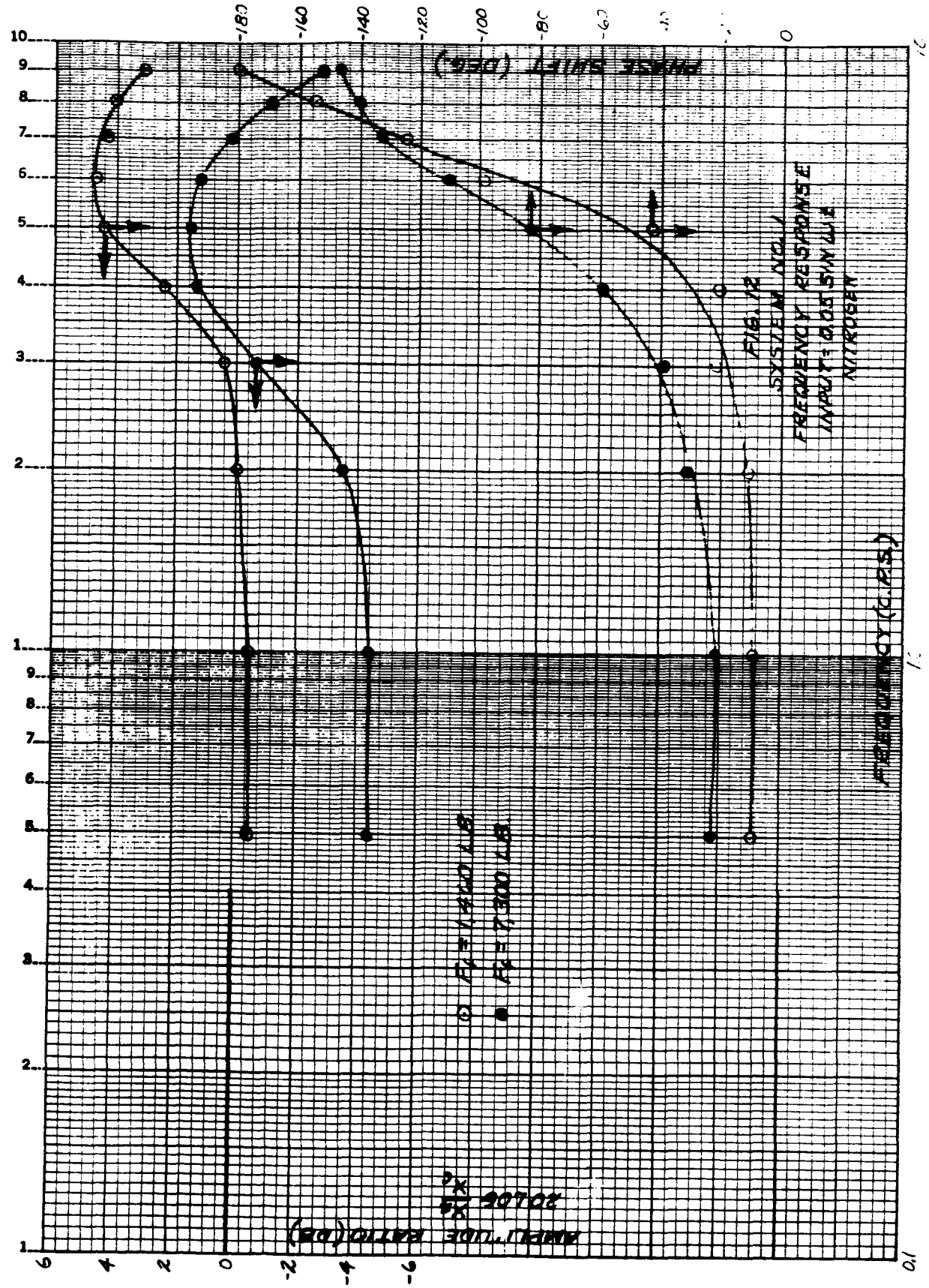
FIG. 12
SYSTEM NO. 1
FREQUENCY RESPONSE
INPUT = 0.05 SCFM
NITROGEN
Pi = 1440 LB
Pi = 1300 LB
K&E SEMI-LOGARITHMIC 359-81
KEUFFEL & ESSER CO.
2 CYCLES X 70 DIVISIONS

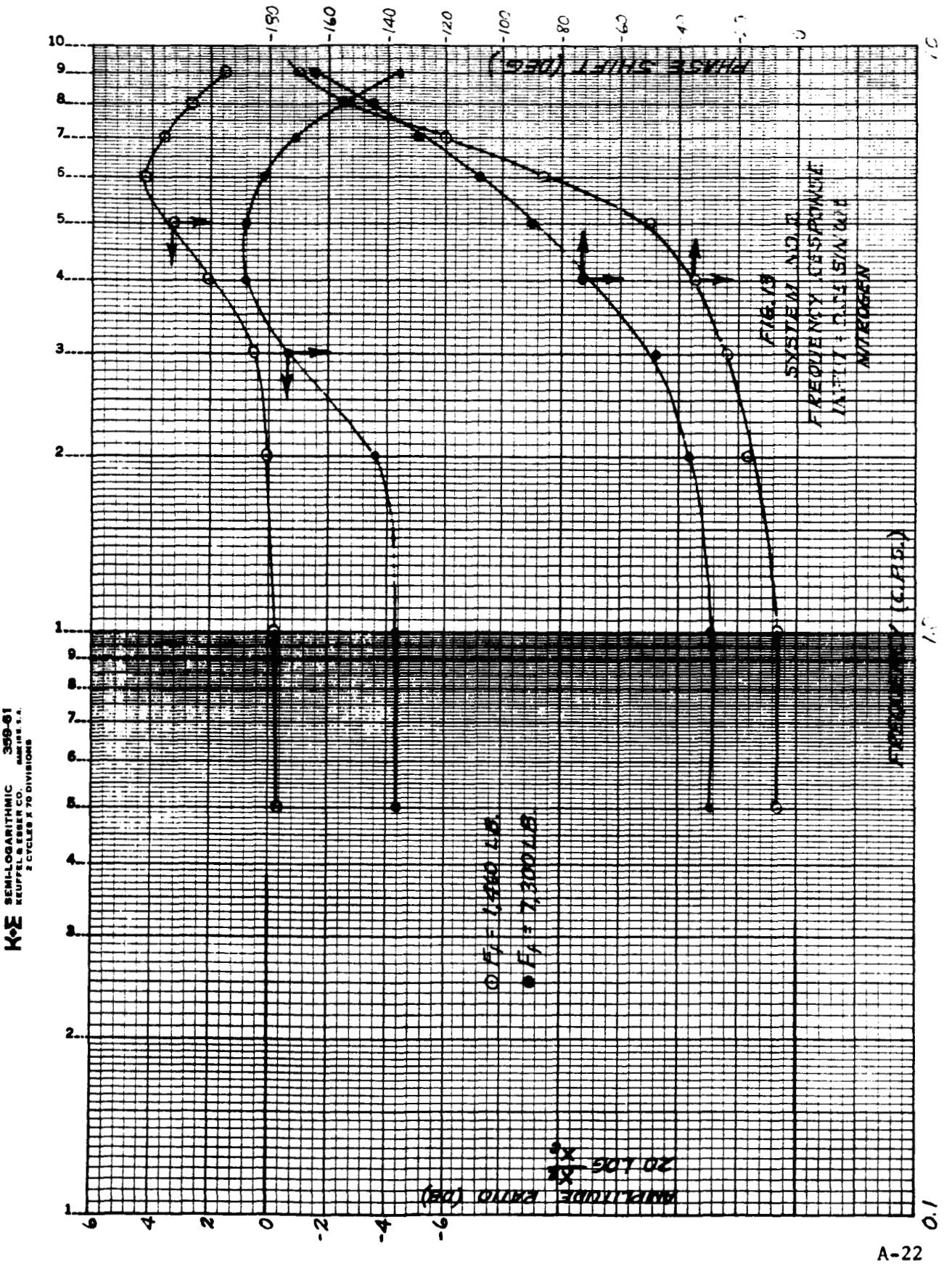

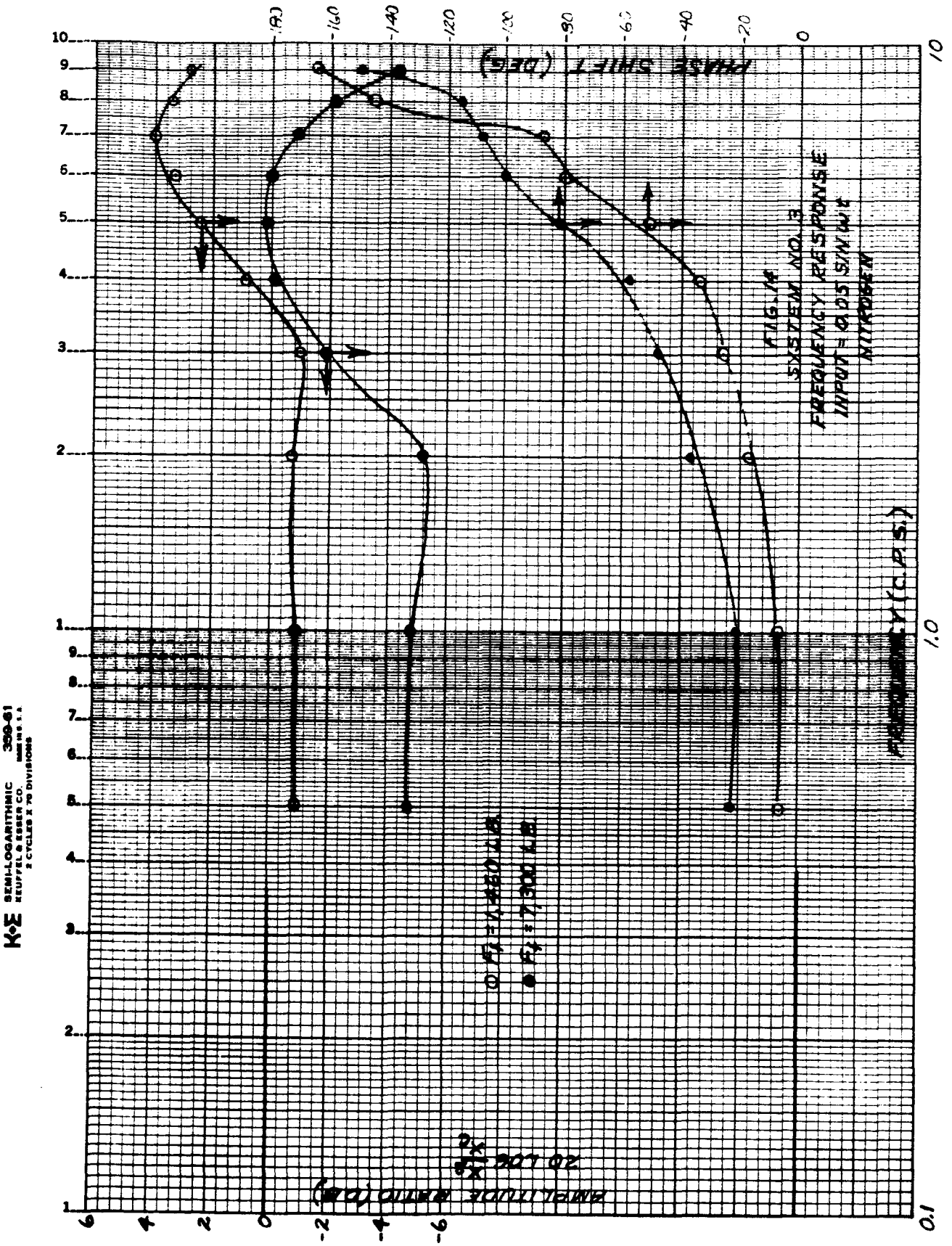
FIG. 14
SYSTEM NO. 3
FREQUENCY RESPONSE
INPUT = 0.05 SIN WT
NITROGEN
PHASE SHIFT (DEG.)
AMPLITUDE RATIO (DB)
FREQUENCY (C.P.S.)
K&E SEMI-LOGARITHMIC 359-61
KEUFFEL & ESSER CO.
2 CYCLES X 90 DIVISIONS

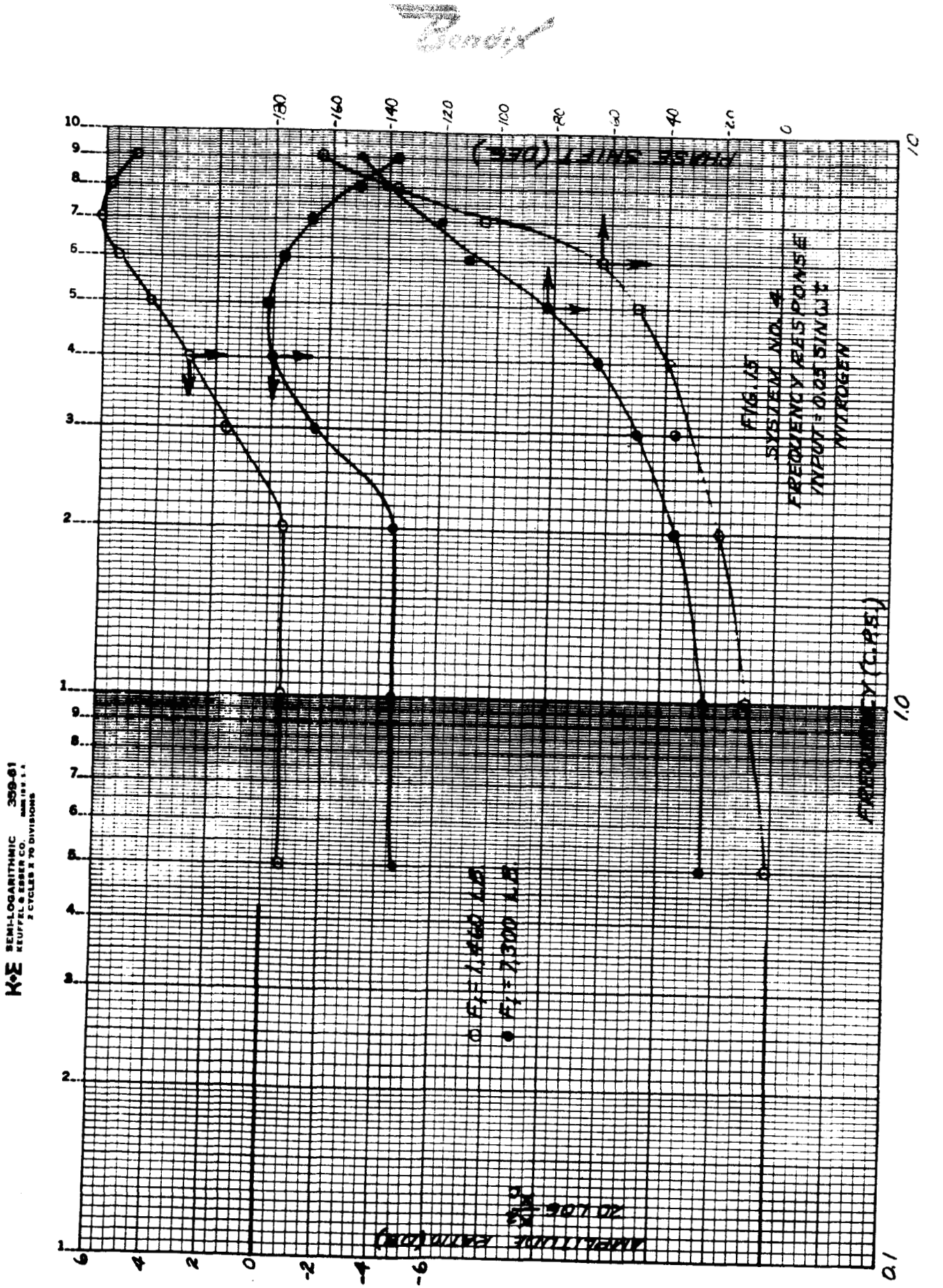

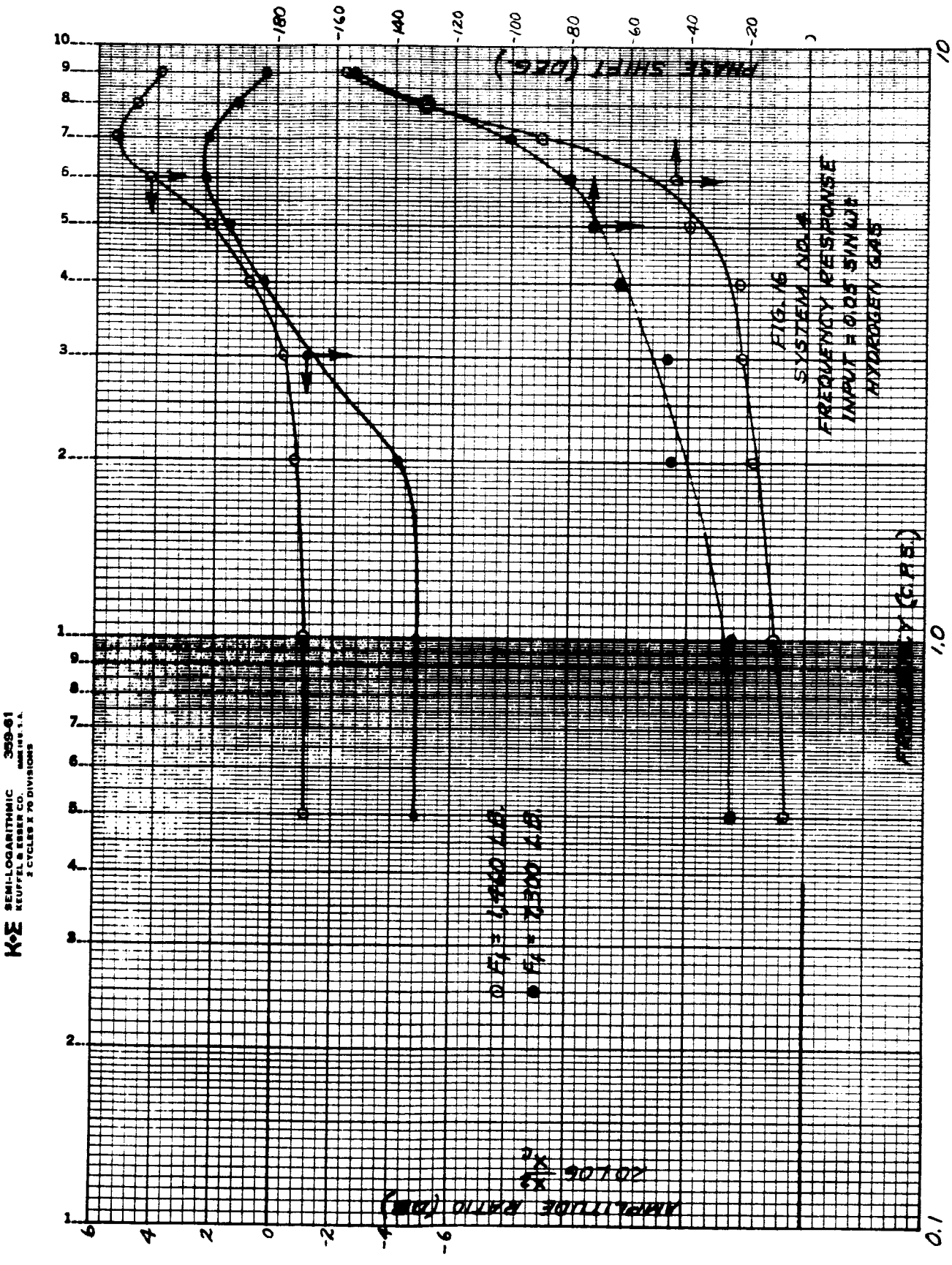

Bendix

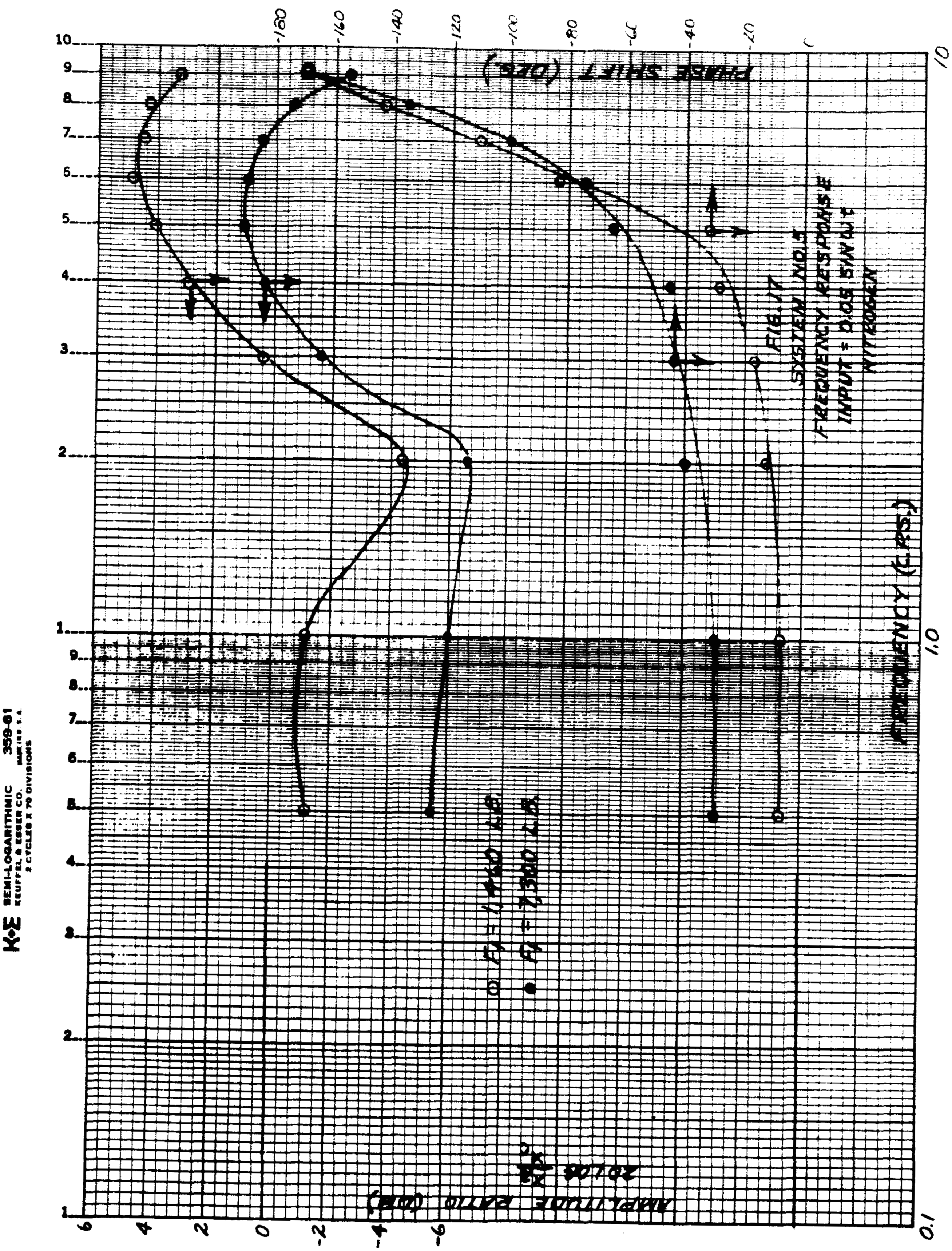
FIG. 17
SYSTEM NO. 5
FREQUENCY RESPONSE
INPUT = 0.05 SIN ωt
NITROGEN
PHASE SHIFT (DEG.)
FREQUENCY (C.P.S.)
AMPLITUDE RATIO (DB)
20 LOG X/Xo
○ FA = 1,440 LB.
● FA = 2,300 LB.
K+E SEMI-LOGARITHMIC 359-61
KEUFFEL & ESSER CO.
2 CYCLES X 70 DIVISIONS

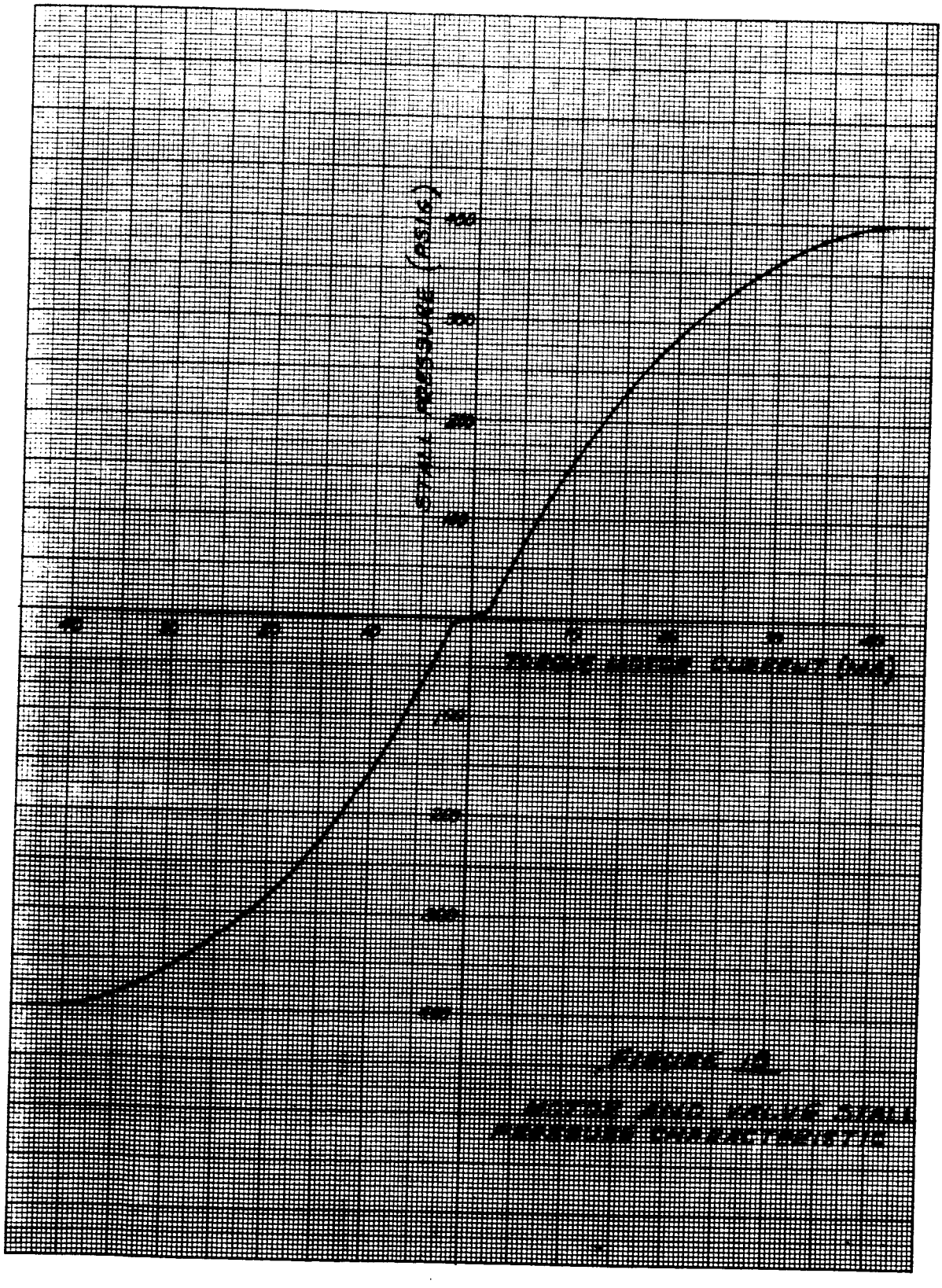

Figure 4B

REGULATOR AND SHUTOFF VALVE ASSEMBLY CHARACTERISTICS

K&E 10 X 10 TO THE CM. 359-14
KEUFFEL & ESSER CO. MADE IN U.S.A.

APPENDIX B

DYNAMIC ANALYSIS OF VORTEX VALVES

DYNAMIC ANALYSIS OF VORTEX VALVES

1.0 PURPOSE OF INVESTIGATION

To develop a mathematical model of a vortex valve which will predict reasonably accurate results for both steady state and transient response for step inputs of control pressure.

2.0 SUMMARY OF RESULTS

2.1 The steady state mass flow rate data from the computer checked very close with steady state test data. The deviations were +13.0%, +1.6%, and -4.5% at control to supply pressure differences of 0, 2, and 4 psia, respectively. This range covers the majority of the working range of the vortex valve. (See Figure II.)

2.2 The dynamic results of the computer data and actual test data compared within the range of interpretation of the data and the ability of the test equipment to produce a step change in control pressure. (See Figure II.)

2.3 The transient characteristics of the vortex valve can be closely reproduced by a simple time delay and first-order lag for linearized studies about steady state points. The magnitude of the time delay and the first-order lag vary with valve configuration, pressure and flow levels, and the operating limit of the vortex valve.

3.0 VORTEX VALVE ANALYSIS

A search was made for a mathematical model that would yield reasonably accurate transient and steady state response to changes in control pressure.

Previous work on steady state models has shown that an inviscous flow assumption gives poor correlation with test data in the pressure spectrum of high tangential velocities (Mach .5 to Mach 1.0), while an assumption of constant radial velocity profile has good correlation in the region of high tangential velocities but has poor correlation in the region of low tangential velocities (Mach 0 to Mach .2).

This model was selected as a compromise between these two assumptions, by using an arbitrary energy loss factor which has an increasing effect as the tangential velocity approaches sonic velocity.

A closer examination of the model as well as preliminary test data indicates a rather shallow slope of the radial pressure gradients within the vortex valve except in the vicinity of the exit port. This shallow slope indicates that the effects of compressability of the fluid may be neglected for a first-order approximation. For this reason, at transient it is assumed that there is a weight flow balance of mass flow leaving the vortex valve with the mass flow entering the vortex valve, although compressability is considered when calculating radial and tangential velocity profiles.

The radial mass flow rate at any time is controlled by the pressure drop across the exit of the valve with an average upstream pressure equal to the pressure (P_e) calculated at the outer radius of the exit port.

The supply flow enters through an area large enough so that the pressure at the outer parameter of the vortex valve is equal to the supply pressure and independent of any changes in mass flow through the valve.

To simplify calculations, the assumption is made that the compression and expansion of the fluid within the vortex valve is isothermal.

With the preceding assumptions in mind, the following equations may be derived:

$$\frac{\delta P}{\delta r} = \frac{PV^2}{rgRT} \qquad (1)$$

$$\frac{dr}{dt} = \dot{r} = (-)\frac{RTW_e}{2\pi LPr} \qquad (2)$$

$$W_e = \frac{26.88\, A_e \sqrt{P_a(P_e - P_a)}}{\sqrt{RT}} \qquad \frac{P_a}{P_e} \geq .528 \qquad (3)$$

$$W_e = \frac{13.44\, A_e\, P_e}{\sqrt{RT}} \qquad \frac{P_a}{P_e} \leq .528 \qquad (4)$$

$$W_c = \frac{26.88 A_c \sqrt{P_s(P_c - P_s)}}{\sqrt{RT}} \qquad \frac{P_s}{P_c} \geq .528 \qquad (5)$$

$$V_c = 26.88 \sqrt{\frac{RT(P_c - P_s)}{P_c}} \qquad \frac{P_s}{P_c} \geq .528 \qquad (6)$$

$$W_c = \frac{13.44\ A_c\ P_c}{\sqrt{RT}} \qquad \frac{P_s}{P_c} \leq .528 \qquad (7)$$

$$V_c = 13.44 \sqrt{RT} \qquad \frac{P_s}{P_c} \leq .528 \qquad (8)$$

$$W_s = W_e - W_c \qquad (9)$$

$$V_o = \frac{V_c W_c}{W_c + |W_s|} \qquad (10)$$

$$\frac{\delta V}{\delta r} = -\frac{V}{r} + \frac{V}{V_s}\left\{\frac{V}{r} - \left(\frac{\delta V}{\delta t}\right)\frac{1}{r}\right\} \qquad (11)$$

$$V_s = 13.44 \sqrt{RT} \qquad (12)$$

The preceding equations were incorporated into a digital computer program designed to give a high degree of accuracy with a minimum amount of computer time.

A block diagram of the computer program is shown on Figure III. A sketch of a typical vortex valve is shown on Figure I.

The preceding equations may be solved for a steady state solution in the form of:

$$\ell n\left(\frac{P_e}{P_s}\right) = (-)\ .468 \left\{ \ell n \left[\frac{\frac{V_o}{V_s} + \frac{r_e}{r_o}\left(1 - \frac{V_o}{V_s}\right)}{\frac{r_e}{r_o}} \right] + \frac{\frac{V_o}{V_s}\left(1 - \frac{V_o}{V_s}\right)\left(1 - \frac{r_e}{r_o}\right)}{\frac{V_o}{V_s} + \frac{r_e}{r_o}\left(1 - \frac{r_e}{r_o}\right)} \right\} \qquad (13)$$

It should be noted that the steady state solution of the pressure turn down ratio of the valve depends only on the Mach number of the outer perimeter, and the radius ratio of the valve. This suggests that the steady state performance of the vortex valve will be unaffected by the type of gas used, and the temperature of the gas.

The time delay may be approximated by the equation:

$$t_d = \frac{\left[\left(\frac{D_o}{D_e}\right)^2 - 1\right] L}{13.44\ N\sqrt{RT}}$$

t_d = dead time - seconds

D_o = outer diameter - inch

D_e = exit core diameter - inch

R = gas constant - in.lb./lb. °F

13.44 = flow constant based on ratio of specific heats - $(in./sec.^2)^{1/2}$

N = turn down ratio of valve

$N = W_e/W_e^1$

W_e = exit weight flow at test point

W_e^1 = exit weight flow with no control pressure

4.0 COMPUTATION PROCEDURE

The Univac 1107 computer located at Notre Dame was used for running this computer program.

The physical dimensions of the vortex valve, and the characteristics of the gas were included as input data to the program. The program used time increments of .0002 second with instruction to change input pressure conditions after .0300 second of time had elapsed. The program was terminated when no additional input instructions were available.

The solution time on the computer is approximately 20 seconds per increment of control pressure. This increment covers a problem time of .0300 second and includes a total of 150 sub-increments of time.

The very short running time on the computer makes this program a very economical method of optimizing vortex valve designs without going through an elaborate hardware test program.

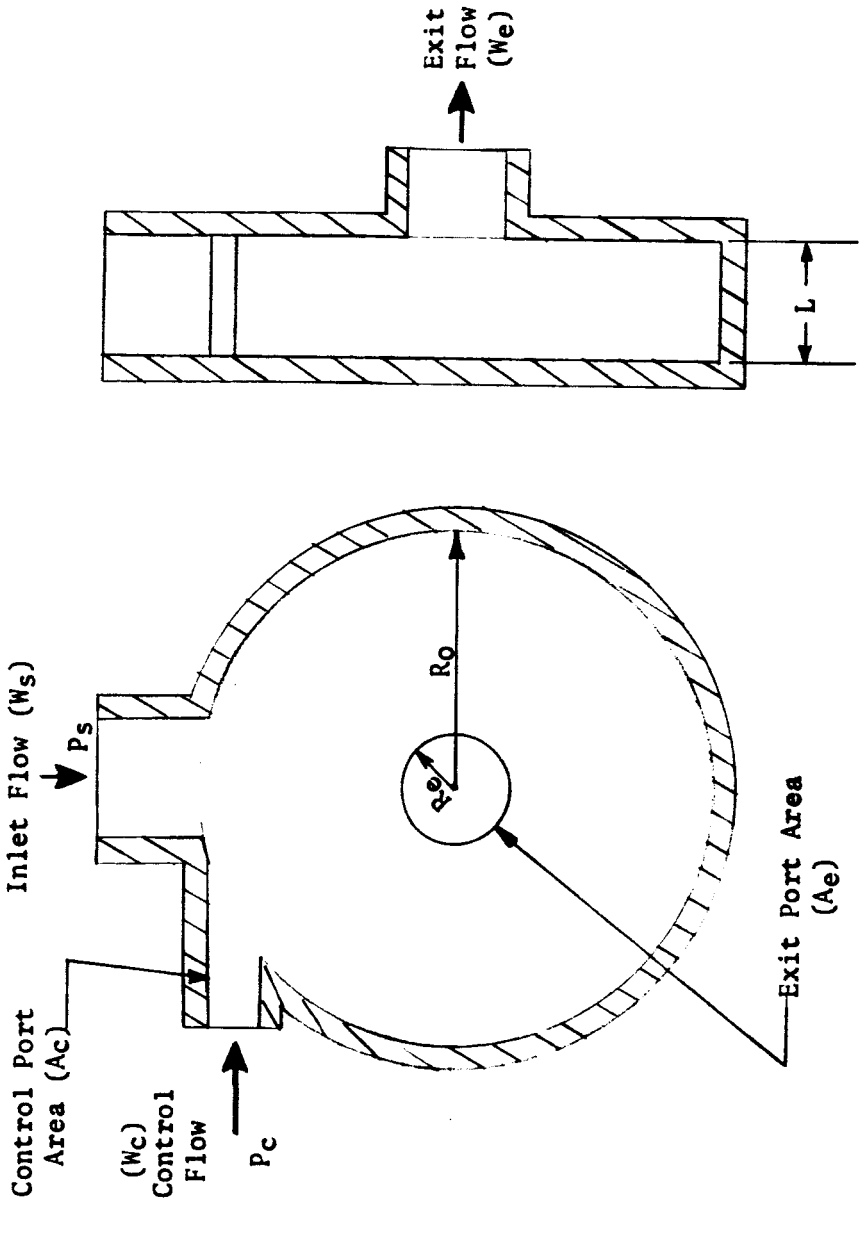

FIGURE 1 VORTEX VALVE

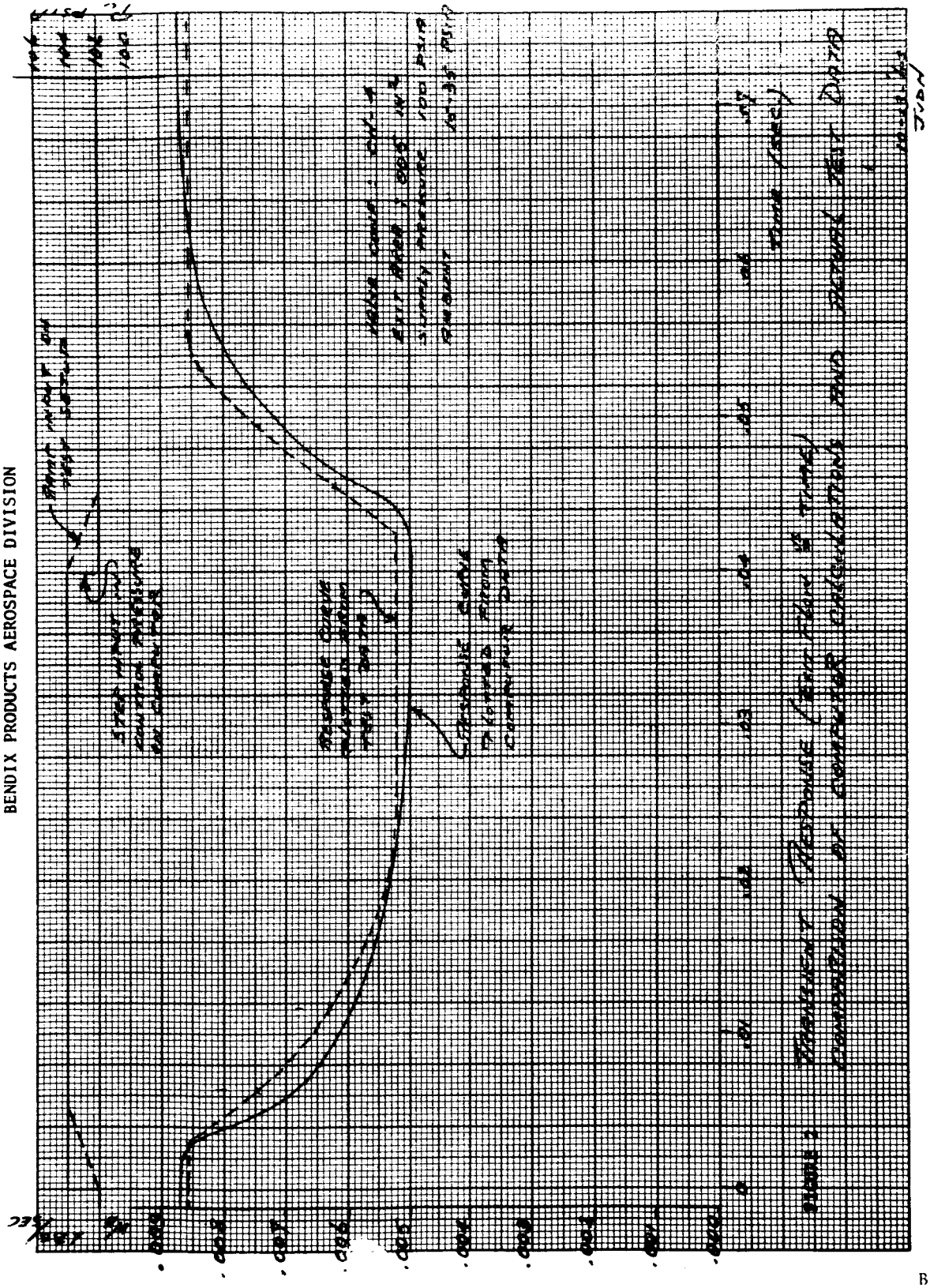

THE BENDIX CORPORATION
BENDIX PRODUCTS AEROSPACE DIVISION

K&E 10 X 10 TO THE ½ INCH 359-11 KEUFFEL & ESSER CO. MADE IN U.S.A.

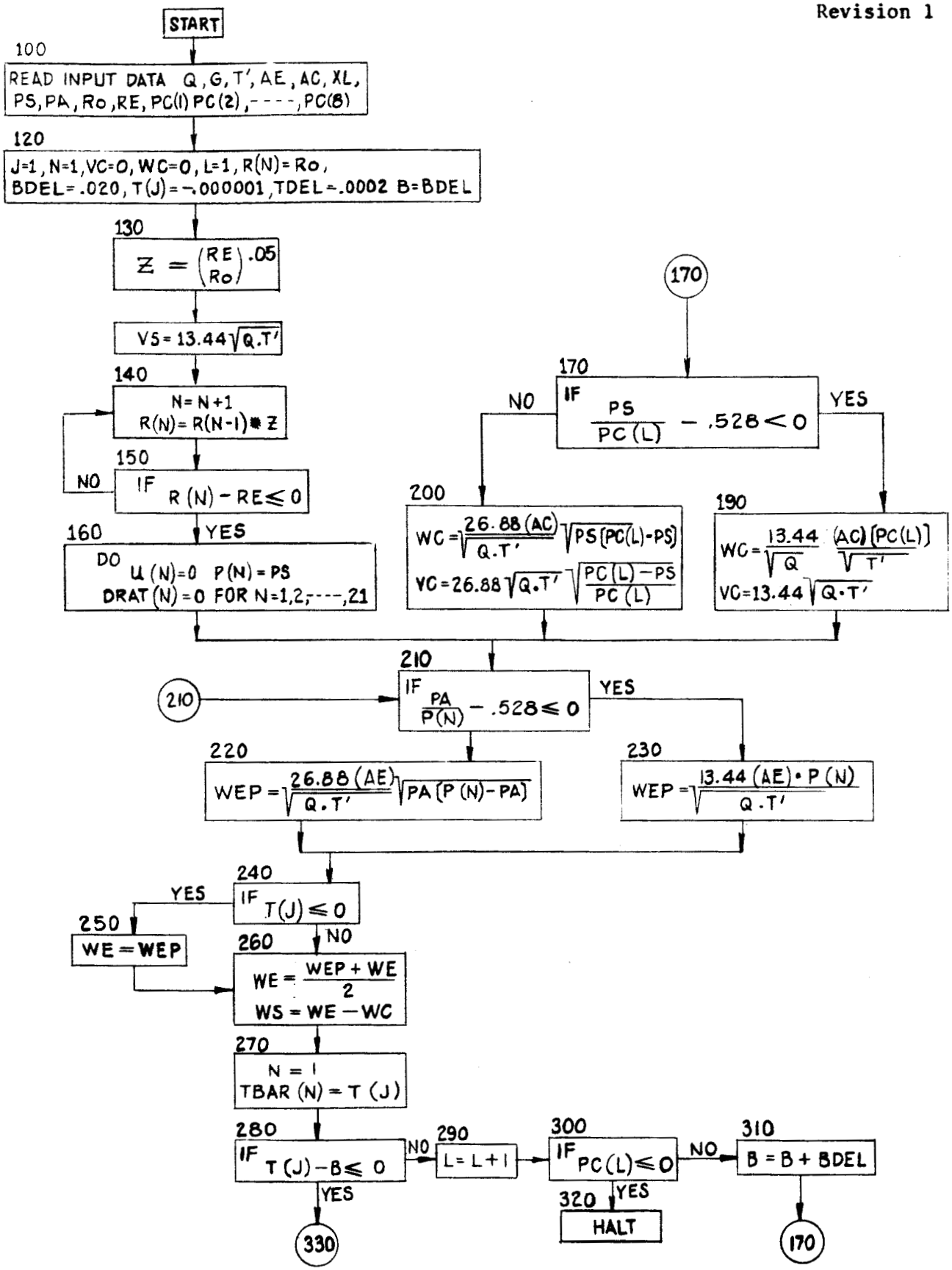
START
100
READ INPUT DATA Q, G, T', AE, AC, XL, PS, PA, Ro, RE, PC(1) PC(2), ----, PC(8)
120
J=1, N=1, VC=0, WC=0, L=1, R(N)=Ro, BDEL=.020, T(J)=-.000001, TDEL=.0002 B=BDEL
130
Z = (RE/Ro) .05
VS = 13.44 √(Q.T')
140
N=N+1
R(N)=R(N-1)*Z
150
NO
IF R(N) - RE ≤ 0
YES
160
DO U(N)=0 P(N)=PS
DRAT(N)=0 FOR N=1,2;---,21
170
170
IF PS/PC(L) - .528 < 0
NO
YES
200
WC = (26.88 (AC)/√(Q.T')) √(PS (PC(L)-PS))
VC = 26.88 √(Q.T') √((PC(L)-PS)/PC(L))
190
WC = (13.44/√Q) (AC) √(PC(L))
VC = 13.44 √(Q.T')
210
210
IF PA/P(N) - .528 ≤ 0
YES
220
WEP = (26.88 (AE)/√(Q.T')) √(PA (P(N)-PA))
230
WEP = (13.44 (AE) • P(N))/√(Q.T')
240
YES
IF T(J) ≤ 0
250
WE = WEP
260
NO
WE = (WEP + WE)/2
WS = WE - WC
270
N = 1
TBAR(N) = T(J)
280
IF T(J) - B ≤ 0
NO
290
L = L + 1
300
IF PC(L) ≤ 0
NO
310
B = B + BDEL
YES
320
HALT
330
170

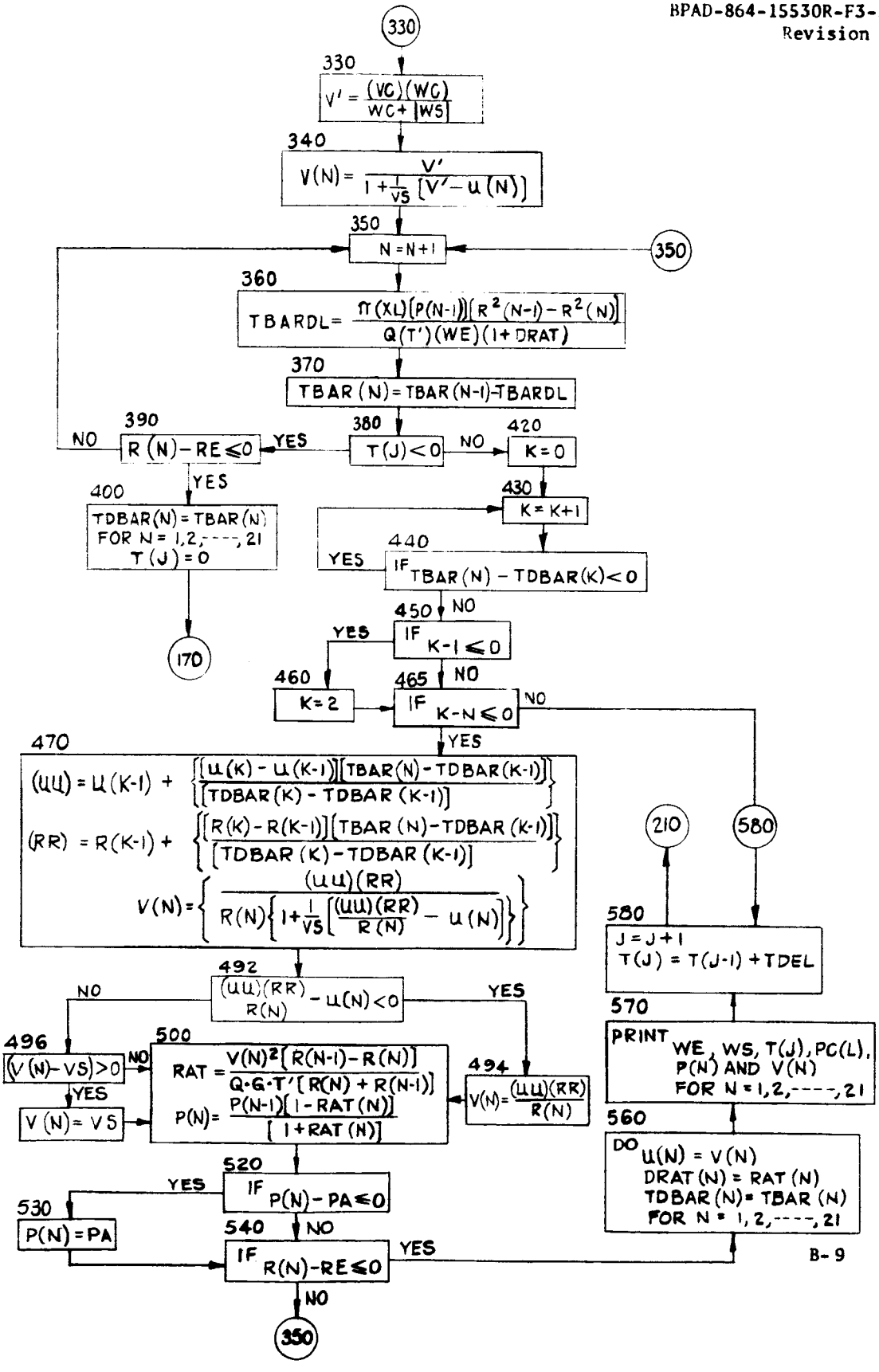
330
330
$V' = \frac{(VC)(WC)}{WC + |WS|}$
340
$V(N) = \frac{V'}{1 + \frac{1}{VS}[V' - U(N)]}$
350
N = N+1
350
360
$TBARDL = \frac{\pi(XL)[P(N-1)][R^2(N-1) - R^2(N)]}{Q(T')(WE)(1+DRAT)}$
370
TBAR(N) = TBAR(N-1) - TBARDL
380
T(J) < 0
NO
420
K = 0
YES
390
R(N) - RE ≤ 0
NO
YES
400
TDBAR(N) = TBAR(N)
FOR N = 1,2,---,21
T(J) = 0
170
430
K = K+1
440
IF TBAR(N) - TDBAR(K) < 0
YES
NO
450
IF K-1 ≤ 0
YES
460
K = 2
465
IF K-N ≤ 0
NO
YES
470
$(UU) = U(K-1) + \left\{\frac{[U(K) - U(K-1)][TBAR(N) - TDBAR(K-1)]}{[TDBAR(K) - TDBAR(K-1)]}\right\}$
$(RR) = R(K-1) + \left\{\frac{[R(K) - R(K-1)][TBAR(N) - TDBAR(K-1)]}{[TDBAR(K) - TDBAR(K-1)]}\right\}$
$V(N) = \left\{\frac{(UU)(RR)}{R(N)\left\{1 + \frac{1}{VS}\left[\frac{(UU)(RR)}{R(N)} - U(N)\right]\right\}}\right\}$
492
$\frac{(UU)(RR)}{R(N)} - U(N) < 0$
NO
YES
496
(V(N) - VS) > 0
NO
YES
V(N) = VS
500
$RAT = \frac{V(N)^2[R(N-1) - R(N)]}{Q \cdot G \cdot T'[R(N) + R(N-1)]}$
$P(N) = \frac{P(N-1)[1 - RAT(N)]}{[1 + RAT(N)]}$
494
$V(N) = \frac{(UU)(RR)}{R(N)}$
520
IF P(N) - PA ≤ 0
YES
530
P(N) = PA
540
IF R(N) - RE ≤ 0
NO
YES
350
210
580
580
J = J+1
T(J) = T(J-1) + TDEL
570
PRINT WE, WS, T(J), PC(L), P(N) AND V(N) FOR N = 1,2,---,21
560
DO U(N) = V(N)
DRAT(N) = RAT(N)
TDBAR(N) = TBAR(N)
FOR N = 1,2,---,21